



# Tensor rank bounds for point singularities in $\mathbb{R}^3$

C. Marcati<sup>1,3</sup> · M. Rakhuba<sup>2</sup> · Ch. Schwab<sup>3</sup>

Received: 23 September 2020 / Accepted: 7 January 2022 / Published online: 14 April 2022  
© The Author(s) 2022

## Abstract

We analyze rates of approximation by quantized, tensor-structured representations of functions with isolated point singularities in  $\mathbb{R}^3$ . We consider functions in countably normed Sobolev spaces with radial weights and analytic- or Gevrey-type control of weighted semi-norms. Several classes of boundary value and eigenvalue problems from science and engineering are discussed whose solutions belong to the countably normed spaces. It is shown that quantized, tensor-structured approximations of functions in these classes exhibit tensor ranks bounded polylogarithmically with respect to the accuracy  $\varepsilon \in (0, 1)$  in the Sobolev space  $H^1$ . We prove *exponential convergence rates* of three specific types of quantized tensor decompositions: quantized tensor train (QTT), transposed QTT and Tucker QTT. In addition, the bounds for the patchwise decompositions are uniform with respect to the position of the point singularity. An auxiliary result of independent interest is the proof of exponential convergence of *hp*-finite element approximations for Gevrey-regular functions with point singularities in the unit cube  $Q = (0, 1)^3$ . Numerical examples of function approximations and of Schrödinger-type eigenvalue problems illustrate the theoretical results.

**Keywords** Quantized tensor train · Tensor networks · Low-rank approximation · Exponential convergence · Schrödinger equation

---

Communicated by: Ivan Oseledets

✉ C. Marcati  
carlo.marcati@sam.math.ethz.ch

M. Rakhuba  
mrakhuba@hse.ru

Ch. Schwab  
christoph.schwab@sam.math.ethz.ch

- <sup>1</sup> Present address: Dipartimento di Matematica, Università degli Studi di Pavia, 27100 Pavia, Italy
- <sup>2</sup> CS Department, HSE University, Pokrovsky Boulevard 11, Moscow, 109028 Russian Federation
- <sup>3</sup> Seminar für Angewandte Mathematik (SAM), ETH Zürich, Rämistrasse 101, 8092, Zürich, Switzerland

**Mathematics Subject Classification (2010)** Primary 35A35; 15A69 · 35J15 · 41A25 · 41A46 · 65N30

## 1 Introduction

Recent years have seen the emergence of *structured numerical linear algebra* in scientific computing and data science. We mention only formatted matrix algebras, such as  $\mathcal{H}$ -matrices (e.g., [33] and the references there) and tensor formats (e.g., [32, 43, 46, 62, 67] and the references there). To date, the impact of these methods was, first and foremost, on the corresponding scientific computing applications: being abstracted from fast multipole methods, formatted computational matrix algebras impact directly the numerical solution of elliptic and parabolic partial differential equations (see, e.g., [6, 27, 35]). Numerical tensor algebras, derived from quantum chemistry (e.g., [6, 72] and the references there) have obvious applications in data science, where massive  $n$ -way data naturally arises and needs to be efficiently handled numerically. Furthermore, tensor-structured formats have, in recent years, been linked to deep neural networks (see [45, 51] and the references there). We now comment on more specific developments in these areas which are directly related to the present paper, and the mathematical results obtained in it.

We are concerned with the approximation of functions with isolated point singularities using tensor-structured representations. In particular, we approximate, using quantized tensor decompositions, three-dimensional arrays of coefficients associated with the finite element projection of functions over trilinear Lagrange basis functions.

*Quantization* refers to the reshaping of an array of coefficients of size  $2^\ell \times 2^\ell \times 2^\ell$  into a multidimensional array of size  $2 \times \dots \times 2$ . The application of tensor decompositions (e.g., the Tensor-Train decomposition [65], which leads to the QTT—quantized tensor train decomposition, introduced in [42, 64]) to such an array can lead to a reduction in complexity and number of parameters.

The number of parameters in a decomposition is related to the *rank* of the decomposition—i.e., the generalization of matrix rank to multi-dimensional arrays. Having a priori knowledge that a function of interest, e.g., the solution to a partial differential equation, can be approximated by a low-rank tensor decomposition, allows for the application of tensor-structured algorithms that avoid working with full  $2^\ell \times 2^\ell \times 2^\ell$  arrays of coefficients.

In particular, here we consider functions in weighted Sobolev spaces with radial weights and analytic- or Gevrey-type control of weighted semi-norms. Such functions arise in a variety of scientific applications: nonlinear Schrödinger equations (e.g., [11, 13] and the references there), Hartree-Fock and density functional theory equations, continuum models of point defects [53], blowup solutions in evolution equations with critical nonlinearity (e.g., [70] and the references there) to name but a few.

The main result of the present paper is *exponential convergence of tensor-structured approximations of point singularities in  $\mathbb{R}^3$* , i.e., they admit tensor ranks bounded polylogarithmically with respect to the accuracy  $\varepsilon \in (0, 1)$  of the approximation, measured in the Sobolev space  $H^1$ .

An auxiliary result of independent interest is the exponential convergence of  $hp$ -finite element (FE) approximations for the class of functions considered. Due to the piecewise polynomial structure of  $hp$ -FE approximants, we can obtain their quantized representations with exact rank bounds that depend only on the dimensions of  $hp$ -spaces. This, in turn, leads to the desired rank bounds of the functions of interest.

One of the advantages of using quantized tensor decompositions—compared with the direct application of  $hp$ -FE approximations—is the relative ease of implementation. The adaptation of the number of parameters in the decomposition to the approximated function is based on well-known numerical linear algebra tools such as QR and SVD decompositions. Moreover, there exist open source codes with the implementation of basic linear algebra operations including solution of linear systems, which can be used independently of a particular application.

Note also that we do not need to know a priori the type and exact location of the singularity of the solution to solve PDEs in quantized tensor-structured formats. The nonlinear structure of the decomposition allows for an “automatic” adaptation of the tensor compressed representation to the regularity of the function. This is by contrast to  $hp$  methods, where mesh and polynomial degree refinements are programmed explicitly depending on the type of singularity. Furthermore, while the mesh of an  $hp$  space has to be constructed so that the refinement happens towards the singular point, this a priori knowledge is not necessary in the computation of quantized tensor-structured representation.

## 1.1 Tensor-structured function approximation

With the availability of efficient numerical realizations of tensor-structured numerical linear algebra, a new perspective has been opened towards *computational function approximation*. Here, one compresses arrays of function values in tensor formats; early work in this direction is [78], and [43] contains a bibliography with a large list of ensuing developments based on this idea. An (incomplete) list of references contains [37, 42, 44, 61, 66] where tensor rank bounds for specific functions have been obtained, both analytically and computationally, in the so-called *quantized tensor train (QTT) format*. QTT-formatted numerics for electron structure computations were presented in [41]. An analysis of approximation properties of tensor networks for classes of functions of finite differentiability as expressed by membership in classical Sobolev and Besov spaces of finite order has recently been presented in [1–3].

Subsequently, and more directly related to the present work, rather than rank bounds for individual functions, *tensor rank bounds for solution classes of elliptic PDEs* in one and two spatial dimensions were obtained in [36, 38, 40, 58]. In [40], in particular, it was proved first that functions in countably normed, analytic function classes in polygons  $D \subset \mathbb{R}^2$  admit QTT-structured tensor approximations with tensor ranks bounded polylogarithmically in terms of the approximation accuracy  $\varepsilon$ . The key mathematical argument in the references cited above is based on *analytic regularity results* for solutions of elliptic PDEs in polytopal domains. Such regularity results, implying solutions belong to countably normed spaces, have been obtained

in the past two decades for several broad classes of (boundary value and eigenvalue problems of) elliptic PDEs, in [4, 55, 59].

## 1.2 Contributions

In this work, we obtain rank bounds for the QTT approximation of functions in weighted analytic and Gevrey classes with point and edge singularities. Specifically, we prove polylogarithmic growth of QTT ranks with respect to the accuracy of the approximation. To obtain the bounds, we approximate functions from the weighted Gevrey class by continuous, piecewise polynomial functions on dyadic partitions which are geometrically refined towards the singular supports. These piecewise polynomial approximants are subsequently re-interpolated and compressed to the QTT format. The resulting rank bounds follow from the low-rank structure of piecewise polynomial functions, and the exponential convergence of the piecewise polynomial approximations.

The principal novel contributions of this paper are therefore the *exponential convergence of  $hp$  approximation for weighted Gevrey classes*, and the *polylogarithmic rank bounds of QTT approximations* on these classes.

First, we analyze approximation rates of tensor-structured approximations of smooth functions with isolated point singularities. As compared to exponential convergence results for *analytic* functions with point singularities, we here establish exponential convergence of *hp*-finite element (FE) approximations on geometric meshes of axiparallel quadrilaterals resp. hexahedra analogous to [20] also for Gevrey-regular functions.

We then address tensor-formatted approximations. Generalizing results also in two variables, in the present paper we extend the analysis in [40] to quantized, TT-structured function approximation of functions from countably weighted, Gevrey-type classes. The corresponding results in three spatial variables are novel. They also extend the QTT rank bounds in [40] to Gevrey- $\mathfrak{d}$  regular functions (see Remark 4). They also constitute a building block for the derivation of corresponding QTT rank bounds for edge and face singularities in three space dimensions, which we do not detail here. In particular, we prove in three physical variables for analytic and Gevrey functions with point singularities, for the classical tensor-format, asymptotic upper bounds on quantized tensor ranks at prescribed accuracy  $\varepsilon$  which are better than the corresponding bounds for the transposed TT format introduced in [40] (in two dimensions).

We show numerical results indicating the correctness of the presently obtained results, and also strongly suggesting that similar ranks are achieved in tensor-formatted PDE solvers, provided the PDE solutions belong to the countably normed classes introduced in Section 1.3.2.

## 1.3 Problem formulation

The tensor-formatted function approximation considered in this paper aims at establishing tensor rank bounds for functions in certain classes of locally smooth functions

that admit a point singularity. In this paper, we confine ourselves to the case that the function under consideration admits singular support consisting only of one isolated point (we therefore speak of “point singularities”). Naturally, functions whose singular support comprises of a finite number of *well-separated points* can equally be approximated in the tensor-formats discussed here, with the same tensor rank bounds, by a localization and superposition argument.

Weighted Sobolev spaces for functions with isolated point singularities have been introduced for the analysis of elliptic problems in polygonal domains, see [47], since they allow for the extension of classical elliptic regularity theory to domains with corners. For an overview of regularity results for elliptic boundary value problems in conical domains, in weighted Sobolev spaces, we refer to the monographs [28, 48, 49, 60].

For elliptic boundary value problems in three space dimensions, weighted Sobolev spaces that accommodate isolated point singularities have also proven important in the mathematical regularity analysis of problems with singular potentials, such as electron structure calculations in quantum physics and quantum chemistry, see, e.g., [21–23].

When a function is regular in weighted Sobolev spaces—specifically, when analytic-type bounds can be derived on the norms of its derivatives—piecewise polynomial approximations can be constructed, for example by *hp* finite elements which converge exponentially (in terms of the number of parameters) [29, 30, 71, 73, 74]. This suggests the existence of an underlying low-rank structure in suitable tensor formats; for this reason, we are here interested in the derivation of rank bounds for functions that belong to weighted analytic- and Gevrey-type classes.

A theory of analytic regularity in weighted Sobolev spaces has been developed for several classes of important physical problems and we mention an incomplete list. Solutions to scalar elliptic problems with constant coefficients belong to analytic-type weighted spaces [15, 16], as do the flow and pressure obtained with the Stokes [31] and Navier-Stokes [59] equations in polygons. Furthermore, eigenfunctions to three-dimensional linear [55] and nonlinear [54] Schrödinger equations are weighted analytic. In quantum chemistry, the wave functions computed with the non-relativistic Hartree-Fock models for electronic structure calculations are also analytic in weighted Sobolev spaces [56, Section 7.4], [12], with point singularities at the nuclei. We refer to Section 1.3.3 for some explicit examples in this sense. Other instances of the occurrence of point singularities in otherwise smooth solutions comprise general relativity (see, e.g., [10, 79] and the references there) and solutions of parabolic evolution equations with critical nonlinearity (see, e.g., [70] and the references there). The results of the present work apply to all the problems cited above, whose solutions are weighted analytic, in the spaces that we detail in Section 1.3.2 below.

We consider the following setting for quantized, tensor train (TT)-formatted function approximation in  $Q = (0, 1)^3$ , with one point singularity at the origin, where the functions belong to countably normed, weighted Sobolev spaces, where the weights are powers of  $r = |x|$ , the Euclidean distance of the point  $x \in Q$  from the origin.

### 1.3.1 Kondrat’ev-type weighted Sobolev spaces

For integer  $s \geq 0$ , a real parameter  $\gamma \in \mathbb{R}$ , and summability exponent  $1 \leq q < \infty$ , we introduce the *homogeneous weighted Sobolev spaces*

$$\mathcal{K}_\gamma^{s,q}(Q) = \left\{ v \in L^q(Q) : r^{|\alpha|-\gamma} \partial^\alpha u \in L^q(Q), \forall \alpha, |\alpha| \leq s \right\}$$

with seminorm

$$|w|_{\mathcal{K}_\gamma^{s,q}(Q)} = \left( \sum_{|\alpha|=s} \|r^{|\alpha|-\gamma} \partial^\alpha w\|_{L^q(Q)}^q \right)^{1/q}, \tag{1}$$

and norm

$$\|w\|_{\mathcal{K}_\gamma^{s,q}(Q)} = \left( \sum_{k=0}^s |w|_{\mathcal{K}_\gamma^{k,q}(Q)}^q \right)^{1/q}.$$

Our focus will be mostly on *non-homogeneous weighted Sobolev spaces* (remark the different weight exponent)

$$\mathcal{J}_\gamma^{s,q}(Q) = \left\{ v \in L^q(Q) : r^{s-\gamma} \partial^\alpha u \in L^q(Q), \forall \alpha, |\alpha| \leq s \right\},$$

with norm

$$\|w\|_{\mathcal{J}_\gamma^{s,q}(Q)} = \left( \sum_{|\alpha| \leq s} \|r^{s-\gamma} \partial^\alpha w\|_{L^q(Q)}^q \right)^{1/q}.$$

In the following, we will always consider the case where  $q = 2, 0 < \gamma - 3/2 < 1$ , and  $s > \gamma - 3/2$ . Under those hypotheses, as shown in [14, Proposition 3.18], the above norm is equivalent to

$$\|w\|_{\mathcal{J}_\gamma^{s,2}(Q)} \simeq \left( \|w\|_{L^2(Q)}^2 + \sum_{k=1}^s |w|_{\mathcal{K}_\gamma^{k,2}(Q)}^2 \right)^{1/2}. \tag{2}$$

Non-homogeneous spaces allow for functions with non trivial Taylor expansion at the singularity and have been used, for this reason, in the analysis of problems in non smooth domains with Neumann boundary conditions and of elliptic problems with singular potentials. For a thorough analysis of the relationship between homogeneous and non-homogeneous spaces, we refer the reader to [49] and [14].

### 1.3.2 Gevrey and analytic function classes

We define the weighted Kondrat’ev-type class of functions of infinite regularity

$$\mathcal{K}_\gamma^{\infty,q}(Q) = \bigcap_{s \in \mathbb{N}} \mathcal{K}_\gamma^{s,q}(Q).$$

Evidently,  $C_0^\infty(Q) \subset \mathcal{K}_\gamma^{\infty,q}(Q)$  Furthermore, for constants  $C, A > 0$  and  $\mathfrak{d} \geq 1$ , we introduce the *countably normed, homogeneous weighted Gevrey-type* (analytic-type when  $\mathfrak{d} = 1$ ) class

$$\mathcal{K}_\gamma^{\mathfrak{d},q}(Q; C, A, \mathfrak{d}) = \left\{ v \in \mathcal{K}_\gamma^{\infty,q}(Q) : |v|_{\mathcal{K}_\gamma^{s,q}(Q)} \leq CA^s (s!)^\mathfrak{d}, \text{ for all } s \in \mathbb{N}_0 \right\}.$$

The *countably normed, non-homogeneous weighted classes*  $\mathcal{J}_\gamma^{\infty,q}(Q)$  are then defined as in the homogeneous case, while the *non-homogeneous Gevrey/analytic classes* are given by

$$\mathcal{J}_\gamma^{\omega,q}(Q; C, A, \delta) = \left\{ v \in \mathcal{J}_\gamma^{\infty,q}(Q) : |v|_{\mathcal{K}_\gamma^{s,q}(Q)} \leq CA^s (s!)^\delta, \text{ integer } s > \gamma - 3/2 \right\}. \tag{3}$$

We write  $\mathcal{K}_\gamma^{s,2}(Q) = \mathcal{K}_\gamma^s(Q)$  and  $\mathcal{J}_\gamma^{s,2}(Q) = \mathcal{J}_\gamma^s(Q)$ ; similarly we omit the summability exponent  $q$  when it equals 2 in the notation for the weighted Gevrey classes.

### 1.3.3 Model problems

We illustrate the scope of problems by listing several concrete boundary-value and eigenvalue problems whose solutions are known to belong to the weighted analytic classes  $\mathcal{K}_\gamma^\omega(\Omega)$  and  $\mathcal{J}_\gamma^\omega(\Omega)$ . Although the focus here is on three-dimensional problems, we start by considering a polygon  $\Omega \subset \mathbb{R}^2$  with  $n \geq 3$  straight sides and corners  $c_i, i = 1, \dots, n$ . In this setting, the space  $\mathcal{K}_\gamma^\omega(\Omega)$  contains the *corner weight function*  $r_P = \prod_{i=1}^n |x - c_i|$ , i.e., the seminorm (1) is replaced, for  $1 \leq q < \infty$ , by

$$|w|_{\mathcal{K}_\gamma^{s,q}(\Omega)} = \left( \sum_{|\alpha|=s} \|r_P^{|\alpha|-\gamma} \partial^\alpha w\|_{L^q(\Omega)}^q \right)^{1/q}.$$

Then, given an analytic (in  $\overline{\Omega}$ ) external force field  $f$ , the *Stokes equations*

$$-v\Delta u + \nabla p = f \text{ in } \Omega, \quad \nabla \cdot u = 0 \text{ in } \Omega$$

and the viscous, incompressible *Navier-Stokes equations*

$$-v\Delta u + (u \cdot \nabla)u + \nabla p = f \text{ in } \Omega, \quad \nabla \cdot u = 0 \text{ in } \Omega \tag{4}$$

with homogeneous Dirichlet (“no-slip”) boundary conditions have been shown in [31, 59] to admit solutions in  $\mathcal{K}_\gamma^\omega(\Omega)$  with  $\gamma > 3/2$ . Specifically, for the non-linear boundary value problem (4) we require a “small data assumption” which is well-known to ensure uniqueness of Leray-Hopf solutions, see, e.g., [25, Chapter IV, Theorem 2.2]. See Remark 4 for further comments on the implication of the present work on two-dimensional problems.

In the three-dimensional setting, energy minimization problems in quantum physics/chemistry can be transformed into eigenvalue problems whose solutions are in the weighted analytic class (3). We consider here a set of isolated point singularities situated at  $n$  nuclei in positions  $R_i \in \mathbb{R}^3, i = 1, \dots, n$ , and function spaces with weight function  $r$  such that  $r \simeq |x - R_i|$  in the vicinity of each  $R_i$ , and  $r \simeq 1$  far from all singularities resp. all nuclei.

A first example is given by a *nonlinear Schrödinger equation* with polynomial nonlinearity. Consider a compact domain without boundary  $\Omega$  (e.g., a periodic unit cell) and a potential  $V$  such that there exists  $\beta < 2$  and a constant  $A_V > 0$  such that

$$\forall \alpha \in \mathbb{N}_0^3 : \quad \|r^{\beta+|\alpha|} \partial^\alpha V\|_{L^\infty(\Omega)} \leq A_V^{|\alpha|+1} |\alpha|!.$$

Then, the eigenfunction  $u$  corresponding to the smallest eigenvalue (i.e., the “ground state”) of the nonlinear Schrödinger equation

$$-\frac{1}{2}\Delta u + Vu + |u|^2u = \lambda u, \quad \|u\|_{L^2(\Omega)} = 1 \tag{5}$$

is in  $\mathcal{J}_\gamma^\varpi(\Omega)$  for some  $\gamma > 3/2$ , see [56, Section 7.3]. Note that (5) is the Euler-Lagrange equation of the minimization problem

$$\inf \left\{ \int_\Omega |\nabla v|^2 + Vv^2 + \frac{1}{2}v^4, v \in H^1(\Omega), \|v\|_{L^2(\Omega)} = 1 \right\}.$$

As a second example we consider the *Hartree-Fock equation*. Let  $V_C$  be the potential of the Coulomb interaction exerted on electrons by nuclei with charge  $Z_i$  assumed to be pointlike and situated at positions  $R_i \in \mathbb{R}^3, i = 1, \dots, n$ , i.e.,

$$V_C(x) = -\sum_{i=1}^n \frac{Z_i}{|x - R_i|}.$$

The Hartree-Fock model consists in finding the smallest  $N$  eigenvalues  $\varepsilon_i$  and the corresponding  $L^2(\mathbb{R}^3)$ -orthonormal eigenfunctions  $\psi_i, i = 1, \dots, N$ , such that

$$\left(-\frac{1}{2}\Delta + V_C\right)\psi_i + \left(\frac{1}{|x|} \star \rho_\psi\right)\psi_i - \sum_{j=1}^N \left(\frac{1}{|x|} \star (\psi_j\psi_i)\right)\psi_j = \varepsilon_i\psi_i, \quad i = 1, \dots, N \tag{6}$$

with  $\rho_\psi = \sum_{i=1}^N \psi_i^2$ . Then, under some conditions on the potential  $V_C$  so that the solution exists [52], the eigenfunctions are weighted analytic:

$$\psi_i \in \mathcal{J}_\gamma^\varpi(\mathbb{R}^3), \quad i = 1, \dots, N,$$

see [56, Section 7.4]. Problem (6) is the Euler-Lagrange equation of the minimization problem (see [12, Section 9])

$$\inf \left\{ E^{\text{HF}}(\psi_1, \dots, \psi_N), \psi_i \in H^1(\mathbb{R}^3) : \int_{\mathbb{R}^3} \psi_i\psi_j = \delta_{ij} \right\},$$

where

$$E^{\text{HF}}(\psi_1, \dots, \psi_N) = \sum_{i=1}^N \int_{\mathbb{R}^3} |\nabla\psi_i|^2 + \int_{\mathbb{R}^3} V\rho_\psi + \frac{1}{2} \int_{\mathbb{R}^3} \rho_\psi(x) \left(\frac{1}{|x|} \star \rho_\psi\right) - \frac{1}{2} \int_{\mathbb{R}^3} \int_{\mathbb{R}^3} \frac{\tau_\psi(x, y)}{|x - y|},$$

with  $\tau_\psi(x, y) = \sum_{i=1}^N \psi_i(x)\psi_i(y)$ .



*Remark 1 (Near-Singularity)* While functions of the form  $(r \in \mathbb{R}_+, \omega \in \mathbb{S}_2$  spherical coordinates)

$$u_a(r, \omega) = (r^2 + a^2)^{\beta/2} v(\omega), \quad v \text{ analytic in } \mathbb{S}_2 \tag{7}$$

are, for real, nonzero values of  $a$  and for  $\beta > 0$ , formally (mathematically) smooth, their behavior approaches that of functions with point singularities at the origin when  $|a| \ll 1$ . Specifically, if  $|a| \leq a_{\max}$ , there exist positive constants  $C$  and  $A$  independent of  $a$  such that  $u_a \in \mathcal{J}_\gamma^\omega(Q; C, A, 1)$  for  $\gamma < \beta + 3/2$ ; hence, the bounds obtained in the present paper allow for the derivation of rank bounds for the quantized tensor-formatted approximations considered, which are *uniform as the parameter  $a \downarrow 0$*  for functions of the form (7).

The same remark applies to certain *merging point singularities* as arise, for example, in binary star or black hole models. Consider, e.g., two nuclei situated at locations  $R_1 = -\varepsilon e_1, R_2 = \varepsilon e_1$  in  $\mathbb{R}^3$  at distance  $2\varepsilon$  for small  $\varepsilon > 0$ . Denoting by  $r_i = |x - R_i|, i = 1, 2$ , and  $r = |x|$ , we find  $v(x) = r_1^2 + r_2^2 = 2(r^2 + \varepsilon^2)$  i.e., once more a function of the above form with  $a = \varepsilon$ .

### 1.4 Structure of this paper

In Section 2, we review the definitions and notation of quantized, tensor-structured function approximation which are to be employed throughout the remainder of the article, extending the concepts of [66]. In Sections 2.2–2.7, in particular, we introduce the *tensor train* (TT), the *quantized TT format* (QTT), *transposed quantized TT format* (QT3) and the *Tucker quantized TT format* (TQTT), some of which allow to prove better rank bounds on functions with point singularities.

Section 3 introduces tools from numerical analysis which we require in the arguments for the TT rank bounds for function approximation. Section 3.1 introduces in particular the notion of “*uniform background mesh*” (never directly accessed in the QTT formats) which is the basis for all quantized TT function representations. Section 3.2 recapitulates several notions and auxiliary results from the theory of so-called *hp*-approximation from [73, 74, 77]. Section 4 introduces a combined (quasi) interpolation projector, which was introduced in [40] (in two dimensions) and which is crucial in establishing the rank bounds. Section 5 then contains statements and proofs of the main results of the present paper: tensor rank bounds for generic functions in the various countably normed classes introduced in Section 1.3 above. These bounds are obtained for functions with the singularity at a corner of the domain; they are extended to the case of an internal singular point (and to a patchwise formulation that allows for more complex domains) in Appendix B.

Section 6 presents detailed numerical experiments which exhibit actual TT rank bounds in the various formats for model singular functions in three space dimensions. The Section 7 provides a brief summary of the main results, and possible further research directions. Appendix A contains (novel) auxiliary results on exponential rates of convergence of *hp*-approximations for Gevrey-regular functions in  $\mathbb{R}^3$  with point singularities, generalizing [20] to axiparallel geometric meshes of hexahedra with 1-irregular edges and faces.

## 2 Tensor-structured representations

The mathematical issue in tensor-formatted function approximation consists in finding a compressed representation/approximation of three-way tensors

$$A \in \mathbb{R}^{2^\ell \times 2^\ell \times 2^\ell},$$

for  $\ell \in \mathbb{N}$ . All techniques that we examine are based on the *Quantized Tensor Train* (QTT) representation, see, e.g., [38, 40, 42, 64, 66] and the references there. In particular, we will analyze three tensor compressed representations, that we call here (*classic*) *QTT*, *transposed QTT* (QT3), and *Tucker QTT* (TQTT) representation, respectively. The difference between these schemes lies in the arrangement of the three physical dimensions of the tensor  $A$  in the corresponding TT format in the following, after a brief introduction of QTT representations, we detail the three formats mentioned.

### 2.1 Notation

Throughout, we adopt the following notation, from [40]. Given  $n \in \mathbb{N}$  indices  $i_1, \dots, i_n$  such that  $i_j \in \{0, \dots, k_j - 1\}$  for all  $j = 1, \dots, n$ , we write

$$\overline{i_1 \dots i_n} = i_1 \prod_{j=2}^n k_j + i_2 \prod_{j=3}^n k_j + \dots + i_n.$$

In what follows, the term *tensor* will generically denote a multi-dimensional array. Furthermore, for an axiparallel  $d$ -dimensional ( $d \leq 3$ ) subset  $K \in Q$ , the space  $\mathbb{Q}_p(K)$  is the tensor product space of  $d$ -variate polynomials in  $K$  of maximum polynomial degree  $p$  in each variable. Furthermore, we will indicate by a colon “:” a whole slice of a tensor. For example, given a four-dimensional tensor  $A \in \mathbb{R}^{n_1 \times n_2 \times n_3 \times n_4}$  with entries  $a_{i,j,k,l}$ , we will write

$$A_{i,:,:,l} = \{a_{i,j,k,l}\}_{j=1,\dots,n_2,k=1,\dots,n_3} \in \mathbb{R}^{n_2 \times n_3}.$$

### 2.2 Tensor train (TT) format

Tensor Trains (TT) [65], also known as Matrix Product States (MPS) in the computational physics community [72], provide an efficient way to represent high-dimensional tensors, provided these tensors have an underlying low-rank structure. Let  $d \gg 1$ , and consider the  $d$ -dimensional tensor

$$B \in \mathbb{R}^{n_1 \times \dots \times n_d}. \tag{8}$$

The *Tensor Train representation* of the  $d$ -variate tensor  $B$  in (8) is given in terms of the *core tensors*<sup>1</sup>

$$U^k : \{0, \dots, n_k - 1\} \rightarrow \mathbb{R}^{r_{k-1} \times r_k} \quad k = 1, \dots, d,$$

<sup>1</sup>The cores  $U^k$  can be naturally considered as three-dimensional arrays  $\tilde{U}^k \in \mathbb{R}^{r_{i-1} \times n_i \times r_i}$  so that  $(U^k(i_k))_{\alpha_{k-1}, \alpha_k} = \tilde{U}^k_{\alpha_{k-1}, i_k, \alpha_k}$ ,  $\alpha_{k-1} = 1, \dots, r_{k-1}$ ,  $\alpha_k = 1, \dots, r_k$ . Using the three-variate arrays

where  $r_k \in \mathbb{N}$  (with the restriction  $r_0 = r_d = 1$ ) and such that [65, Eq. (1.2)]

$$B_{i_1, \dots, i_d} = U^1(i_1) \cdots U^d(i_d). \tag{10}$$

Suppose for ease of presentation that  $r_i = r$  and  $n_i = n$  for all  $i$ . Then, the TT representation (10) has

$$N_{\text{dof}} = \mathcal{O}(dnr^2)$$

parameters. The TT format is therefore an efficient decomposition if a  $d$ -way tensor can be written as a tensor train with *low ranks*  $r_i$ . Due to the equality in (10) the representation we have introduced is an *exact* TT representation; in practice, a matrix may not admit an exact low-rank TT representation, but a low-rank *approximation* could instead be available.

### 2.3 Rank bound analysis of TT representations

To examine the issue of low-rank approximation of high-dimensional tensors, we require the concept of *unfolding matrices* (“unfoldings” for short), used to derive *rank bounds* on the TT representation of a tensor.

**Definition 1** (Unfolding matrix) Let  $d \in \mathbb{N}$  and  $n_i \in \mathbb{N}$  for  $i = 1, \dots, d$ . Given a tensor  $B \in \mathbb{R}^{n_1 \times \dots \times n_d}$ , we define for all  $q = 1, \dots, d - 1$  its *unfolding matrices*  $B^{(q)} \in \mathbb{R}^{n_1 \cdots n_q \times n_{q+1} \cdots n_d}$  as

$$B^{(q)}_{i_1 \dots i_q, i_{q+1} \dots i_d} = B_{i_1, \dots, i_d}, \quad \text{for all } i_k = 1, \dots, n_k \text{ and } k = 1, \dots, d$$

i.e., the matrix with row index given by the concatenation of the first  $q$  indices, and column index given by the concatenation of the remaining ones.

In the case that the unfolding matrices of a tensor can be approximated by low-rank matrices, then a low-rank TT approximation exists. This is made precise in the following result.

**Proposition 1** [65, Theorem 2.2] Let  $B \in \mathbb{R}^{n_1 \times \dots \times n_d}$  such that its unfolding matrices  $B^{(q)}$  can be decomposed as

$$B^{(q)} = R^q + E^q, \quad \text{rank } R^q = r_q, \quad \|E^q\|_F \leq \varepsilon_q, \quad \text{for all } q = 1, \dots, d - 1.$$

There exists a tensor  $C$  with TT representation (10) and TT ranks  $r_q$  such that

$$\|B - C\|_F^2 \leq \sum_{q=1}^{d-1} \varepsilon_q^2.$$

notation, the TT decomposition of  $B$  can be written as

$$B_{i_1, \dots, i_d} = \sum_{\alpha_0=1}^{r_0} \cdots \sum_{\alpha_d=1}^{r_d} \tilde{U}_{\alpha_0, i_1, \alpha_1}^1 \cdots \tilde{U}_{\alpha_{d-1}, i_d, \alpha_d}^d, \tag{9}$$

which is also used in [65, Eq. (1.3)]. For clarity of presentation, we use the representation (10), which is more compact than (9) (and equivalent to it). We also do not distinguish between the mappings  $U^k$  and the three-dimensional arrays  $\tilde{U}^k$ .

The above theorem includes as a sub-case the rank bound of exact TT representation, by affirming the existence of an exact TT rank  $r_q$  representation of a tensor with unfolding matrix rank bounded by  $r_q, q = 1, \dots, d - 1$ .

### 2.4 Quantized tensor train (QTT) format in one physical dimension

We introduce QTT representations in the simplified setting of QTT approximation of vectors

$$v \in \mathbb{R}^{2^\ell}, \tag{11}$$

for  $\ell \in \mathbb{N}$ . Generalizations to the multi-dimensional case will be the subject of the next sections.

The QTT decomposition introduced in [42, 64] extends the use of the TT approximation to the case of *low-dimensional* tensors with a large number of elements. To do so, the low-dimensional tensor is reshaped into a high-dimensional one, which is subsequently TT-(re)approximated. Applied to the vector in (11), algorithmically this is achieved by reshaping it into the  $\ell$ -dimensional tensor  $\tilde{v}$  such that

$$\tilde{v}_{i_1, \dots, i_\ell} = v_{\overline{i_1 \dots i_\ell}},$$

where  $i_k \in \{0, 1\}$  for all  $k = 1, \dots, \ell$ . The tensor  $\tilde{v}$  can then be represented in TT form. We formalize this representation in the following definition.

**Definition 2** (Univariate QTT decomposition) Given  $\ell \in \mathbb{N}$  and a vector  $v \in \mathbb{R}^{2^\ell}$ ,  $v$  admits a *QTT representation* with QTT ranks  $r_0, \dots, r_\ell$  and QTT cores  $U^i : \{0, 1\} \rightarrow \mathbb{R}^{r_{i-1} \times r_i}$  if

$$v_{\overline{i_1 \dots i_\ell}} = U^1(i_1) \cdots U^\ell(i_\ell), \quad \text{for all } (i_1, \dots, i_\ell) \in \{0, 1\}^\ell.$$

As before, the tensor cores can also be interpreted as three-way arrays in  $\mathbb{R}^{r_{i-1} \times 2 \times r_i}$ .

### 2.5 Classic QTT format in three physical space dimensions

The ‘‘classic QTT’’ format is the straightforward generalization of the univariate QTT format in Definition 2 to the multivariate case.

In this way, a three-dimensional tensor  $A \in \mathbb{R}^{2^\ell \times 2^\ell \times 2^\ell}$  is reshaped into the tensor

$$\tilde{A}^{\text{qtt}} \in \mathbb{R}^{\overbrace{2 \times \dots \times 2}^{3\ell \text{ times}}} \quad \text{such that} \quad \tilde{A}^{\text{qtt}}_{i_1, \dots, i_\ell, j_1, \dots, j_\ell, k_1, \dots, k_\ell} = A_{\overline{i_1 \dots i_\ell, j_1 \dots j_\ell, k_1 \dots k_\ell}} \tag{12}$$

for all  $i_n, j_n, k_n \in \{0, 1\}$ , which is subsequently TT-decomposed.

**Definition 3** (Classic QTT decomposition) Given  $A \in \mathbb{R}^{2^\ell \times 2^\ell \times 2^\ell}$  for an  $\ell \in \mathbb{N}$ , we say that  $A$  admits a *classic QTT decomposition* with ranks  $r_0, \dots, r_{3\ell}$  and cores  $U^1, \dots, U^\ell, V^1, \dots, V^\ell, W^1, \dots, W^\ell$  if

$$A_{\overline{i_1 \dots i_\ell, j_1 \dots j_\ell, k_1 \dots k_\ell}} = U^1(i_1) \cdots U^\ell(i_\ell) V^1(j_1) \cdots V^\ell(j_\ell) W^1(k_1) \cdots W^\ell(k_\ell) \tag{13}$$

for all  $i_n, j_n, k_n \in \{0, 1\}$ , and where

$$\begin{aligned} U^n &: \{0, 1\} \rightarrow \mathbb{R}^{r_{n-1} \times r_n}, & V^n &: \{0, 1\} \rightarrow \mathbb{R}^{r_{\ell+n-1} \times r_{\ell+n}}, \\ W^n &: \{0, 1\} \rightarrow \mathbb{R}^{r_{2\ell+n-1} \times r_{2\ell+n}}, \end{aligned} \tag{14}$$

for  $n = 1, \dots, \ell$ . We have the restriction on the ranks  $r_0 = r_{3\ell} = 1$ .

We denote by  $\mathfrak{T}^{\text{qtt}} : \mathbb{R}^{2^\ell \times 2^\ell \times 2^\ell} \xrightarrow{\text{3}\ell \text{ times}} \mathbb{R}^{2 \times \dots \times 2}$  the ‘‘classic QTT’’ tensorization given by

$$\mathfrak{T}^{\text{qtt}}(A) = \tilde{A}^{\text{qtt}}, \tag{15}$$

with  $\tilde{A}^{\text{qtt}}$  defined in (12).

The (classic) QTT decomposition is symbolically depicted in tensor network format in Fig. 1a.

### 2.6 Transposed order QTT format in three physical space dimensions

In the *transposed order QTT* format (referred to as ‘‘QT3’’ format) introduced first in [40], after reshaping the tensor  $A$  as in (12), the indices from the different (three) physical dimensions are regrouped together, resulting in a tensor

$$\tilde{A}^{\text{qt3}} \in \mathbb{R}^{\overbrace{8 \times \dots \times 8}^{\ell \text{ times}}} \quad \text{such that} \quad \tilde{A}^{\text{qt3}}_{i_1 j_1 k_1, \dots, i_\ell j_\ell k_\ell} = A_{i_1 \dots i_\ell, j_1 \dots, j_\ell, k_1 \dots k_\ell} \tag{16}$$

for all  $i_n, j_n, k_n \in \{0, 1\}$ . The tensor  $\tilde{A}^{\text{qt3}}$  is subsequently *TT-decomposed*, as specified in the next definition.

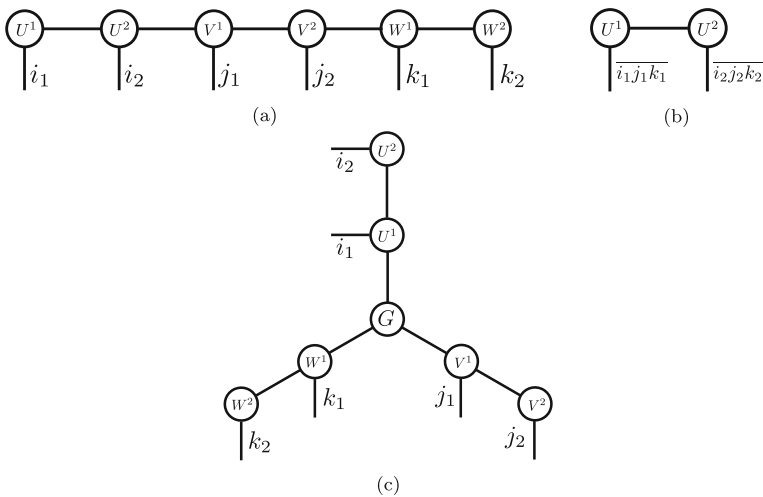


**Fig. 1** Tensor networks for the QTT (a), transposed QTT (QT3) (b), and Tucker QTT (TQTT) representations (c). Each node represents a tensor with edges in the network indicating indices. An edge connecting two nodes is a contracted index (corresponding to tensor multiplication). This can be seen comparing the networks with equations (13), (17), and (20)

**Definition 4** (Transposed order QTT) Let  $\ell \in \mathbb{N}$  and let  $A \in \mathbb{R}^{2^\ell \times 2^\ell \times 2^\ell}$ . The tensor  $A$  admits a transposed QTT decomposition with tensor ranks  $r_0, \dots, r_\ell$  and cores  $U_1, \dots, U_\ell$  if

$$A_{\overline{i_1 \dots i_\ell, j_1 \dots j_\ell, k_1 \dots k_\ell}} = U^1(\overline{i_1 j_1 k_1}) \dots U^\ell(\overline{i_\ell j_\ell k_\ell}), \tag{17}$$

for all  $i_n, j_n, k_n \in \{0, 1\}$ , and where  $U^n : \{0, \dots, 7\} \rightarrow \mathbb{R}^{r_{n-1} \times r_n}$ , for  $n = 1, \dots, \ell$ . We have the restriction on the ranks  $r_0 = r_\ell = 1$ .

We denote by  $\mathfrak{T}^{\text{qt3}} : \mathbb{R}^{2^\ell \times 2^\ell \times 2^\ell} \rightarrow \mathbb{R}^{\overbrace{8 \times \dots \times 8}^{\ell \text{ times}}}$  the ‘‘transposed QTT’’ tensorization given by

$$\mathfrak{T}^{\text{qt3}}(A) = \tilde{A}^{\text{qt3}}, \tag{18}$$

with  $\tilde{A}^{\text{qt3}}$  defined in (16).

A representation of the transposed order QTT decomposition in tensor network format is given in Fig. 1b.

### 2.7 Tucker QTT

The Tucker QTT (TQTT) decomposition is a combination of the Tucker and the QTT decompositions, first considered in [18]. A tensor  $A \in \mathbb{R}^{2^\ell \times 2^\ell \times 2^\ell}$  is represented in the Tucker decomposition if

$$A_{ijk} = \sum_{\beta_1=1}^{R_1} \sum_{\beta_2=1}^{R_2} \sum_{\beta_3=1}^{R_3} G_{\beta_1 \beta_2 \beta_3} U_{\beta_1}(i) V_{\beta_2}(j) W_{\beta_3}(k),$$

where  $R_1, R_2, R_3 \in \mathbb{N}$  are the Tucker ranks, the tensor  $G \in \mathbb{R}^{R_1 \times R_2 \times R_3}$  is the Tucker core and the Tucker factors  $U, V, W$  can be considered as matrices  $U \in \mathbb{R}^{2^\ell \times R_1}$ ,  $V \in \mathbb{R}^{2^\ell \times R_2}$ ,  $W \in \mathbb{R}^{2^\ell \times R_3}$ . In the TQTT decomposition, the factor matrices  $U, V, W$  are given by QTT decompositions, where, e.g., for  $U$ , only one of the QTT cores depends on the corresponding column number  $\beta_1$ :

$$\begin{aligned} U_{\beta_1}(i) &= U_{\beta_1}^1(i_1)U^2(i_2) \dots U^\ell(i_\ell), & i &= \overline{i_1 \dots i_\ell}, \\ V_{\beta_2}(j) &= V_{\beta_2}^1(j_1)V^2(j_2) \dots V^\ell(j_\ell), & j &= \overline{j_1 \dots j_\ell}, \\ W_{\beta_3}(k) &= W_{\beta_3}^1(k_1)W^2(k_2) \dots W^\ell(k_\ell), & k &= \overline{k_1 \dots k_\ell}. \end{aligned} \tag{19}$$

We denote the QTT ranks of  $U, V, W$  as  $\{r_0, r_1, \dots, r_\ell\}$ ,  $\{s_0, s_1, \dots, s_\ell\}$  and  $\{t_0, t_1, \dots, t_\ell\}$  with the constraints  $r_0 = R_1, s_0 = R_2, t_0 = R_3$  and  $r_\ell = s_\ell = t_\ell = 1$ .

**Definition 5** (Tucker QTT (TQTT) representation) Let  $\ell \in \mathbb{N}$  and let  $A \in \mathbb{R}^{2^\ell \times 2^\ell \times 2^\ell}$ .  $A$  admits a Tucker QTT decomposition with Tucker ranks  $R_1, R_2, R_3$  and QTT ranks  $r_0, r_1, \dots, r_\ell, s_0, \dots, s_\ell, t_0, \dots, t_\ell$  if there exist a Tucker core  $G \in \mathbb{R}^{R_1 \times R_2 \times R_3}$  and

QTT cores  $U^1, \dots, U^\ell, V^1, \dots, V^\ell, W^1, \dots, W^\ell$  defined as in (19) such that

$$\begin{aligned}
 & A_{\overline{i_1 \dots i_\ell, j_1 \dots, j_\ell, k_1 \dots k_\ell}} \\
 &= \sum_{\substack{R_1, R_2, R_3 \\ \beta_1, \beta_2, \beta_3=1}} G_{\beta_1, \beta_2, \beta_3} U_{\beta_1}^1(i_1) U^2(i_2) \dots U^\ell(i_\ell) \\
 & \quad V_{\beta_2}^1(j_1) V^2(j_2) \dots V^\ell(j_\ell) W_{\beta_3}^1(k_1) W^2(k_2) \dots W^\ell(k_\ell).
 \end{aligned} \tag{20}$$

### 2.8 Degrees of freedom

Supposing for ease of notation that  $r_n = r_{\text{qtt}}$  for the classic QTT representation,  $r_n = r_{\text{qt3}}$  for the transposed one, and  $r_n = s_n = t_n = r_{\text{tqtt}}$  and  $R_1 = R_2 = R_3 = R$  for Tucker QTT, the number  $N_{\text{dof}}$  of parameters in the QTT representations is bounded as

$$N_{\text{dof}} = \begin{cases} 2((3\ell - 2)r_{\text{qtt}}^2 + 2r_{\text{qtt}}) = \mathcal{O}(\ell r_{\text{qtt}}^2) & \text{classic QTT} \\ 8((\ell - 2)r_{\text{qt3}}^2 + 2r_{\text{qt3}}) = \mathcal{O}(\ell r_{\text{qt3}}^2) & \text{transposed QTT} \\ R^3 + 6((\ell - 2)r_{\text{tqtt}}^2 + (R + 1)r_{\text{tqtt}}) = \mathcal{O}(R^3 + \ell r_{\text{tqtt}}^2 + Rr_{\text{tqtt}}) & \text{Tucker QTT.} \end{cases} \tag{21}$$

### 3 Functional setting

Our analysis will require the introduction of two different meshes and of two respective finite element spaces in the cube  $Q$ . The first one is a *uniform tensor product mesh* with distance between nodes given by  $h_\ell = 2^{-\ell}$ . This mesh contains  $2^\ell$  nodes in every physical direction; given a function  $f$  defined over  $Q$ , the point values of  $f$  at the mesh points can be grouped in a three-dimensional tensor of dimension  $2^\ell \times 2^\ell \times 2^\ell$ , which can be QTT-approximated in the formats introduced in the previous section. Note that, in practice, one does not need to compute the values of the function at all  $2^{3\ell}$  mesh points, see, e.g., [63], as this would undermine the efficiency of tensor compressed methods. For this reason, the background mesh is also referred to as “virtual” mesh in the literature, see for example [38–40, 68].

Furthermore, tensor-formatted closed forms of some discrete differential operators exist, see, e.g., [37, 42, 44]. This can be used to discretize certain partial differential equations in quantized tensor format, as it will be shown in the sequel. The space of (tensor-formatted) functions on the uniform mesh is the space of  $\mathbb{Q}_1$  finite elements, i.e., the tensor product of one-dimensional Lagrange functions associated with mesh nodes.

The second finite dimensional space we introduce is the *auxiliary hp space*. This space is introduced here only for proving tensor rank bounds of the QTT-structured approximation. It is never accessed during numerical computation in the tensor formats. The *hp* space is, in particular, an  $H^1$ -conforming finite element space, on a mesh with elements geometrically refined towards the origin. The polynomial degree of functions in the *hp* space is, instead, increasing polynomially with the number of geometric mesh layers. This is made more precise in Section 3.2 below. The role of

the auxiliary  $hp$  finite element approximation is to provide an *exponentially convergent, continuous and piecewise polynomial approximation* on a *bisection geometric partition which is compatible with the background mesh in the  $\mathbb{Q}_1$ -approximation* for generic functions in the weighted Sobolev space  $\mathcal{J}_\gamma^\omega(Q)$ .

A function in  $v \in \mathcal{J}_\gamma^\omega(\Omega)$  can then be approximated—with exponential accuracy—by its projection  $v_{hp}$  into the  $hp$  space. By re-interpolating  $v_{hp}$  on the background mesh and QTT-compressing the resulting tensor, we establish existence of quantized, tensor-structured approximations with polylogarithmic bounds on the QTT ranks and the number of QTT parameters. The quasi-interpolation operator from  $v$  to its representation on the background mesh is introduced in Section 3.3.

For simplicity, we will consider here functions that have zero trace on the part of the boundary not abutting at the origin, i.e., on

$$\Gamma = \{(x_1, x_2, x_3) \in \partial Q : x_1 x_2 x_3 \neq 0\} .$$

We denote by  $H_\Gamma^1(Q)$  the subspace of  $H^1(Q)$  functions with zero trace on  $\Gamma$ . We then fix  $\gamma \in \mathbb{R}$  such that  $\gamma - 3/2 \in (0, 1)$ , two constants  $C_X, A_X > 0$ , and a regularity exponent  $\mathfrak{d} \geq 1$  and denote by

$$X = \mathcal{J}_\gamma^\omega(Q; C_X, A_X, \mathfrak{d}) \cap H_\Gamma^1(Q)$$

the weighted space of Gevrey- $\mathfrak{d}$ -regular functions with zero trace on  $\Gamma$  that will be considered henceforth.

### 3.1 Low order background FE space $X^\ell$

We introduce the so-called “background” (sometimes also referred to as “virtual”) FE space discussed above. Here, it will consist of the space of continuous, piecewise trilinear functions on a uniform mesh of axiparallel hexahedral elements of size  $2^{-\ell}$  (so-called  $\mathbb{Q}_1$ -FEM), which we now introduce.

#### 3.1.1 Uniform background mesh $\mathcal{T}^\ell$

In  $Q = (0, 1)^3$ , we introduce the uniform mesh  $\mathcal{T}^\ell$  with nodes  $x_{i,j,k} \in 2^{-\ell}\mathbb{N}_0^3 \cap \bar{Q}$ , for  $(i, j, k) \in \{0, \dots, 2^\ell\}^3$ . For a refinement level  $\ell \in \mathbb{N}$ , we write  $I_j^\ell = (2^{-\ell}j, 2^{-\ell}(j + 1))$ ,  $j = 0, \dots, 2^\ell - 1$ . Then,  $\mathcal{T}^\ell = \{I_i^\ell \times I_j^\ell \times I_k^\ell : i, j, k = 0, \dots, 2^\ell - 1\}$ .

#### 3.1.2 Background finite element space

For  $(i, j, k) \in \{0, \dots, 2^\ell - 1\}^3$ , we denote by  $\varphi_{i,j,k}$  the locally trilinear, continuous nodal Lagrange functions which satisfy

$$\varphi_{i,j,k}(x_{m,n,p}) = \delta_{im}\delta_{jn}\delta_{kp}, \quad (i, j, k) \in \{0, \dots, 2^\ell - 1\}^3, (m, n, p) \in \{0, \dots, 2^\ell\}^3,$$

where  $\delta_{im}$  denotes the Kronecker delta symbol for indices  $i$  and  $m$ .

The space of continuous, locally trilinear Lagrange functions on the (background) mesh  $\mathcal{T}^\ell$  is

$$X^\ell = \text{span}\{\varphi_{i,j,k} : (i, j, k) \in \{0, \dots, 2^\ell - 1\}^3\}.$$



Note that the basis functions  $\varphi_{i,j,k}$  and the space  $X^\ell$  are algebraic tensor products of the corresponding univariate functions, resp. spaces. We remark that for every  $v \in X^\ell$  holds  $v|_\Gamma = 0$ .

*Remark 2*  $X^\ell$  contains functions that vanish on  $\Gamma$ . We limit ourselves to this case for simplicity of notation; the extension of our analysis to functions with nonzero trace on  $\Gamma$  involves additional technicalities. We refer to [40] for the two-dimensional case.

### 3.1.3 Lagrange interpolation operator $\mathcal{I}^\ell$

We denote by  $\mathcal{I}^\ell$  the Lagrange interpolation operator on the uniform tensor mesh  $\mathcal{T}^\ell$ . I.e.,  $\mathcal{I}^\ell : C(\bar{Q}) \rightarrow X^\ell$  is defined as

$$(\mathcal{I}^\ell v)(x) = \sum_{(i,j,k) \in \{0, \dots, 2^\ell - 1\}^3} v(x_{i,j,k}) \varphi_{i,j,k}(x), \quad x \in \bar{Q}.$$

### 3.1.4 Analysis and synthesis operators

For  $\ell \in \mathbb{N}$ ,  $\mathcal{A}^\ell : X^\ell \rightarrow \mathbb{R}^{2^\ell \times 2^\ell \times 2^\ell}$  and  $\mathcal{S}^\ell : \mathbb{R}^{2^\ell \times 2^\ell \times 2^\ell} \rightarrow X^\ell$  are the analysis and synthesis operators, such that

$$(\mathcal{A}^\ell v)_{i,j,k} = v^\ell(x_{i,j,k}), \quad (\mathcal{S}^\ell v)(x) = \sum_{i,j,k=0}^{2^\ell-1} v_{i,j,k} \varphi_{i,j,k}(x). \quad (22)$$

## 3.2 Auxiliary *hp* space

We obtain the QTT rank bounds on TT-formatted approximations by comparison with *hp*-approximations. To this end, we introduce the *hp*-FE spaces. We start with *l-irregular meshes of axiparallel hexahedra* with geometric refinement towards the singularity of the function of interest (“geometric meshes” for short).

### 3.2.1 Geometric mesh

Let  $\ell \in \mathbb{N}$ . For  $i = 0, \dots, \ell$ , let

$$J_{1,i}^\ell = (2^{i-\ell-1}, 2^{i-\ell}) \quad \text{and} \quad J_{0,i}^\ell = (0, 2^{i-\ell}).$$

Then, for  $k \in \{0, \dots, \ell\}$  and  $a, b, c \in \{0, 1\}$ , define the non-overlapping cubes

$$K_{abc,k}^\ell = J_{a,k}^\ell \times J_{b,k}^\ell \times J_{c,k}^\ell$$

see Fig. 2.

Denoting  $\mathcal{N} = \{001, \dots, 111\}$ , the auxiliary geometric mesh is given by

$$\mathcal{G}^\ell = \{K_{n,k}^\ell, k \in \{1, \dots, \ell\}, n \in \mathcal{N}\} \cup K_{000,0}^\ell.$$

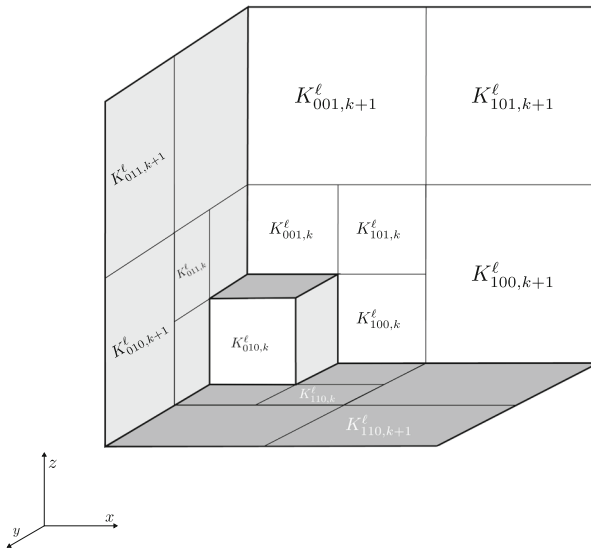


**Fig. 2** Elements  $K_{n,j}^{\ell}$ , for fixed  $\ell$ , for  $j = k, k + 1$ , and for  $n \in \{001, \dots, 110\}$ . Element  $K_{111}$  not visible in this projection

Element  $K_{000,0}^{\ell}$  has one vertex coinciding with the origin. We collect all elements at the same refinement level in *mesh layers*

$$\mathcal{L}_0^{\ell} = \{K_{000,0}\}, \quad \mathcal{L}_j^{\ell} = \{K_{n,j}, n \in \mathcal{N}\} \text{ for } j = 1, \dots, \ell. \quad (23)$$

We also introduce the one- and two-dimensional versions of the geometric mesh as

$$\mathcal{G}_{2d}^{\ell} = \{K_{n,k}^{\ell}, k \in \{1, \dots, \ell\}, n \in \{01, 10, 11\}\} \cup K_{00,0}^{\ell},$$

where  $K_{ab,k}^{\ell} = J_{a,k}^{\ell} \times J_{b,k}^{\ell}$ , and

$$\mathcal{G}_{1d}^{\ell} = \{J_{1,k}^{\ell}, k \in \{1, \dots, \ell\}\} \cup J_{0,0}^{\ell}. \quad (24)$$

see Fig. 3.

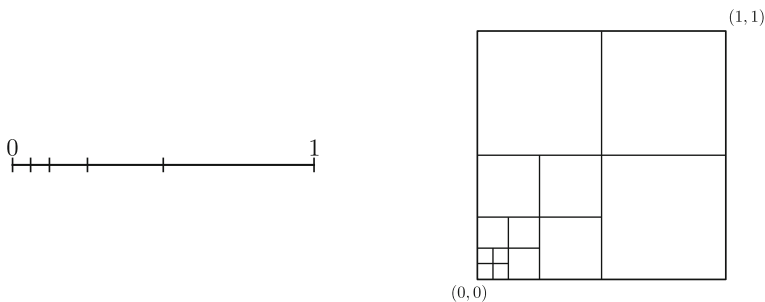


**Fig. 3** Univariate geometric mesh  $\mathcal{G}_{1d}^{\ell}$  (left) and bivariate geometric mesh  $\mathcal{G}_{2d}^{\ell}$  (right) with subdivision ratio 1/2

We remark that for  $q \in \mathbb{N}, k = 1, \dots, 2^q - 1, j = 1, \dots, q - 1$ , and for all integer  $\ell > q$

$$I_k^q \subset J_{1, \lfloor \log_2 k \rfloor + 1}^q \quad J_{1, j}^q = J_{1, \ell - q + j}^\ell.$$

Furthermore, for  $p = 1, \dots, q - 1$  and all  $m = p + 1, \dots, q - 1$ , there holds

$$J_{1, p}^q \subset J_{0, m}^q.$$

### 3.2.2 $hp$ space

The  $hp$  space is formally introduced as

$$X_{hp}^{\ell, p} = \{v \in H^1(Q) : v|_{K_{n, j}^\ell} \in \mathbb{Q}_p(K_{n, j}^\ell), \text{ for all } n \in \mathcal{N}, j = 1, \dots, \ell \text{ and } n = 000, j = 0\}. \quad (25)$$

Note that, as a consequence of the existence of a continuous  $hp$  approximation to functions in  $\mathcal{J}_\gamma^\infty(Q)$  proved in Appendix A and in [73], the space  $X_{hp}^{\ell, p}$  is well defined by (25).

### 3.2.3 $hp$ approximation

We provide a brief presentation of (novel)  $hp$ -interpolation error bounds which are exponential in the number of degree of freedom for functions in the Gevrey-type classes  $\mathcal{K}_\gamma^{\varpi, q}(Q; C, A, \vartheta), \mathcal{J}_\gamma^{\varpi, q}(Q; C, A, \vartheta)$  defined in Section 1.3.2. We consider here *axiparallel, geometric partitions* of  $Q = (0, 1)^3$  into hexahedral elements; this entails, of course, irregular nodes and faces so that  $hp$ -interpolants are to be constructed in a two-stage process: first, an elementwise  $hp$ -(quasi)interpolant with analytic error bounds and second, *polynomial face jump liftings* which preserve the analytic bounds. We refer to the Appendix and to, e.g., [73] for details on this.

In the analytic case, i.e., when  $\vartheta = 1$  such exponential error bounds are well-known (e.g., [73]). However, for  $\vartheta > 1$ , these bounds are novel; for regular geometric meshes of tetrahedra, corresponding bounds have recently been established in [20].

We introduce in Appendix A the projector  $\Pi_{hp}^{\ell, p} : \mathcal{J}_\gamma^\infty(Q) \rightarrow X_{hp}^{\ell, p}$ , defined for  $\gamma > 3/2$ . We recall here that given a function  $v \in \mathcal{J}_\gamma^\infty(Q)$ , for  $\gamma > 3/2$ , then  $\Pi_{hp}^{\ell, p} v \in H^1(Q) \cap C(\bar{Q})$ , i.e., the projector is *conforming* in  $H^1(Q)$ . Furthermore for all  $u \in \mathcal{J}_\gamma^\varpi(Q; C, A, \vartheta)$ , with  $\gamma > 3/2$ , there exist  $p \simeq \ell^\vartheta$ , and positive  $C_{hp}, b_{hp}$  (depending on  $C, A, \vartheta$ ) such that for every  $\ell \in \mathbb{N}$  holds

$$\|u - \Pi_{hp}^{\ell, p} u\|_{H^1(Q)} \leq C_{hp} \exp(-b_{hp} \ell), \quad (26)$$

and  $\dim(X_{hp}^{\ell, p}) \simeq \ell p^3 \simeq \ell^{3\vartheta+1}$ , see Proposition 3 in Appendix A.

### 3.3 Quasi interpolation operator $\mathfrak{P}^\ell$

We recall that

$$X = \left\{ v \in \mathcal{J}_\gamma^\varpi(Q; C_X, A_X, \vartheta) : v|_\Gamma = 0 \right\},$$

where  $\Gamma = \{(x_1, x_2, x_3) \in \partial Q : x_1 x_2 x_3 \neq 0\}$  and for  $\gamma > 3/2$ , positive constants  $C_X$  and  $A_X$ , and Gevrey exponent  $\vartheta \geq 1$ . We also fix  $p \simeq \ell^\vartheta$  such that (26) holds and define the quasi-interpolation operator  $\mathfrak{P}^\ell : X \rightarrow X^\ell$  as

$$\mathfrak{P}^\ell u = \mathcal{I}^\ell \Pi_{\text{hp}}^{\ell,p} u. \tag{27}$$

### 4 Quasi interpolation error

We give here (specifically, in Proposition 2) an estimate on the error introduced by the quasi-interpolation operator  $\mathfrak{P}^\ell$  defined in Section 3.3. We start by estimating, in the following lemma, the error introduced by interpolating the  $hp$  projection of a function in  $X$ .

**Lemma 1** *Let  $\ell \in \mathbb{N}$ ,  $u \in X$ ,  $\mathcal{I}^\ell : C(\bar{Q}) \rightarrow X^\ell$  and  $\Pi_{\text{hp}}^{\ell,p} : X \rightarrow X_{\text{hp}}^{\ell,p}$  defined in Sections 3.1.3 and 3.2.3, respectively. Then there exist constants  $C, b_{\mathcal{I}} > 0$  such that*

$$\| (\text{Id} - \mathcal{I}^\ell) \Pi_{\text{hp}}^{\ell,p} u \|_{H^1(Q)} \leq C \exp(-b_{\mathcal{I}} \ell).$$

*Proof* There holds

$$\| (\text{Id} - \mathcal{I}^\ell) \Pi_{\text{hp}}^{\ell,p} u \|_{H^1(Q)}^2 = \sum_{j=0}^{\ell} \sum_{K \in \mathcal{L}_j^\ell} \| (\text{Id} - \mathcal{I}^\ell) \Pi_{\text{hp}}^{\ell,p} u \|_{H^1(K)}^2, \tag{28}$$

where the mesh layers  $\mathcal{L}_j^\ell$  are defined in (23). The quantity on the right-hand side of this equation is an upper bound for the error of interpolation over a uniform mesh of axiparallel cubes of edge length  $2^{-\ell}$ . The axiparallel cubes  $K_{n,j}^\ell$  are affine equivalent to the reference element  $\widehat{K} = (-1, 1)^3$ . Furthermore, since  $u \in X$ , by Remark 8 in the Appendix there holds  $(\Pi_{\text{hp}}^{\ell,p} u)|_\Gamma = 0$ . Hence there exists  $C > 0$  such that, for all  $(n, j) \in \mathcal{N} \times \{1, \dots, \ell\} \cup (000, 0)$  and for all  $\ell$

$$\| (\text{Id} - \mathcal{I}^\ell) \Pi_{\text{hp}}^{\ell,p} u \|_{H^1(K_{n,j}^\ell)} \leq C 2^{-\ell} | \Pi_{\text{hp}}^{\ell,p} u |_{H^2(K_{n,j}^\ell)}.$$

By the polynomial inverse inequality

$$|v|_{H^2(K)} \leq C \frac{p^2}{h_K} |v|_{H^1(K)},$$

where  $v$  is a polynomial of degree  $p$  and  $h_K$  is the diameter of  $K$  (see, e.g., [24, 77]), recalling that an element  $K_{n,j}^\ell \in \mathcal{L}_j^\ell$  is an axiparallel cube with diameter  $h_j \simeq 2^{-\ell+j}$ ) and using a triangle inequality, there exists a constant  $C > 0$  independent of  $\ell$  and of

$p$  such that

$$\begin{aligned} 2^{-\ell} |\Pi_{\text{hp}}^{\ell,p} u|_{H^2(K_{n,j}^\ell)} &\leq C 2^{-\ell} h_j^{-1} p^2 |\Pi_{\text{hp}}^{\ell,p} u|_{H^1(K_{n,j}^\ell)} \\ &\leq C 2^{-j} p^2 |\Pi_{\text{hp}}^{\ell,p} u|_{H^1(K_{n,j}^\ell)} \\ &\leq C 2^{-j} p^2 \left( |u|_{H^1(K_{n,j}^\ell)} + |u - \Pi_{\text{hp}}^{\ell,p} u|_{H^1(K_{n,j}^\ell)} \right). \end{aligned}$$

Since  $\gamma > 1$ , there exists a uniform constant  $C$  such that, on each  $K_{n,j}^\ell$ ,

$$2^{(\ell-j)(\gamma-1)} \leq Cr_{K_{n,j}^\ell}^{1-\gamma}.$$

From this last inequality and (2)

$$2^{-j} |u|_{H^1(K_{n,j}^\ell)} \leq C 2^{-\ell(\gamma-1)-j(2-\gamma)} \|u\|_{\mathcal{J}_\gamma^1(K_{n,j}^\ell)}. \tag{29}$$

Combining (28) to (29), there exists a constant  $C > 0$  such that for all  $\ell$  holds

$$\begin{aligned} &\| (\text{Id} - \mathcal{I}^\ell) \Pi_{\text{hp}}^{\ell,p} u \|_{H^1(Q)}^2 \\ &\leq C \sum_{j=0}^{\ell} \sum_{K \in \mathcal{L}_j^\ell} 2^{-2j} p^4 \left( |u|_{H^1(K)} + |u - \Pi_{\text{hp}}^{\ell,p} u|_{H^1(K)} \right)^2 \\ &\leq Cp^4 \left( \sum_{j=0}^{\ell} \sum_{K \in \mathcal{L}_j^\ell} 2^{-2\ell(\gamma-1)-2j(2-\gamma)} \|u\|_{\mathcal{J}_\gamma^1(K)}^2 + |u - \Pi_{\text{hp}}^{\ell,p} u|_{H^1(Q)}^2 \right). \end{aligned}$$

Then, by (26) and since  $p \simeq \ell^\delta$ ,

$$\| (\text{Id} - \mathcal{I}^\ell) \Pi_{\text{hp}}^{\ell,p} u \|_{H^1(Q)}^2 \leq C \ell^{4\delta} \left( 2^{-2\ell \min(\gamma-1, 1)} \|u\|_{\mathcal{J}_\gamma^1(Q)}^2 + C_{\text{hp}}^2 e^{-2b_{\text{hp}}\ell} \right).$$

Absorbing the terms algebraic in  $\ell$  into the exponential by a change of constant concludes the proof. □

**Proposition 2** *Let  $0 < \varepsilon_0 < 1$  and  $u \in X$ . Then for all  $0 < \varepsilon \leq \varepsilon_0$  there exists  $\ell \in \mathbb{N}$  such that*

$$\|u - \mathfrak{P}^\ell u\|_{H^1(Q)} \leq \varepsilon,$$

where  $\mathfrak{P}^\ell u \in X^\ell$  is defined in (27) and there exists  $C > 0$  independent of  $\varepsilon$  such that

$$\ell \leq C \lceil \log \varepsilon \rceil.$$

*Proof* By a triangle inequality, Lemma 1, and Proposition 3 (recalled above in (26)),

$$\|u - \mathfrak{P}^\ell u\|_{H^1(Q)} \leq \|u - \Pi_{\text{hp}}^{\ell,p} u\|_{H^1(Q)} + \|(\text{Id} - \mathcal{I}^\ell) \Pi_{\text{hp}}^{\ell,p} u\|_{H^1(Q)} \leq C \exp(-b\ell),$$

where  $C$  and  $b$  are independent of  $\ell$ . The choice  $\ell = \lceil b^{-1} \log(\frac{C}{\varepsilon}) \rceil$  and adjusting the value of  $C$  concludes the proof. □

### 5 QTT-formatted approximation of $u \in \mathcal{J}_\gamma^w(Q)$

We now state and prove our main results. For Gevrey-regular functions in  $Q = (0, 1)^3$  with point singularity at the origin, and for each of the three tensor formats (QTT, QT3, TQTT), we prove bounds on the ranks which are sufficient to achieve a prescribed approximation accuracy  $\varepsilon \in (0, 1)$  in the norm  $H^1(Q)$ . This is the relevant norm for linear, second order, elliptic PDEs.

#### 5.1 Tensor rank bounds for QTT approximation

**Lemma 2** *Let  $0 < \varepsilon_0 < 1$  and  $u \in X$ . Then, for all  $0 < \varepsilon \leq \varepsilon_0$  there exist  $\ell \in \mathbb{N}$  and  $v_{\text{qtt}}^\ell = \mathfrak{P}^\ell u$  such that  $\|u - v_{\text{qtt}}^\ell\|_{H^1(Q)} \leq \varepsilon$  and  $v_{\text{qtt}}^\ell$  admits a QTT-formatted representation with*

$$N_{\text{dof}} \leq C |\log \varepsilon|^{4\mathfrak{d}+3}$$

degrees of freedom, for  $C > 0$  independent of  $\varepsilon$ .

*Proof* We consider the unfolding matrices  $V^{(q)}$  of  $\mathfrak{T}^{\text{qtt}}(\mathcal{A}^\ell(v_{\text{qtt}}^\ell))$ , with  $\mathfrak{T}^{\text{qtt}}$  defined in (15) and  $\mathcal{A}^\ell$  in (22). We first consider the case  $q \in \{1, \dots, \ell - 1\}$ . In this case,

$$V_{\xi_1, \xi_2 \eta \zeta}^{(q)} = v_{\text{qtt}}^\ell(x_{\xi_1 \xi_2, \eta, \zeta}^\ell),$$

for  $\xi_1 = 0, \dots, 2^q - 1, \xi_2 = 0, \dots, 2^{\ell-q} - 1$ , and for  $\eta, \zeta = 0, \dots, 2^\ell - 1$ . Now, introduce the reference line  $S_1$  as  $S_1 = (0, 1) \times \{0\} \times \{0\}$ . For each element  $K \in \mathcal{G}_{1\text{d}}^q$ , we denote its left and right endpoints as  $y_0^K$  and  $y_1^K$ , so that  $(y_0^K, y_1^K) = K$ . On  $S_1$ , we introduce a geometric mesh

$$\mathcal{G}_{S_1}^q = \{K \times \{0\} \times \{0\}, K \in \mathcal{G}_{1\text{d}}^q\},$$

and the univariate discontinuous FE space

$$X_{S_1}^q = \left\{ v \in L^\infty(S_1) : v|_K \in \mathbb{Q}_p(K) \text{ for all } K \in \mathcal{G}_{S_1}^q \right. \\ \left. \text{and } v \text{ is right continuous at the nodes of } \mathcal{G}_{1\text{d}}^q \right\}.$$

We require the function to be right continuous at its discontinuity points, i.e., for any two neighboring intervals  $K_\sharp$  and  $K_b$  with  $y_0^{K_b} < y_1^{K_b} = y_0^{K_\sharp} < y_1^{K_\sharp}$  and a function  $v \in X_{S_1}^q$  such that

$$v = \begin{cases} v_b & \text{in } K_b \\ v_\sharp & \text{in } K_\sharp, \end{cases}$$

we have  $v(y_1^{K_b}) = v(y_0^{K_\sharp}) = v_\sharp(y_0^{K_\sharp})$ . We also consider the affine transformation

$$\varphi_{ijk}^{-1} : (x_1, x_2, x_3) \mapsto (x_1 + 2^{-\ell}i, x_2 + 2^{-\ell}j, x_3 + 2^{-\ell}k),$$

so that, for all  $\xi_1 = 0, \dots, 2^q - 1, \xi_2 = 0, \dots, 2^{\ell-q} - 1$ , and  $\eta, \zeta = 0, \dots, 2^\ell - 1$ ,

$$\varphi_{\xi_2 \eta \zeta}^{-1}(x_{\xi_1 \xi_2, \eta, \zeta}^\ell) = (2^{-q}\xi_1, 0, 0).$$

Now, for all  $\xi_1 \in \{0, \dots, 2^q - 1\}$ ,

$$x_{\overline{\xi_1 \xi_2, \eta, \zeta}} \in \varphi_{\overline{\xi_2 \eta \zeta}}(S_1) = \overline{I_{\xi_1}^q} \times \{2^{-\ell} \eta\} \times \{2^{-\ell} \zeta\}.$$

Then, for each  $\xi_2 \in \{0, \dots, 2^{\ell-q} - 1\}$  and for each  $\eta, \zeta \in \{0, \dots, 2^\ell - 1\}$  there exists a piecewise polynomial  $p_{\overline{\xi_2 \eta \zeta}} \in X_{S_1}^q$  such that

$$\begin{aligned} v_{\text{qtt}}^\ell \left( x_{\overline{\xi_1 \xi_2, \eta, \zeta}} \right) &= \left( v_{\text{qtt}}^\ell \circ \varphi_{\overline{\xi_2 \eta \zeta}} \right) \left( \varphi_{\overline{\xi_2 \eta \zeta}}^{-1} \left( x_{\overline{\xi_1 \xi_2, \eta, \zeta}} \right) \right) \\ &= \left( v_{\text{qtt}}^\ell \circ \varphi_{\overline{\xi_2 \eta \zeta}} \right) \left( (2^{-q} \xi_1, 0, 0) \right) \\ &= p_{\overline{\xi_2 \eta \zeta}} \left( (2^{-q} \xi_1, 0, 0) \right) \end{aligned}$$

for all  $\xi_1 = 0, \dots, 2^q - 1$ . The piecewise polynomial  $p_{\overline{\xi_2 \eta \zeta}}$  is constructed as follows. For each  $K = (y_0^K, y_1^K) \in \mathcal{G}_{\text{id}}^q \setminus (0, 2^{-q})$  the function  $v_{\text{qtt}}^\ell \circ \varphi_{\overline{\xi_2 \eta \zeta}}$  is a polynomial of degree  $p$  with the first variable in the interval  $(y_0^K - 2^{-\ell \xi_2}, y_1^K - 2^{-\ell \xi_2})$ , therefore, *a fortiori*, denoting  $\tilde{J}^K = (y_0^K, y_1^K - 2^{-\ell \xi_2})$

$$v_{\text{qtt}}^\ell \circ \varphi_{\overline{\xi_2 \eta \zeta}} \in \mathbb{Q}_p(\tilde{J}^K \times \{0\} \times \{0\}).$$

Hence, by extension, there exists a polynomial  $p_{\overline{\xi_2 \eta \zeta}}^K$  such that  $p_{\overline{\xi_2 \eta \zeta}}^K \in \mathbb{Q}_p(K \times \{0\} \times \{0\})$  and

$$p_{\overline{\xi_2 \eta \zeta}}^K = v_{\text{qtt}}^\ell \circ \varphi_{\overline{\xi_2 \eta \zeta}} \text{ in } \tilde{J}^K \times \{0\} \times \{0\}.$$

When  $K = (0, 2^{-q})$ , we let  $p_{\overline{\xi_2 \eta \zeta}}^K$  be any polynomial of degree  $p$  satisfying  $p_{\overline{\xi_2 \eta \zeta}}^K(0, 0, 0) = (v_{\text{qtt}}^\ell \circ \varphi_{\overline{\xi_2 \eta \zeta}})(0, 0, 0)$ . Finally,  $p_{\overline{\xi_2 \eta \zeta}} \in X_{S_1}^q$  is defined piecewise as  $p_{\overline{\xi_2 \eta \zeta}}^K$  in each element. Note that the property of right-continuity is crucial for the exactness of the piecewise polynomial at mesh nodes.

Remarking that there exists a constant  $C > 0$  such that for every  $p, q$  holds  $\dim(X_{S_1}^\ell) \leq Cqp$  and taking a basis  $\{e_n\}_n$  of  $X_{S_1}^\ell$ , we can write

$$V^{(q)} = BW,$$

where  $B_{\xi_1, n} = e_n((2^{-q} \xi_1, 0, 0))$ , for  $n = 1, \dots, \dim(X_{S_1}^\ell)$  and  $\xi_1$  as above, and  $W$  is a  $\dim(X_{S_1}^\ell) \times 2^{3\ell-q}$  matrix of coefficients. Hence, there exists  $\tilde{C} > 0$  such that for all  $q = 1, \dots, \ell$  it holds

$$r_q = \text{rank}(V^{(q)}) \leq \dim(X_{S_1}^\ell) \leq \tilde{C} \ell^{d+1}.$$

We now consider the case where  $\ell < q < 2\ell$  and denote  $\tilde{q} = q - \ell$ . Then,

$$V_{\overline{\xi \eta_1, \eta_2 \zeta}}^{(q)} = v_{\text{qtt}}^\ell(x_{\overline{\xi, \eta_1 \eta_2, \zeta}}),$$

for  $\xi, \zeta = 0, \dots, 2^\ell - 1, \eta_1 = 0, \dots, 2^{\tilde{q}} - 1$ , and  $\eta_2 = 0, \dots, 2^{\ell-\tilde{q}} - 1$ . We introduce the two-dimensional slice

$$S_2^{\tilde{q}} = \{0\} \times (0, 2^{-\tilde{q}}) \times (0, 1),$$

with associated mesh

$$\mathcal{G}_{S_2^{\tilde{q}}}^{\tilde{q}} = \{\{0\} \times K \text{ for all } K \in \mathcal{G}_{2d}^\ell \text{ such that } K \subset (0, 2^{-\tilde{q}}) \times (0, 1)\},$$

and the corresponding FE space

$$X_{S_2^{\tilde{q}}} = \{v \in H^1(S_2^{\tilde{q}}) : v|_K \in \mathbb{Q}_p(K) \text{ for all } K \in \mathcal{G}_{S_2^{\tilde{q}}}\}.$$

Consider the affine transformations

$$\psi_{i,j} : (0, x_2, x_3) \mapsto (2^{-\ell}i, x_2 + 2^{-\tilde{q}}j, x_3).$$

Then,  $x_{\xi, \overline{\eta_1 \eta_2}, \zeta} \in \psi_{\xi, \eta_1}(S_2^{\tilde{q}})$ . Moreover, for each  $\xi, \eta_1$  there exists a piecewise polynomial  $p_{\xi \eta_1}^{\tilde{q}} \in X_{S_2^{\tilde{q}}}$  such that

$$\left(v_{\text{qtt}}^{\ell} \circ \psi_{\xi, \eta_1}\right) \left(\left(\psi_{\xi, \eta_1}\right)^{-1}\left(x_{\xi, \overline{\eta_1 \eta_2}, \zeta}\right)\right) = p_{\xi \eta_1}^{\tilde{q}}(x_{0, \eta_2}, \zeta)$$

for all  $\eta_2 = 0, \dots, 2^{\ell-\tilde{q}} - 1$  and  $\zeta = 0, \dots, 2^{\ell} - 1$ , see Fig. 4.

Since  $\dim(X_{S_2^{\tilde{q}}}) \leq C\ell p^2$ , we obtain, reasoning as before,

$$r_q = \text{rank}(V^{(q)}) \leq C\ell p^2 \leq C\ell^{2\mathfrak{d}+1} \quad q = \ell + 1, \dots, 2\ell - 1.$$

It remains to consider  $q$  with  $2\ell \leq q < 3\ell$ . We sketch their treatment, which follows the same line of reasoning as in the preceding cases. Every row of the unfolding matrix  $V^{(q)}$  contains the evaluation of  $v_{\text{qtt}}^{\ell}$  on  $2^{3\ell-q}$  equispaced points belonging to a line parallel to the  $z$ -axis. Hence, there exists a space of piecewise polynomials with less than  $C(3\ell - q)p$  degrees of freedom such that each row of  $V^{(q)}$  can be written as linear combination of elements of the space, thus implying the existence of a constant  $C > 0$  such that

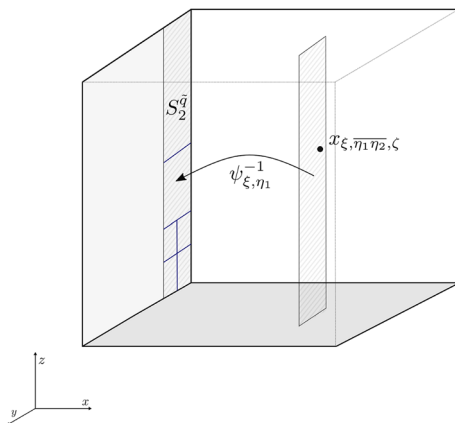
$$r_q = \text{rank}(V^{(q)}) \leq C\ell p \leq C\ell^{\mathfrak{d}+1} \quad q = 2\ell, \dots, 3\ell - 1.$$

The proof is concluded by remarking that

$$N_{\text{dof}} \leq C \sum_{q=1}^{3\ell-1} r_q r_{q+1} \leq C\ell^{4\mathfrak{d}+3},$$

choosing  $\ell \simeq |\log \varepsilon|$  and using Proposition 2. □

**Fig. 4** Slice  $S_2^{\tilde{q}}$ , with geometric mesh  $\mathcal{G}_{S_2^{\tilde{q}}}$  (in blue) and action of domain mapping  $\psi_{\xi, \eta_1}$





*Remark 3* In the proof of Lemma 2, we use a slightly different technique to treat the cases  $q \in \{1, \dots, \ell\}$  and  $q \in \{\ell + 1, \dots, 3\ell\}$ : in the first, we show that the columns of the unfolding matrices are point evaluations of piecewise polynomials, while in the latter we show a similar result for the rows of the unfolding matrices. It is possible to prove bounds on  $r_1, \dots, r_\ell$  by using the same procedure as the one used for  $q \geq 2\ell + 1$ : one would introduce the three-dimensional slice

$$\tilde{S}_1 = (0, 2^{-q}) \times (0, 1)^2,$$

the mesh

$$\tilde{\mathcal{G}}_{S_1}^q = \{K \in \mathcal{G}^q : K \subset \tilde{S}_1\},$$

and the space

$$\tilde{X}_{S_1}^q = \left\{ v \in H^1(\tilde{S}_1^q) : v \in \mathbb{Q}_p(K), \forall K \in \tilde{\mathcal{G}}_{S_1}^q \right\}.$$

Then, using the affine transformation

$$\tilde{\varphi}_{\xi_1} : (x_1, x_2, x_3) \mapsto (x_1 + 2^{-q}\xi_1, x_2, x_3),$$

one obtains that for all  $\xi_1 \in \{1, \dots, 2^q - 1\}$ ,

$$\left( v_{\text{qt3}}^\ell \circ \tilde{\varphi}_{\xi_1} \right) \in \tilde{X}_{S_1}^q,$$

which implies by the same reasoning as used in the proof that for  $q \in \{1, \dots, \ell\}$

$$r_q \leq C \dim \tilde{X}_{S_1}^q \leq C \ell p^3.$$

This bound is weaker than the one obtained in the proof of Lemma 2 (and would impact the final bound on  $N_{\text{dof}}$ ).

The same effect would manifest itself if we changed the direction of the decomposition in the case  $q \in \{2\ell + 1, \dots, 3\ell\}$ .

### 5.2 Rank bounds for transposed order QTT representations

**Lemma 3** *Let  $0 < \varepsilon_0 < 1$  and  $u \in X$ . Then, for all  $0 < \varepsilon \leq \varepsilon_0$  there exists  $\ell \in \mathbb{N}$  and  $v_{\text{qt3}}^\ell = \mathfrak{P}^\ell u$  such that  $\|u - v_{\text{qt3}}^\ell\|_{H^1(Q)} \leq \varepsilon$  and  $v_{\text{qt3}}^\ell$  admits a transposed QTT representation with*

$$N_{\text{dof}} \leq C |\log \varepsilon|^{6\delta+1}$$

*degrees of freedom, with  $C > 0$  independent of  $\varepsilon$ .*

*Proof* By Proposition 2, for all  $0 < \varepsilon \leq \varepsilon_0$  exists  $\ell \in \mathbb{N}$  such that  $\|u - \mathfrak{P}^\ell u\|_{H^1(Q)} \leq \varepsilon$ , with

$$\ell \leq C |\log \varepsilon|,$$

and  $C$  independent of  $\varepsilon$ . Let then  $q \in \{1, \dots, \ell - 1\}$ ; we consider the  $q$ th unfolding matrix of the transposed QTT representation of  $v_{\text{qt3}}^\ell$ , i.e., the  $q$ th unfolding matrix of  $\mathfrak{T}^{\text{qt3}}(\mathcal{A}^\ell(v_{\text{qt3}}^\ell))$ , as defined in (18). This is the matrix with entries

$$U_{\xi_1 \eta_1 \zeta_1, \xi_2 \eta_2 \zeta_2}^{(q)} = \mathcal{A}^\ell(v_{\text{qt3}}^\ell)_{\xi_1 \xi_2, \eta_1 \eta_2, \zeta_1 \zeta_2} = v_{\text{qt3}}^\ell(x_{\xi_1 \xi_2, \eta_1 \eta_2, \zeta_1 \zeta_2}) \tag{30}$$

with  $\xi_1, \eta_1, \zeta_1 \in \{0, \dots, 2^q - 1\}$  and  $\xi_2, \eta_2, \zeta_2 \in \{0, \dots, 2^{\ell-q} - 1\}$ . Following the proof of Lemma 2, we introduce a reference cube

$$S^q = (0, 2^{-q})^3$$

and a reference space

$$X_{S^q} = \mathbb{Q}_p(S^q).$$

Then, let  $\varphi_{i,j,k}$  be the map from the reference square to the space of points of the row  $\overline{ijk}$  of the unfolding matrix, i.e.,

$$\varphi_{i,j,k} : (x_1, x_2, x_3) \mapsto (x_1 + 2^{-q}i, x_2 + 2^{-q}j, x_3 + 2^{-q}k),$$

so that  $x_{\overline{\xi_1 \xi_2, \eta_1 \eta_2, \zeta_1 \zeta_2}} \in \varphi_{\xi_1, \eta_1, \zeta_1}(S^q)$  for all  $\xi_1, \eta_1, \zeta_1 \in \{0, \dots, 2^q - 1\}$ , see Fig. 5.

Remark that

$$\left\{ x_{\overline{\xi_1 \xi_2, \eta_1 \eta_2, \zeta_1 \zeta_2}} \right\}_{\substack{\xi_1, \eta_1, \zeta_1 \in \{0, \dots, 2^q - 1\} \\ \xi_2, \eta_2, \zeta_2 \in \{0, \dots, 2^{\ell-q} - 1\}}} \subset \overline{I_{\xi_1}^q} \times \overline{I_{\eta_1}^q} \times \overline{I_{\zeta_1}^q}.$$

Suppose now  $\overline{\xi_1 \eta_1 \zeta_1} > 0$ : then, there exists a single element  $K \in \mathcal{G}^\ell$  such that

$$\overline{I_{\xi_1}^q} \times \overline{I_{\eta_1}^q} \times \overline{I_{\zeta_1}^q} \subset \overline{K},$$

thus,

$$v_{\text{qt3}}^\ell \circ \varphi_{\xi_1, \eta_1, \zeta_1} \in X_{S^q}.$$

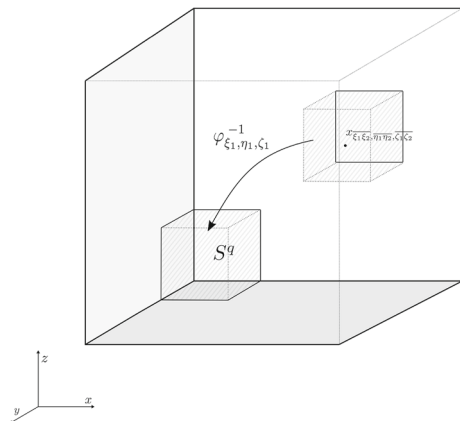
This implies that, for each  $\xi_1, \eta_1, \zeta_1: \overline{\xi_1 \eta_1 \zeta_1} > 0$ , there exists a polynomial  $p_{\overline{\xi_1 \eta_1 \zeta_1}} \in X_{S^q}$  that interpolates  $v_{\text{qt3}}^\ell \circ \varphi_{\xi_1, \eta_1, \zeta_1}$  in the reference cube, i.e.,

$$\left( v_{\text{qt3}}^\ell \circ \varphi_{\xi_1, \eta_1, \zeta_1} \right) \left( \varphi_{\xi_1, \eta_1, \zeta_1}^{-1} \left( x_{\overline{\xi_1 \xi_2, \eta_1 \eta_2, \zeta_1 \zeta_2}} \right) \right) = p_{\overline{\xi_1 \eta_1 \zeta_1}}(x_{\xi_2, \eta_2, \zeta_2}).$$

Note that for  $\xi_1 = \eta_1 = \zeta_1 = 0$ , the function  $v_{\text{qt3}}^\ell \circ \varphi_{\xi_1, \eta_1, \zeta_1}$  is not a polynomial, which increases the dimension of the row space of  $U^{(q)}$  by 1. Since  $\dim(X_{S^q}) \leq Cp^3$ , and using the same arguments as in the proof of Lemma 2 it can be concluded that

$$r_q = \text{rank}(U^{(q)}) \leq \dim(X_{S^q}) + 1 \leq C\ell^{3D}$$

Fig. 5 Reference cube  $S^q$  for transposed order QTT and representation of  $\varphi_{\xi_1, \eta_1, \zeta_1}$



which gives, due to (21), a total number of degrees of freedom  $N_{\text{dof}} \leq C\ell^{6\text{d}+1}$ . The fact that  $\ell \lesssim |\log \varepsilon|$  concludes the proof.  $\square$

### 5.3 Rank bounds of QTT approximations

In this section, we prove rank bounds for the QTT approximation. We start by proving, in Lemma 4 below, rank bounds for the *block QTT decomposition* of collections of piecewise polynomial functions. Block QTT decompositions are precisely defined in the following.

**Definition 6** (Block QTT decomposition) Let  $\ell \in \mathbb{N}$  and let  $A_\alpha : \{0, \dots, 2^\ell - 1\} \rightarrow \mathbb{R}$  for every  $\alpha = 1, \dots, s$ . We say that the collection  $\{A_\alpha\}_\alpha$  admits a *block QTT decomposition* with ranks  $r_0, \dots, r_\ell$  and cores  $U^1, U^2, \dots, U^\ell$ , if

$$A_\alpha(\overline{i_1 \dots i_\ell}) = U_\alpha^1(i_1)U^2(i_1) \cdots U^\ell(i_\ell) \quad \forall (i_1, \dots, i_\ell) \in \{0, 1\}^\ell, \forall \alpha \in \{1, \dots, s\},$$

for all  $i_n \in \{0, 1\}$ , and with  $U^n : \{0, 1\} \rightarrow \mathbb{R}^{r_{n-1} \times r_n}$  for all  $n = 1, \dots, \ell$ . By  $U_\alpha^1(i_1)$  we indicate the  $\alpha$ th row of  $U^1(i_1)$ . We have the restriction on the ranks  $r_0 = s, r_\ell = 1$ .

We also need the definition, on the geometric mesh  $\mathcal{G}_{1\text{d}}^\ell$  (see (24)), of the univariate *hp*-FE space

$$X_{\text{hp},1\text{d}}^{\ell,p} = \{v \in H^1((0, 1)) : v|_K \in \mathbb{Q}_p(K), \text{ for all } K \in \mathcal{G}_{1\text{d}}^\ell\}.$$

**Lemma 4** Let  $\{w_\alpha\}_{\alpha=1}^s \subset X_{\text{hp},1\text{d}}^{\ell,p}$ , and let  $W_\alpha : \{0, \dots, 2^\ell - 1\} \rightarrow \mathbb{R}$  be such that  $W_\alpha(i) = w_\alpha(2^{-\ell}i)$ , for all  $\alpha = 1, \dots, s$  and  $i = 0, \dots, 2^\ell - 1$ . Then the collection  $\{W_\alpha\}_{\alpha=1}^s$  admits a *block QTT representation* with ranks  $r_n \leq s + p + 1$  for all  $n = 1, \dots, \ell - 1$ .

*Proof* We provide a constructive proof with explicit formulas for the QTT cores. In the proof, the  $m$ -by- $n$  matrix with zero entries will be denoted by  $\mathbf{O}_{m \times n}$ , while the  $n$ -by- $n$  identity matrix will be written as  $\mathbf{I}_n$ . Let

$$q(x) = \mathbf{a}^\top \mathbf{m}(x),$$

where

$$\mathbf{a} = [a_0 \ a_1 \ \dots \ a_p]^\top \quad \mathbf{m}(x) = [1 \ x \ x^2 \ \dots \ x^p]^\top$$

be a polynomial of degree  $\leq p$  and  $\mathbf{q} = \{q(x_i)\}_{i=0}^{2^\ell-1} \in \mathbb{R}^{2^\ell}$ ,  $x_i = 2^{-\ell}i$ . Then  $\mathbf{q}$  admits the *exact, explicit QTT representation* [26, 42, 66] with ranks  $r_k = p + 1$ :

$$\mathbf{q}_i = Q^1(i_1)Q^2(i_2) \cdots Q^\ell(i_\ell), \quad i = \overline{i_1 \dots i_\ell},$$

where

$$\begin{aligned}
 Q^1(i_1) &= \boldsymbol{\varphi}^{\mathbf{a}}(2^{-1}i_1) \equiv [\varphi_0^{\mathbf{a}}(2^{-1}i_1) \dots \varphi_p^{\mathbf{a}}(2^{-1}i_1)], \\
 &\text{with } \varphi_m^{\mathbf{a}}(x) = a_m + \sum_{k=m+1}^p a_k C_k^m x^{k-m}, \quad m = 0, \dots, p, \\
 Q^k(i_k) &= \mathbf{Q}(2^{-k}i_k), \quad k = 2, \dots, \ell - 1, \\
 &\text{with } \mathbf{Q}(x)_{ij} = \begin{cases} C_i^{i-j} x^{i-j} & i > j, \\ C_i^0 & i = j, \\ 0 & \text{otherwise,} \end{cases} \quad i, j = 0, \dots, p, \\
 Q^\ell(i_\ell) &= \mathbf{m}(2^{-\ell}i_\ell).
 \end{aligned} \tag{31}$$

Let now  $w_\alpha \in X_{\text{hp},1\text{d}}^{\ell,p}$ ,  $\alpha = 1, \dots, s$  be given by polynomials with the coefficients  $\mathbf{a}_k^{(\alpha)}$ ,  $k = 1, \dots, \ell + 1$  on subintervals  $[2^{-k}, 2^{1-k})$  for  $k = 1, \dots, \ell$  and  $[0, 2^{-\ell})$  for  $k = \ell + 1$ .

Consider the points  $x_{\overline{i_1 \dots i_\ell}}$ . The case of  $i_1 = 1$  and any  $i_n \in \{0, 1\}$ ,  $n = 2, \dots, \ell$  corresponds to the equispaced mesh points  $x_{\overline{i_1 \dots i_\ell}}$  from the interval  $[1/2, 1)$ . Similarly, the case  $i_1 = \dots = i_{k-1} = 0, i_k = 1$  and any  $i_n \in \{0, 1\}$ ,  $n = k + 1, \dots, \ell$  corresponds to  $x_{\overline{i_1 \dots i_\ell}} \in [2^{-k}, 2^{1-k})$ .

We conclude that  $w_\alpha(x_{\overline{0 \dots 0 i_{k+1} \dots i_\ell}})$  are polynomials sampled in equidistant points. By utilizing this fact, explicit formulas (31) for the polynomial parts and combining expressions for each of them, we obtain:

$$W_\alpha(i) = w_\alpha(2^{-\ell}i) = W_\alpha^1(i_1)W^2(i_2) \dots W^\ell(i_\ell), \quad i = \overline{i_1 \dots i_\ell},$$

where

$$\begin{aligned}
 W_\alpha^1(i_1) &= \begin{cases} [\Phi_1(2^{-1}i_1) \mathbf{O}_{s \times s}], & i_1 = 1 \\ [\mathbf{O}_{s \times (p+1)} \mathbf{I}_s], & i_1 = 0 \end{cases} \\
 W^k(i_k) &= \begin{cases} \begin{bmatrix} \mathbf{Q}(2^{-k}i_k) \mathbf{O}_{(p+1) \times s} \\ \Phi_k(2^{-1}i_k) \mathbf{O}_{s \times s} \end{bmatrix}, & i_k = 1 \\ \begin{bmatrix} \mathbf{Q}(2^{-k}i_k) \mathbf{O}_{(p+1) \times s} \\ \mathbf{O}_{s \times (p+1)} \mathbf{I}_s \end{bmatrix}, & i_k = 0 \end{cases} \quad k = 2, \dots, \ell - 1 \\
 W^\ell(i_\ell) &= \begin{cases} \begin{bmatrix} \mathbf{m}(2^{-\ell}i_\ell) \\ (\mathbf{a}_\ell^{(1)})^\top \mathbf{m}(2^{-\ell}i_\ell) \\ \dots \\ (\mathbf{a}_\ell^{(s)})^\top \mathbf{m}(2^{-\ell}i_\ell) \end{bmatrix}, & i_\ell = 1 \\ \begin{bmatrix} \mathbf{m}(2^{-\ell}i_\ell) \\ (\mathbf{a}_{\ell+1}^{(1)})^\top \mathbf{m}(2^{-\ell}i_\ell) \\ \dots \\ (\mathbf{a}_{\ell+1}^{(s)})^\top \mathbf{m}(2^{-\ell}i_\ell) \end{bmatrix}, & i_\ell = 0 \end{cases}
 \end{aligned}$$

and where we used the notation

$$\Phi_k(x) \equiv \begin{bmatrix} \varphi^{a_k^{(1)}}(x) \\ \vdots \\ \varphi^{a_k^{(s)}}(x) \end{bmatrix} \in \mathbb{R}^{s \times (p+1)}, \quad k = 1, \dots, \ell.$$

For fixed  $i_k, k = 2, \dots, \ell - 1$ , the matrices  $W^k(i_k)$  are of size  $(p + s + 1) \times (p + s + 1)$ . We conclude that the ranks of the collection  $\{W_\alpha\}_\alpha$  are bounded from above by  $p + s + 1$ . This completes the proof. □

**Lemma 5** *Let  $0 < \varepsilon_0 < 1$  and  $u \in X$ . Then, there exists a constant  $C > 0$  (depending on  $u$  and on  $\varepsilon_0$ ) such that for all  $0 < \varepsilon \leq \varepsilon_0$  there exists  $\ell \in \mathbb{N}$  and  $v_{\text{qtt}}^\ell = \mathfrak{P}^\ell u$ , such that  $\|u - v_{\text{qtt}}^\ell\|_{H^1(Q)} \leq \varepsilon$ . Furthermore,  $v_{\text{qtt}}^\ell$  admits a TQTT representation with*

$$N_{\text{dof}} \leq C |\log \varepsilon|^{3\mathfrak{d}+3}$$

*degrees of freedom.*

*Proof* Consider the three-dimensional array  $V = \mathcal{A}^\ell(v_{\text{qtt}}^\ell)$ , with entries

$$V_{\xi, \eta, \zeta} = v_{\text{qtt}}^\ell(x_{\xi, \eta, \zeta}).$$

We start by showing that the 1-rank of  $V$ , i.e., the column rank of

$$V_{(1)} = V_{\xi, \eta, \bar{\zeta}}$$

is bounded by  $C\ell p$ , for  $C > 0$  independent of  $\ell, p$ . Indeed, for all  $\eta, \zeta \in \{0, \dots, 2^\ell - 1\}$ , the column  $\{V_{\xi, \eta, \bar{\zeta}}\}_\xi$  contains the evaluation of a piecewise polynomial in the finite dimensional space

$$X_{\text{hp}, 1\text{d}}^{\ell, p} = \{v \in H^1((0, 1)) : v|_K \in \mathbb{Q}_p(K), \text{ for all } K \in \mathcal{G}_{1\text{d}}^\ell\},$$

i.e., there exists  $p_{\eta\bar{\zeta}} \in X_{\text{hp}, 1\text{d}}^{\ell, p}$  such that

$$V_{\xi, \eta, \bar{\zeta}} = p_{\eta\bar{\zeta}}(2^{-\ell}\xi) \quad \text{for all } \xi \in \{0, \dots, 2^\ell - 1\}.$$

Since  $\dim(X_{\text{hp}, 1\text{d}}^{\ell, p}) \leq C\ell p$ , we have that  $\text{rank}(V_{(1)}) \leq C\ell^{\mathfrak{d}+1}$ . We write  $R = \dim(X_{\text{hp}, 1\text{d}}^{\ell, p})$ , denote by  $\{b_n\}_{n=1}^R$  a basis for  $X_{\text{hp}, 1\text{d}}^{\ell, p}$ , and repeat the argument above in the other two cardinal directions. It follows that there exists a Tucker decomposition such that, for  $\xi, \eta, \zeta \in \{0, \dots, 2^\ell - 1\}$ ,

$$V_{\xi, \eta, \zeta} = \sum_{\beta_1=1}^R \sum_{\beta_2=1}^R \sum_{\beta_3=1}^R G_{\beta_1, \beta_2, \beta_3} U_{\beta_1}(\xi) V_{\beta_2}(\eta) W_{\beta_3}(\zeta), \tag{32}$$

where  $R \leq C\ell^{\mathfrak{d}+1}$  and such that

$$U_{\beta_1}(\xi) = b_{\beta_1}(2^{-\ell}\xi), \quad V_{\beta_2}(\eta) = b_{\beta_2}(2^{-\ell}\eta), \quad W_{\beta_3}(\zeta) = b_{\beta_3}(2^{-\ell}\zeta), \tag{33}$$

for all  $\beta_1, \beta_2, \beta_3 \in \{1, \dots, R\}$ , see [32, Chapter 8].

Applying Lemma 4 to the Tucker factors  $U, V, W$ , we obtain their block QTT representation with tensor ranks  $\{R, r_{\text{QTT}}, \dots, r_{\text{QTT}}, 1\}$  bounded as

$$r_{\text{QTT}} = R + p + 1 \leq C\ell^{\mathfrak{d}+1}.$$

To store Tucker factors in the block QTT format, we need to store

$$N_{\text{dof}}^{\text{factors}} = 3 \cdot 2 \cdot (r_{\text{QTT}}R + r_{\text{QTT}}^2(\ell - 2) + r_{\text{QTT}}) \leq C\ell^{2\mathfrak{d}+3}$$

parameters of the decomposition. Storing the Tucker core requires an additional

$$N_{\text{dof}}^{\text{core}} = R^3 \leq C\ell^{3\mathfrak{d}+3}$$

parameters. This gives the following bound for the overall number of degrees of freedom in the TQTT representation

$$N_{\text{dof}} = N_{\text{dof}}^{\text{core}} + N_{\text{dof}}^{\text{factors}} \leq C\ell^{3\mathfrak{d}+3}.$$

Choosing  $\ell \simeq |\log \varepsilon|$  and using Proposition 2 completes the proof. □

### 5.4 Exponential convergence of QTT approximations of $u \in \mathcal{J}_\gamma^{\mathfrak{w}}(\mathcal{Q})$

From Proposition 2 and Lemmas 2, 3, and 5, we obtain the following estimate for the QTT-Finite Element approximation of functions in  $\mathcal{J}_\gamma^{\mathfrak{w}}(\mathcal{Q})$ . In the following theorem, we introduce a tag  $\text{qtd} \in \{\text{qtt}, \text{tqtt}, \text{qt3}\}$ , which generically denotes quantized tensor decomposition.

**Theorem 1** *Assume  $\gamma > 3/2$ ,  $C_u > 0$ ,  $A_u > 0$ ,  $\mathfrak{d} \geq 1$ , and  $0 < \varepsilon_0 \ll 1$ . Furthermore, assume the function  $u$  belongs to the weighted Gevrey class  $u \in \mathcal{J}_\gamma^{\mathfrak{w}}(\mathcal{Q}; C_u, A_u, \gamma, \mathfrak{d}) \cap H_F^1(\mathcal{Q})$ . Then, there exists a constant  $C > 0$  such that, for all  $0 < \varepsilon \leq \varepsilon_0$ , there exists  $\ell \in \mathbb{N}$  and  $v_{\text{qtd}}^\ell \in X^\ell$  such that*

$$\|u - v_{\text{qtd}}^\ell\|_{H^1(\mathcal{Q})} \leq \varepsilon$$

and  $v_{\text{qtd}}^\ell$  admits a representation with

$$N_{\text{dof}} \leq C|\log \varepsilon|^\kappa$$

degrees of freedom, with

$$\kappa = \begin{cases} 4\mathfrak{d} + 3 & \text{for classic QTT} \\ 6\mathfrak{d} + 1 & \text{for transposed order QTT} \\ 3\mathfrak{d} + 3 & \text{for Tucker QTT} \end{cases}.$$

**Remark 4** (Rank bounds of QTT-formatted approximations of two-dimensional corner singularities) Using the same techniques for the two-dimensional case (which was already considered for the transposed order QTT in [40] in the analytic class, i.e., for  $\mathfrak{d} = 1$ ) results in the bound

$$\kappa = \begin{cases} 2\mathfrak{d} + 3 & \text{for classic QTT,} \\ 4\mathfrak{d} + 1 & \text{for transposed order QTT.} \end{cases}$$

In the case of two spatial variables, the Tucker QTT format is easily reduced to the classic QTT format for the index ordering  $i_\ell, \dots, i_1, j_1, \dots, j_\ell$ .

## 6 Numerical experiments

In this section, we support the obtained theoretical results with numerical experiments. First, in Section 6.1, we construct FE approximants to functions defined in  $Q = (0, 1)^3$  with point singularities in three quantized tensor formats: QTT, transposed order QTT (QT3) and Tucker QTT (TQTT), see Fig. 1 for their tensor network representations. We note that for all formats under consideration, the numerically observed asymptotic behavior of rank versus error is better than that of theoretical estimates.

In Section 6.2, we consider an elliptic eigenvalue problem with a singular potential — the Schrödinger equation for a hydrogen atom. We approximate the solution using the finite element method with a tensor of coefficients represented the TQTT format. The numerical results suggest that convergence rates of QTT-formatted approximations are slightly higher than those achieved by the *hp*-FEM.

We note that optimization algorithms, e.g., SVD, that we use to approximate tensors are based on optimization in  $L^2$ -type norms. Nevertheless, in numerical experiments, we also calculate  $H^1$  errors for function approximation problem (Section 6.1) as well as eigenvalue errors (Section 6.2) that are associated with the computation of derivatives. We observe that these errors behave in agreement with the theoretical bounds.

### 6.1 QTT-FE approximation of functions with point singularities

In this section, we present the numerical results on function approximation. We will detail the approximation technique in Remark 5, while the details on the explicit construction of prolongation matrices for the computation of the error will be postponed to Appendix C.

Let us consider the following smooth functions in  $Q = (0, 1)^3$  that exhibit singularities at the origin  $x = (0, 0, 0)$ :

$$u(x) = |x|^\alpha m(x), \quad x = (x_1, x_2, x_3) \in Q,$$

where  $\alpha > 0$  defines the strength of the singularity and  $m(x) = (1 - x_1^2)(1 - x_2^2)(1 - x_3^2)$  is chosen to ensure zero values of the function on  $\Gamma$ . Note that the function  $m(x)$  does not affect the singularity at the origin and can be represented with tensor ranks bounded from above by 3 for QTT and TQTT formats and by 9 for QT3 format.

Recall that by  $\mathcal{I}^\ell$  we denote the Lagrange interpolation operator on the uniform tensor mesh  $\mathcal{T}^\ell$ :

$$\mathcal{I}^\ell v = \sum_{(i,j,k) \in \{0, \dots, 2^\ell - 1\}^3} v(x_{i,j,k}) \varphi_{i,j,k}.$$

In practice,  $u_{\text{qtd}}^\ell$  will be an approximation of  $\mathcal{I}^\ell u$  obtained by applying to  $\mathcal{A}^\ell \mathcal{I}^\ell u$  the exponential sums representation (see Remark 5) and by interpolating on a staggered

grid (see Remark 6). We introduce the rank-truncated representation of  $u_{\text{qtd}}^\ell$ ,  $\text{qtd} \in \{\text{qtt}, \text{qtqt}, \text{qt3}\}$  based on the rounding procedure:

$$u_{\text{qtd}}^{\ell, \delta} = \mathcal{S}^\ell \left( \text{round}_{\text{qtd}}(\mathcal{A}^\ell u_{\text{qtd}}^\ell, \delta) \right),$$

where  $\text{round}_{\text{qtd}}$  is a rounding operation that aims at reducing the numerical  $\text{qtd}$ -rank of  $\mathcal{A}^\ell u_{\text{qtd}}^\ell$  with the relative Euclidean error threshold  $\delta$ . The rounding procedure is based on a sequence of QR and SVD decompositions, see [65, Alg. 2] for TT (covers QTT and QT3 cases) and [18, Alg. 1] for two-level QTT-Tucker (covers the TQTT case with minor modifications).

For given  $u_{\text{qtd}}^{\ell, \delta}$ , we approximate the error  $\widehat{\varepsilon}_\ell$  in the seminorm  $|\cdot|_{H^1(Q)}$ :

$$\widehat{\varepsilon}_\ell = \frac{|u_{\text{qtd}}^{\ell, \delta} - u|_{H^1(Q)}}{|u|_{H^1(Q)}} = \frac{\|\nabla u_{\text{qtd}}^{\ell, \delta} - \nabla u\|_{L^2(Q)}}{\|\nabla u\|_{L^2(Q)}},$$

by using the respective quantized tensor approximation of  $u$  obtained on an equispaced mesh of axiparallel cubes with  $L := 30$  levels of binary refinement of  $Q = (0, 1)^3$ :

$$\widehat{\varepsilon}_\ell \approx \varepsilon_\ell \equiv \frac{\|\nabla u_{\text{qtd}}^{\ell, \delta} - \mathcal{I}_0^L(\nabla u)\|_{L^2(Q)}}{\|\mathcal{I}_0^L(\nabla u)\|_{L^2(Q)}}. \tag{34}$$

Here  $\mathcal{I}_0^L(\nabla u) = (\mathcal{I}_{0,1}^L(\partial_{x_1} u), \mathcal{I}_{0,2}^L(\partial_{x_2} u), \mathcal{I}_{0,3}^L(\partial_{x_3} u))^\top$  with  $\mathcal{I}_{0,\beta}^L$ ,  $\beta = 1, 2, 3$  being interpolation operators on a span of  $\{\partial_{x_\beta} \varphi_{i,j,k}\}_{i,j,k}$ .

In Fig. 6, we present the convergence plots of the relative error  $\varepsilon_\ell$  defined in (34) for  $\delta = 10^{-10}$  versus the background mesh levels  $\ell$  for different  $\alpha$  and for different quantized tensor formats. In all the cases, we observe empirical convergence in close correspondence with the rate

$$\varepsilon_\ell = \mathcal{O} \left( 2^{-\min\{\alpha+1/2, 1\}\ell} \right), \quad \alpha > -\frac{1}{2}.$$

This can be anticipated from classical FE interpolation error bounds on an equispaced, cartesian mesh in  $Q$ , for functions  $[x \mapsto |x|^\alpha]$  in three spatial dimensions.

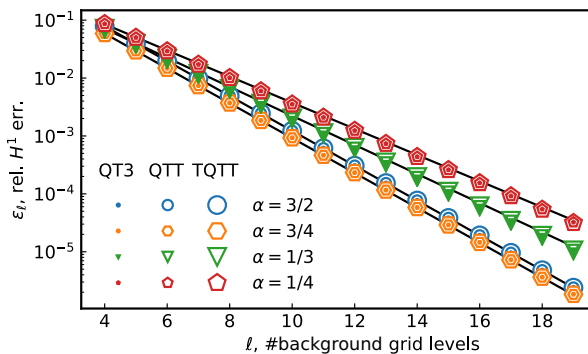


**Fig. 6** Number of background mesh levels versus the relative error in  $|\cdot|_{H^1(D)}$  seminorm for singularity exponent  $\alpha = 3/2, 3/4, 1/3, 1/4$  and for different quantized tensor formats: QTT, QT3 (transposed QTT), TQTT (Tucker QTT). The black lines correspond to  $\varepsilon_\ell = \mathcal{O}(2^{-\min\{\alpha+1/2, 1\}\ell})$  convergence



Let us first fix  $\alpha = 3/2$ . In Fig. 7, we present  $\varepsilon_\ell$  versus the effective number of degrees of freedom  $N_{\text{dof}}$  for three different tensor formats. On each gray dotted line we plot the error  $\varepsilon_\ell$  for one fixed  $\ell$  and for various values of  $\delta$ . The envelopes of the computed errors with respect to  $N_{\text{dof}}$  are highlighted with large empty markers.

In Fig. 8, we depict  $\varepsilon_\ell$  versus  $N_{\text{dof}}$  for  $\alpha = 3/2, 3/4, 1/3$ , and  $1/4$  obtained as envelopes of the set of points obtained for different  $\delta$  (see Fig. 7 for  $\alpha = 3/2$ ). By plotting  $\log_{10} \log_2 \varepsilon_\ell^{-1}$  against  $\log_{10} N_{\text{dof}}$ , we numerically estimate the constant  $\kappa$  in the empirical exponential rate of convergence

$$\varepsilon_\ell = C \exp(-bN_{\text{dof}}^{1/\kappa}), \tag{35}$$

for some positive constants  $b$  and  $C$ . Indeed, by first applying  $\log_2$  to both sides of (35), we arrive at  $\log_2 \varepsilon_\ell^{-1} = \tilde{b}N_{\text{dof}}^{1/\kappa} - \log_2 C$ ,  $\tilde{b} = -b \log 2$ . Assuming  $\log_2 C$  is small compared with  $N_{\text{dof}}^{1/\kappa}$  and taking  $\log_{10}$  of both sides, we obtain

$$\log_{10} \log_2 \varepsilon_\ell^{-1} \approx \kappa^{-1} \log_{10} N_{\text{dof}} + \log_{10} \tilde{b}.$$

In all the numerical examples considered, we observe  $\kappa < 6$ , i.e., higher convergence rates than those predicted by our quantized tensor rank bounds. We also observe lower rates of convergence than those of  $hp$ -FE approximations of corner singularities in three spatial dimensions (see (43)), i.e., we find  $\kappa > 4$ .

Figures 7 and 8 illustrate the fact that in the range of  $\ell$  considered, the transposed order QTT representation requires more degrees of freedom to achieve a given accuracy  $\varepsilon$  than the two other formats even though it has empirical convergence (35) with slightly smaller values of  $\kappa$ . Among the tensor formats and for the examples considered, the TQTT format requires the smallest number of degrees of freedom to achieve a prescribed accuracy  $\varepsilon$ .

*Remark 5* (Approximation of singular functions by exponential sums) To numerically evaluate the relative errors  $\varepsilon_\ell$  for all functions under consideration we used the following procedure. For each background mesh level  $\ell$ , we approximated the function using the exponential sums representation. Specifically, we obtain the quantized tensor representations by applying the trapezoidal quadrature rule on a uniform mesh

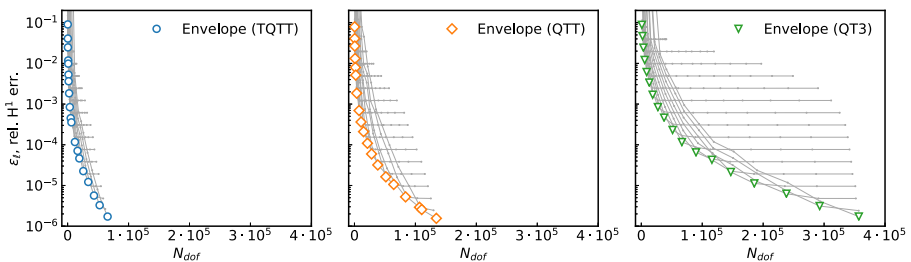


**Fig. 7** Each gray dotted line represents dependence of the estimated relative seminorm  $|\cdot|_{H^1(D)}$  error values  $\varepsilon_\ell$  on the rounding parameter  $\delta$  for fixed  $\ell$  as suggested by (34). Empty markers represent convex envelope of the gray dotted lines. The limits for both axes coincide for each of the plots

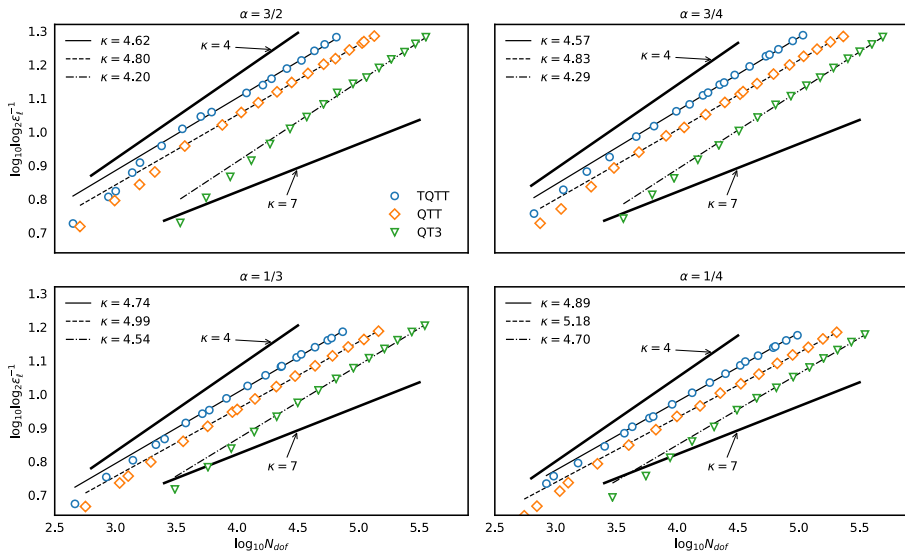


**Fig. 8** Effective number of degrees of freedom w.r.t. the estimated relative seminorm  $|\cdot|_{H^1(D)}$  error values  $\epsilon_\ell$  for  $\alpha = 3/2, 3/4, 1/3$  and  $1/4$ . Reference lines with  $\kappa = 4$  and  $\kappa = 7$  correspond to the  $hp$  approximation and the obtained (for QTT and QT3) theoretical convergence bounds respectively

to the following integral [9, 34]

$$(\sqrt{y})^{-\beta} = \frac{1}{\Gamma(\beta/2)} \int_{-\infty}^{\infty} e^{-ye^t + \beta t/2} dt, \quad \beta > 0, \quad y > 0, \quad (36)$$

for different values of  $\beta$ . A quadrature rule on a uniform mesh applied to (36) leads to an approximate, separated representation:

$$|x|^{-\beta} \approx \sum_{\alpha} \omega_{\alpha} e^{-x_1^2 e^{\alpha}} e^{-x_2^2 e^{\alpha}} e^{-x_3^2 e^{\alpha}}, \quad x = (x_1, x_2, x_3), \quad (37)$$

where  $|x| = (x_1^2 + x_2^2 + x_3^2)^{1/2}$ . Note that (37) only gives us separation of physical variables, while the exponential convergence for Gaussian functions in the QTT format was shown in [19].

The size of the integration interval and the number of points was tuned separately for each beta to ensure the desired accuracy. In this way, an approximation for  $|x|^\beta$ , with  $\beta \in (0, 2)$ , is found by first approximating the radial function  $|x|^{\beta-2}$  since  $\beta - 2 < 0$  and (37) is applicable, and subsequently by multiplying this function by  $|x|^2 = x_1^2 + x_2^2 + x_3^2$ , which has bounded TT ranks:  $|x|^\beta = |x|^2 |x|^{\beta-2}$  for  $\beta \in (0, 2)$ . This allows us to avoid using cross approximation techniques which may experience stability issues at high accuracies (using exponential sums, we obtain approximations with relative accuracy  $10^{-11}$  in  $L^2$  norm). Note that the exponential sums approach can be applied to any of the considered TT formats: QTT, QT3 and TQTT. In this

section, for the QTT-, QT3-formatted arrays and for intermediate computations in TQTT we utilized the `ttpy` library.<sup>2</sup>

*Remark 6* (Interpolation on staggered grid) To conveniently assemble  $|x|^{\beta-2}$  for  $\beta \in (0, 2)$  using exponential sums, while avoiding evaluation at the origin where the function has a singularity, we approximate each  $u(x_{i,j,k})$  as an average of the neighboring points on a staggered grid. Let  $h_\ell = 2^{-\ell}$  and denote by  $\tilde{\mathcal{N}} = \{x_{i,j,k} + h_\ell/2\}_{i,j,k=0}^{2^\ell-1}$  the nodes on the staggered grid. Then, for each  $x_{i,j,k}$ , the set of neighboring points to  $x_{i,j,k}$  on the staggered grid is  $\tilde{\mathcal{N}}_{i,j,k} = \{x \in \tilde{\mathcal{N}} : |x - x_{i,j,k}| \leq h_\ell/2\}$ . We then approximate

$$u(x_{i,j,k}) \approx \frac{1}{\#\tilde{\mathcal{N}}_{i,j,k}} \sum_{x \in \tilde{\mathcal{N}}_{i,j,k}} u(x),$$

where  $\#\tilde{\mathcal{N}}_{i,j,k}$  is the number of points of  $\tilde{\mathcal{N}}_{i,j,k}$ —equal to 8 except for points that lie on  $\partial\Omega \setminus \Gamma$ . We need therefore function evaluations only in the points of a mesh shifted by  $h_\ell/2$  with respect to the original mesh  $\mathcal{T}^\ell$ , and avoid evaluations at the singularity.

After  $u_{\text{qtd}}^\ell$  is accurately approximated for every background mesh level  $\ell$  using exponential sums, we reduce the number of parameters in the corresponding quantized tensor representation `qtd` of  $\mathcal{A}^\ell u_{\text{qtd}}^\ell$  by using `round_qtd`.

### 6.2 QTT-FEM for eigenvalue problems with singular potential

We apply QTT-formatted compression to the numerical solution of the eigenvalue problem (5), linearized and with singular potential  $V$ :

$$\left(-\frac{1}{2}\Delta - \frac{1}{|x|}\right)u(x) = \lambda u(x), \quad x \in \mathbb{R}^3.$$

This is, essentially, Schrödinger’s equation for the hydrogen atom. It is well-known (e.g., [50, Chapter 10]) that the eigenfunctions  $u_{n,l,m}$  can be enumerated by three integer quantum numbers:  $n = 1, 2, \dots$ —principal quantum number,  $l = 0, 1, \dots, n - 1$ —orbital quantum number, and  $m = -l, \dots, l$ , magnetic quantum number. The corresponding eigenvalues are  $\lambda_n = 1/(2n^2)$ . We aim at approximating the 3 smallest eigenvalues  $\lambda_n$  and their respective  $N_{\text{ev}} = 14$  eigenvectors  $u_{n,m,l}$ ,  $n = 1, 2, 3$ .

To solve the problem numerically, we replace  $\mathbb{R}^3$  with a finite domain  $\Omega = (-a, a)^3$ ,  $a = 100$  and impose homogeneous Dirichlet boundary conditions. To discretize the problem, we introduce a mesh with the nodes

$$x_{i,j,k} = -a + (i, j, k)h_\ell, \quad h_\ell = \frac{2a}{2^\ell + 1},$$

<sup>2</sup><https://github.com/oseledets/ttpy/tree/develop/tt> in the `develop` branch (latest commit: `ac03657`)

where  $(i, j, k) \in \{0, 1, \dots, 2^\ell + 1\}^3$ . For  $(i, j, k) \in \{1, \dots, 2^\ell\}^3$ , we denote by  $\varphi_{i,j,k}^\ell$  the piecewise trilinear, continuous nodal Lagrange functions satisfying

$$\varphi_{i,j,k}^\ell(x_{p,q,r}) = \delta_{ip}\delta_{jq}\delta_{kr}, \quad (i, j, k) \in \{1, \dots, 2^\ell\}^3, \quad (p, q, r) \in \{0, \dots, 2^\ell + 1\}^3,$$

and introduce the associated finite element space  $\text{span}\{\varphi_{i,j,k}^\ell\}$ . We discretize the problem using the finite element method. The discretized eigenvalue problem reads

$$\left(\frac{1}{2}D^\ell + V^\ell\right)u^\ell = \lambda^\ell M^\ell u^\ell, \quad u^\ell \in \mathbb{R}^{2^\ell \times 2^\ell \times 2^\ell}, \tag{38}$$

where  $D^\ell$  and  $M^\ell$  are, respectively, stiffness and mass linear operators<sup>3</sup>:

$$(D^\ell)_{i,j,k,p,q,r} = \int_\Omega \nabla \varphi_{i,j,k}^\ell(x) \nabla \varphi_{p,q,r}^\ell(x) dx,$$

$$(M^\ell)_{i,j,k,p,q,r} = \int_\Omega \varphi_{i,j,k}^\ell(x) \varphi_{p,q,r}^\ell(x) dx$$

for  $(i, j, k), (p, q, r) \in \{1, \dots, 2^\ell\}^3$ , and  $V_\ell$  is the matrix of the FE discretization of  $V(x) = -|x|^{-1}$ :

$$(V^\ell)_{i,j,k,p,q,r} = - \int_\Omega \frac{1}{|x|} \varphi_{i,j,k}^\ell(x) \varphi_{p,q,r}^\ell(x) dx.$$

assembled with the exponential sums approach.

To solve the problem, we approximate the eigenvectors corresponding to the smallest eigenvalues in the TQTT format that yields the smallest amount of degrees of freedom for a given error (compared with the QTT and QT3 formats) according to Figs. 6 and 8. Note that due to the extremely refined underlying background meshes with  $2^{3\ell}$  internal equispaced points, the stiffness matrix  $D^\ell$  becomes severely ill-conditioned (its condition number scales as  $h_\ell^{-2}$ , i.e., it grows exponentially in  $\ell$ ). Besides, there arises an effect of ill-conditioning for large  $\ell$  connected purely with the structure of tensor decompositions, see [5]. Therefore, in order to overcome the effect of algebraic and representation ill-conditioning and to accurately approximate the eigenvalues and corresponding eigenvectors of (38), particular attention has to be devoted to technical details of the computation. The overall procedure—based on the preconditioned gradient descent method and on the Rayleigh-Ritz procedure—is summarized in Algorithm 1. In the algorithm, we utilize “derivative-free” formulas [69] (that avoid multiplications by  $D^\ell$ , see Algorithm 1, line 8) for calculating the  $N_{\text{ev}} \times N_{\text{ev}}$  matrix  $F$  given by

$$F_{\alpha\beta}^k = \left\langle u_\alpha^{\ell,k}, \left(\frac{1}{2}D^\ell + V^\ell\right) u_\beta^{\ell,k} \right\rangle, \quad \alpha, \beta = 1, \dots, N_{\text{ev}}, \tag{39}$$

<sup>3</sup>Here, linear operators are mappings  $A : \mathbb{R}^{2^\ell \times 2^\ell \times 2^\ell} \rightarrow \mathbb{R}^{2^\ell \times 2^\ell \times 2^\ell}$  given as 6-dimensional arrays such that the action on  $u \in \mathbb{R}^{2^\ell \times 2^\ell \times 2^\ell}$  is defined by

$$(Au)_{i,j,k} = \sum_{p,q,r=1}^{2^\ell} A_{i,j,k,p,q,r} u_{p,q,r}, \quad (i, j, k) \in \{1, \dots, 2^\ell\}^3.$$

**Algorithm 1** Block eigensolver in TQTT format based on derivative-free formulas. The algorithm is formulated for three-dimensional arrays, implying that all the operations are performed within the TQTT format.

**Require:** Initial guess to eigenvectors  $u_\alpha^{\ell,0}$  and to eigenvalues  $\lambda_\alpha^{\ell,0}, \alpha = 1, \dots, N_{\text{ev}}$ , tolerance parameter  $\delta$ .

**Ensure:** Approximation to eigenvectors  $u_\alpha^\ell(\delta)$  and to eigenvalues  $\lambda_\alpha^\ell(\delta), \alpha = 1, \dots, N_{\text{ev}}$ .

- 1: **for**  $k = 1, 2, \dots$  until converged **do**
- 2:     **for**  $\alpha = 1, \dots, N_{\text{ev}}$  **do**
- 3:         Approximate  $V^\ell u_\alpha^{\ell,k-1}$  using algorithm `mvrk2` from TT-Toolbox.
- 4:         With tolerance  $\delta$  using the ADI-based solver [68], solve

$$\left(\frac{1}{2}D^\ell - \lambda_\alpha^{\ell,k-1} M^\ell\right) u_\alpha^{\ell,k} = -V^\ell u_\alpha^{\ell,k-1}.$$

- 5:         Approximate  $V^\ell u_\alpha^{\ell,k}$  using algorithm `mvrk2` from TT-Toolbox.
- 6:     **for**  $\alpha = 1, \dots, N_{\text{ev}}$  **do**
- 7:         **for**  $\beta = 1, \dots, N_{\text{ev}}$  **do**
- 8:             Calculate  $F_{\alpha\beta}^k = \lambda_\beta^{\ell,k-1} \langle u_\alpha^{\ell,k}, u_\beta^{\ell,k} \rangle + \langle u_\alpha^{\ell,k}, V^\ell u_\beta^{\ell,k} \rangle - \langle u_\alpha^{\ell,k}, V^\ell u_\beta^{\ell,k-1} \rangle$ .
- 9:             Calculate  $G_{\alpha\beta}^k = \langle u_\alpha^{\ell,k}, u_\beta^{\ell,k} \rangle$ .

10:     Solve the generalized eigenvalue problem

$$F^k S = G^k S \Lambda, \quad S \in \mathbb{R}^{N_{\text{ev}} \times N_{\text{ev}}}, \quad \Lambda = \text{diag}(\lambda_1^{\ell,k}, \dots, \lambda_{N_{\text{ev}}}^{\ell,k}) \in \mathbb{R}^{N_{\text{ev}} \times N_{\text{ev}}}.$$

- 11:     **for**  $\alpha = 1, \dots, N_{\text{ev}}$  **do**
- 12:         Calculate  $\tilde{u}_\alpha^{\ell,k} = \text{round}(\sum_{\beta=1}^{N_{\text{ev}}} S_{\alpha\beta} u_\beta^{\ell,k}, \delta)$ .
- 13:         Calculate  $u_\alpha^{\ell,k} = \tilde{u}_\alpha^{\ell,k} / \|\tilde{u}_\alpha^{\ell,k}\|_2$ .
- 14:     Set  $u_\alpha^\ell(\delta) = u_\alpha^{\ell,k}, \lambda_\alpha^\ell(\delta) = \lambda_\alpha^{\ell,k}, \alpha = 1, \dots, N_{\text{ev}}$ .

where  $u_\alpha^{\ell,k}$  are three-dimensional arrays represented in the TQTT format that approximate  $u_\alpha^\ell$  on the  $k$ th step of the iterative process and  $\langle \cdot, \cdot \rangle$  denotes scalar products of three-dimensional arrays:

$$\langle u, v \rangle = \sum_{i,j,k=1}^{2^\ell} u_{i,j,k} v_{i,j,k}, \quad u, v \in \mathbb{R}^{2^\ell \times 2^\ell \times 2^\ell}.$$

To solve the screened Poisson’s equations arising in Algorithm 1, we utilize the algorithm proposed in [68], which is based on the alternating direction implicit method, adapted to tensor formats with the help of rank truncation after each iteration. We also note that in this solver, the stiffness matrix  $D^\ell$  is never formed explicitly in the quantized format, and each ADI step is performed in a derivative-free way. This allows us to avoid the ill-conditioning of QTT [5] and approximate the solution without stability issues.

Let  $\lambda_{n,l,m}^\ell(\delta), n = 1, 2, 3 (N_{\text{ev}} = 14)$  be the eigenvalues obtained by using Algorithm 1 with a tolerance parameter  $\delta$  and sorted by their quantum numbers. Let us

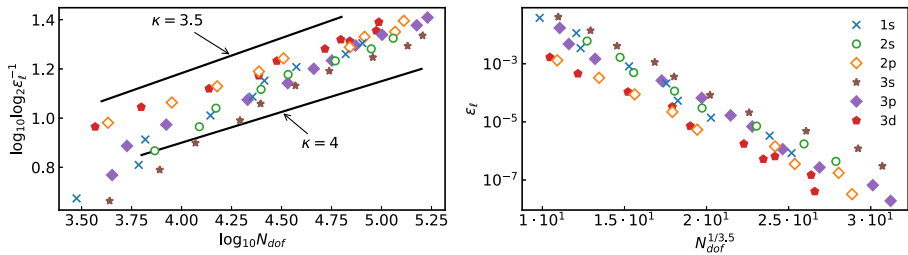


**Fig. 9** Relative errors  $\varepsilon_\ell = |\bar{\lambda}_{n,l}^\ell(\delta) - \lambda_n|/|\lambda_n|$ ,  $n = 1, 2, 3$ ,  $\ell = 0, 1, \dots, n - 1$  in double logarithmic scale (left) and single logarithmic scale (right) with respect to the averaged number of degrees of freedom for the eigenvalue problem (38). In the legend, the numbers 1,2,3 denote the principal quantum number  $n$  and the letters  $s, p, d$  correspond to  $\ell = 0, 1, 2$  respectively

calculate an average numerical eigenvalue for fixed  $n$  and  $l$

$$\bar{\lambda}_{n,l}^\ell(\delta) = \frac{1}{2l + 1} \sum_{m=-l}^l \lambda_{n,l,m}^\ell(\delta), \quad n = 1, 2, 3. \tag{40}$$

To each  $\bar{\lambda}_{n,l}$ , we associate a number of degrees of freedom, which is averaged in  $m$  by analogy with (40). For every  $\ell$ , select the parameters  $\delta^\ell$  as the largest numbers satisfying

$$|\bar{\lambda}_{n,l}^\ell(\delta^\ell) - \lambda_n| \leq c_{n,l} |\lambda_{n,l}^\ell(\delta_{\text{ref}}) - \lambda_n|,$$

where we chose  $\delta_{\text{ref}} = 10^{-10}$  and where the constants  $c_{n,l}$  satisfy  $c_{n,l} > 1$  (the practical choice is  $c_{n,l} = 1.01$ ). In Fig. 9, we present the errors

$$\varepsilon_\ell = \frac{|\bar{\lambda}_{n,l}^\ell(\delta^\ell) - \lambda_n|}{|\lambda_n|},$$

in eigenvalues  $\lambda_n$ ,  $n = 1, 2, 3$  with respect to the effective number of degrees of freedom for the eigenvalue problem (38).

Note that in this section, the implementation is done using the open source library TT-Toolbox<sup>4</sup>, which contains the implementation of the two-level QTT Tucker format [18]. In three space dimensions, this format is equivalent to the TQTT format with negligible overhead.<sup>5</sup>

## 7 Conclusion

We considered several formats of quantized tensor-train decompositions and proved tensor rank bounds for the approximation—with a prescribed error  $\varepsilon \in (0, 1)$  in

<sup>4</sup><https://github.com/oseledets/TT-Toolbox>

<sup>5</sup>In the two-level QTT Tucker format, the Tucker core of size  $R_1 \times R_2 \times R_3$  is additionally decomposed using the TT decomposition, which leads to TT cores of sizes  $R_1 \times R_1, R_1 \times R_2 \times R_3, R_3 \times R_3$ . So, compared with TQTT, the two-level QTT Tucker format leads to the storage of  $\mathcal{O}(R_1^2 + R_3^2)$  additional degrees of freedom.

$H^1(Q)$ —of several classes of Gevrey-smooth functions in the unit cube  $Q = (0, 1)^3$ , with one point singularity situated at the origin. In particular, we considered singularities from Gevrey-type and analytic function spaces with regularity quantified by corresponding derivative bounds in weighted Sobolev norms, with radial weight. For these singularities, we extended the  $hp$  approximation error analysis in [73, 76] to Gevrey-regular solutions with an isolated point singularity.

We then addressed approximation rate bounds in three concrete quantized tensor formats: the quantized tensor train (QTT), the transposed quantized TT (QT3) and the Tucker quantized TT (TQTT) format. Our theoretical TT rank analysis indicated that the tensor ranks and number of degrees of freedom necessary to achieve a prescribed accuracy  $\varepsilon \in (0, 1)$  in norm  $H^1(Q)$  in these format might depend on the format adopted in the quantized approximation (as no lower bounds were shown, these conclusions might be an artifact of our proofs). Numerical results, however, for several model singular functions confirmed the relative rank bounds for the three mentioned formats. These results point the way to QTT-structured solvers for electron structure problems and for other PDE models where solutions exhibit isolated point singularities; for example, continua with point defects, nonlinear Schrödinger and parabolic PDEs with blowup, to name but a few. *Format-adaptive, quantized approximations* as were recently proposed in [7, 8, 61] might result in further quantitative improvement of TT ranks for the presently considered examples.

While our analysis focused only on functions with singular support consisting of one isolated point, we emphasize that corresponding rank bounds are obtained for functions whose singular support consists of a finite number of (well-separated) isolated points; the present results imply the same rank bounds as shown here also for such functions, albeit with the constants in the estimates strongly depending on the separation of the singular supports. With further analysis, the present results extend to other forms of singularities, such as line and face singularities. The details on this shall be reported in [57].

### Appendix A. $hp$ approximation in weighted Gevrey classes

We prove, in this section, the exponential convergence of the  $hp$  approximations to functions in the weighted Gevrey class  $\mathcal{J}_\gamma^\varpi(Q; C, A, \vartheta)$  for  $C, A > 0, \gamma > 3/2, \vartheta \geq 1$ . Specifically, this corresponds to functions  $u \in H^1(Q)$  such that

$$\sum_{|\alpha|=s} \|r^{s-\gamma} \partial^\alpha u\|_{L^2(Q)} \leq CA^s (s!)^\vartheta \quad \text{for all } s \in \mathbb{N}. \tag{41}$$

We recall that the  $hp$  space is defined as

$$X_{hp}^{\ell,p} = \{v \in H^1(Q) : v|_K \in \mathbb{Q}_p(K), \text{ for all } K \in \mathcal{G}^\ell\}.$$

The central (novel) result of this section is the existence—for Gevrey-regular functions in  $\mathcal{J}_\gamma^\varpi(Q)$ —of an exponentially convergent,  $H^1(Q)$  conforming  $hp$ -projector on 1-irregular geometric meshes of hexahedra, as stated in the following proposition.

**Proposition 3** *Let  $\gamma \geq \gamma_0 > 3/2$  and  $\mathfrak{d} \geq 1$ . Then, there exists  $\Pi_{\text{hp}}^{\ell,p} : \mathcal{J}_\gamma^\infty(Q) \rightarrow X_{\text{hp}}^{\ell,p}$  such that for all  $u \in \mathcal{J}_\gamma^\infty(Q; C, A, \mathfrak{d})$  there exist constants  $C_{\text{hp}}$  and  $b_{\text{hp}}$  such that*

$$\|u - \Pi_{\text{hp}}^{\ell,p} u\|_{H^1(Q)} \leq C_{\text{hp}} e^{-b_{\text{hp}} \ell}, \quad \ell \in \mathbb{N}, \tag{42}$$

provided the uniform polynomial degree is  $p \geq c_0 \ell^\mathfrak{d}$  for a sufficiently large constant  $c_0 > 0$  (depending on the constant  $A$  in Eq. (41) and on  $\mathfrak{d}$ ) which is independent of  $\ell$ . The constants  $C_{\text{hp}}, b_{\text{hp}}$  depend on the constants  $C, A$ , and  $\mathfrak{d}$  in  $\mathcal{J}_\gamma^\infty(Q)$ . In terms of  $N_{\text{dof}} = \dim(X_{\text{hp}}^{\ell,p}) \simeq \ell^{3\mathfrak{d}+1}$ , (42) reads

$$\|u - \Pi_{\text{hp}}^{\ell,p} u\|_{H^1(Q)} \leq C_{\text{hp}} \exp\left(-\hat{b}_{\text{hp}} N_{\text{dof}}^{1/(1+3\mathfrak{d})}\right). \tag{43}$$

The rest of the section will be devoted to an overview of the construction of the conforming projector  $\Pi_{\text{hp}}^{\ell,p}$ . This projector has already been exploited and analyzed in detail, e.g., in [73, 74]; here, we wish to sketch its construction for the sake of self-containedness and to provide the necessary detail of the treatment of non-analytic Gevrey-type estimates (i.e., of the cases where  $\mathfrak{d} > 1$ ), which requires some minor modification with respect to the setting of [73, 74]. For positive integers  $p$  and  $s$  such that  $1 \leq s \leq p$ , we write  $\Psi_{p,s} = (p - s)! / (p + s)!$ .

### A.1 Discontinuous projector

We start by introducing a nonconforming projector.

#### A.1.1 Local projector

We denote the reference interval by  $I = (-1, 1)$  and the reference cube by  $\hat{K} = (-1, 1)^3$ . We write also  $H_{\text{mix}}^2(\hat{K}) = H^2(I) \otimes H^2(I) \otimes H^2(I)$ , where  $\otimes$  denotes the Hilbertian tensor product. Let  $p \geq 3$ : as constructed in [17, Appendix A], there exist univariate projectors  $\hat{\pi}_p : H^2(I) \rightarrow \mathbb{P}_p(I)$  such that

$$(\pi_p v)^{(j)}(\pm 1) = v^{(j)}(\pm 1), \quad j = 0, 1, \tag{44}$$

see [73, Lemma 4.1] (the projector  $\pi_p$  is denoted  $\pi_{p,2}$  there). Then, the Hilbertian tensor product projector given by

$$\hat{\Pi}_p = \hat{\pi}_p \otimes \hat{\pi}_p \otimes \hat{\pi}_p \tag{45}$$

has the following property.

**Lemma 6** [75, Remark 5.5] *For every  $p \geq 3$  exists a projector  $\hat{\Pi}_p : H_{\text{mix}}^2(\hat{K}) \rightarrow \mathbb{Q}_p(\hat{K})$  such that for all  $v \in H_{\text{mix}}^2(\hat{K})$  and all integer  $s$  such that  $2 \leq s \leq p$*

$$\|v - \hat{\Pi}_p v\|_{H_{\text{mix}}^2(\hat{K})}^2 \leq C \Psi_{p-1,s-1} \|v\|_{H^{s+5}(\hat{K})}^2,$$

with  $C$  independent of  $p, s$ , and  $v$ .



For all  $K \in \mathcal{G}^\ell$ , we introduce the affine transformation from the reference element to  $K$

$$\Phi_K : \widehat{K} \rightarrow K \quad \text{such that} \quad \Phi_K(\widehat{K}) = K;$$

it follows that for  $v$  defined on  $K$  such that  $v \circ \Phi_K \in H_{\text{mix}}^2(\widehat{K})$  we can define the local projector on  $K$  so that

$$\Pi_p^K v = (\widehat{\Pi}_p(v \circ \Phi_K)) \circ \Phi_K^{-1}. \tag{46}$$

The projector  $\Pi_p^K$  is continuous across regular matching faces.

**Lemma 7** [73, Lemma 4.2] *Let  $K_1, K_2$  be two axiparallel cubes that share one regular face  $F$  (i.e.,  $F$  is a full face of both  $K_1$  and  $K_2$ ). Then, for  $v \in H^6(\text{int}(\overline{K_1} \cup \overline{K_2}))$  the piecewise polynomial*

$$\Pi_p^{K_1 \cup K_2} v = \begin{cases} \Pi_p^{K_1} v & \text{in } K_1, \\ \Pi_p^{K_2} v & \text{in } K_2 \end{cases}$$

is continuous across  $F$ .

*Remark 7* By (44) and (45), if a function  $v$  on  $K$  such that  $v \circ \Phi_K \in H_{\text{mix}}^2(\widehat{K})$  vanishes on a face  $F \subset \partial K$ , then we also have  $(\Pi_p^K v)|_F = 0$ .

### A.1.2 Globally discontinuous $hp$ projector

Starting from the local, elementwise projector (46), a global, *discontinuous* projection operator  $\Pi_{\text{hp,disc}}^{\ell,p}$  is defined in the usual way: with the nonconforming  $hp$ -space

$$X_{\text{hp,disc}}^{\ell,p} = \prod_{K \in \mathcal{G}^\ell} \mathbb{Q}_p(K) = \{v \in L^2(Q) : v|_K \in \mathbb{Q}_p(K), \text{ for all } K \in \mathcal{G}^\ell\};$$

for all  $K \in \mathcal{G}$  and for  $v \in \mathcal{J}_\gamma^\infty(Q)$ , with  $\gamma > 3/2$ ,

$$\Pi_{\text{hp,disc}}^{\ell,p} v|_K = \begin{cases} v(0) & \text{if } K \in \mathcal{L}_0^\ell, \\ \Pi_p^K v & \text{otherwise.} \end{cases} \tag{47}$$

Note that  $v(0)$  is well defined for  $v \in \mathcal{J}_\gamma^1(Q)$  if  $\gamma > 3/2$ , see [49, Lemma 7.1.3]; hence, *a fortiori*,  $\Pi_{\text{hp,disc}}^{\ell,p} : \mathcal{J}_\gamma^\infty(Q) \rightarrow X_{\text{hp,disc}}^{\ell,p}$  is well defined if  $\gamma > 3/2$ .

**Lemma 8** *Let  $u \in \mathcal{J}_\gamma^\infty(Q; C_u, A_u, \vartheta)$ . Then, if  $p \simeq \ell^\vartheta$ , there exist constants  $C, b > 0$  such that*

$$\sum_{K \in \mathcal{G}^\ell} \frac{1}{h_K^2} \|u - \Pi_{\text{hp,disc}}^{\ell,p} u\|_{L^2(K)}^2 + \|\nabla(u - \Pi_{\text{hp,disc}}^{\ell,p} u)\|_{L^2(K)}^2 \leq C e^{-b\ell},$$

with  $\dim(X_{\text{hp,disc}}^{\ell,p}) \simeq \ell^{3\vartheta+1}$ .

*Proof* The proof follows along the lines of the proof of [75, Proposition 5.13]. Denote  $\eta = u - \Pi_{\text{hp,disc}}^{\ell,p} u$  and  $N_K[v]^2 = \|v\|_{L^2(K)}^2/h_K^2 + \|\nabla v\|_{L^2(K)}^2$ .

We start by considering  $K \in \mathcal{L}_j^\ell$  for  $j \geq 1$  and write  $d_K = \text{dist}(K, (0, 0, 0))$ . By Lemma 6, scaling inequalities (see [75, Equations (5.26)–(5.31)]), and the regularity of  $u$  (see (41)),

$$\begin{aligned} N_K[\eta]^2 &\leq C\Psi_{p-1,s-1} \sum_{s+1 \leq |\alpha| \leq s+5} d_K^{2|\alpha|-2} \|\partial^\alpha u\|_{L^2(K)}^2 \\ &\leq C\Psi_{p-1,s-1} \sum_{s+1 \leq |\alpha| \leq s+5} d_K^{2\gamma-2} \|r^{|\alpha|-\gamma} \partial^\alpha u\|_{L^2(K)}^2 \\ &\leq C\Psi_{p-1,s-1} 2^{-2(\ell-j)\gamma+2} A_u^{2(s+5)} ((s+5)!)^{2\mathfrak{d}}. \end{aligned}$$

Then, using the fact that for sufficiently large  $s$  and  $c = 2A_u + 1$ ,

$$\Psi_{p-1,s-1} A_u^{2s} ((s+5)!)^{2\mathfrak{d}} \leq C \left( \frac{2A_u}{2A_u + 1} \right)^{2c^{-1/\mathfrak{d}} p^{1/\mathfrak{d}}},$$

see [20, Equation (42)], choosing  $s = (p/c)^{1/\mathfrak{d}} \simeq \ell$ , with  $c > 1$  sufficiently large, and summing over all mesh layers not touching the origin (“interior mesh layers”), we obtain that there exist  $C_1, b_1 > 0$  such that for every  $\ell \geq 1$  holds

$$\sum_{j=1}^{\ell} \sum_{K \in \mathcal{L}_j^\ell} N_K[\eta]^2 \leq C\Psi_{p-1,s-1} A_u^{2(s+5)} ((s+5)!)^{2\mathfrak{d}} \leq C e^{-2bs} \leq C_1 e^{-2b_1 \ell}. \tag{48}$$

We now consider the element  $K \in \mathcal{L}_0^\ell$ , i.e.,  $K = (0, 2^{-\ell})^3$ . By Hardy’s inequality and choosing  $\gamma > 1$ ,

$$\begin{aligned} N_K[\eta]^2 &= \frac{1}{h_K^2} \|u - u(0)\|_{L^2(K)}^2 + \|\nabla u\|_{L^2(K)}^2 \leq \|r^{-1}(u - u(0))\|_{L^2(K)}^2 + \|\nabla u\|_{L^2(K)}^2 \\ &\leq C \|\nabla u\|_{L^2(K)}^2 \\ &\leq C h_K^{2(\gamma-1)} \|r^{1-\gamma} \nabla u\|_{L^2(K)}^2 \\ &\leq C 2^{-2(\gamma-1)\ell} \|u\|_{\mathcal{J}_\gamma^1(Q)}^2 \leq C_2 e^{-b_2 \ell}. \end{aligned}$$

Finally, the dimension of the  $\mathbb{Q}_p(K)$  space in each element  $K \in \mathcal{G}^\ell$  is given by  $(1 + p)^3$ ; since each non-terminal mesh layer  $\mathcal{L}_j^\ell, j > 0$ , contains 7 elements, we have that  $\dim(X_{\text{hp,disc}}^{\ell,p}) = (1 + p)^3(1 + 7\ell)$ . The observation that  $p \simeq \ell^\mathfrak{d}$  concludes the proof.  $\square$

### A.2 Conforming hp approximation

A conforming  $hp$  approximation is obtained by locally lifting the polynomial face jumps of the discontinuous, piecewise polynomial approximation. Their construction is detailed in [73, Section 5.3].

### A.2.1 Edge and face liftings

Since our discontinuous interpolant is the same as in [73], apart from the nonzero constant in  $\mathcal{L}_0^\ell$  (see (47) and [73, Equation (4.10)]), the construction of the polynomial face jump liftings can be replicated verbatim as in [73]. We recall it here briefly, referring the reader to the aforementioned [73, Section 5.3] for the details.

We start by considering the interface between two mesh levels  $\mathcal{L}_k^\ell$  and  $\mathcal{L}_{k+1}^\ell$ ,  $k \in \mathbb{N}$ . We introduce a local coordinate system  $\hat{x}, \hat{y}, \hat{z}$  and label the faces and edges belonging to the interface as  $F_i, i = 1, 2, 3$  and  $E_i, i = 1, \dots, 9$ , respectively, see Fig. 10. Furthermore, we denote by  $h_E$  the maximum length of all edges  $E_i$ . We refer to Fig. 10 for the precise numbering of edges and faces and for the location of the local system of coordinates. Given two neighboring elements  $K_a$  and  $K_b$  with interface  $f_{ab} = \overline{K}_a \cap \overline{K}_b$ , the jump of a function

$$v = \begin{cases} v^{K_a} & \text{in } K_a \\ v^{K_b} & \text{in } K_b \end{cases}$$

on  $f_{ab}$  is given by

$$[[v]]_{f_{ab}} = v|_{f_{ab}}^{K_a} n_{K_a} + v|_{f_{ab}}^{K_b} n_{K_b},$$

where  $n_{K_a}$  (resp.  $n_{K_b}$ ) is the normal pointing outwards from element  $K_a$  (resp.  $K_b$ ).

Consider face  $F_1$  of Fig. 10: we define the jump of the discontinuous interpolant on this face as

$$[[\Pi_{\text{hp,disc}}^{\ell,p} u]]_{F_1} = [[\Pi_{\text{hp,disc}}^{\ell,p} u]]_{f_{1j}} \quad \text{on } f_{1j}, j = 1, 2, 3, 4$$

where  $f_{1j}$  are the four parts of the face  $F_1$ , see Fig. 10. The jumps on the other faces are defined similarly. The edge jump, e.g., on  $E_1$ , is then defined as

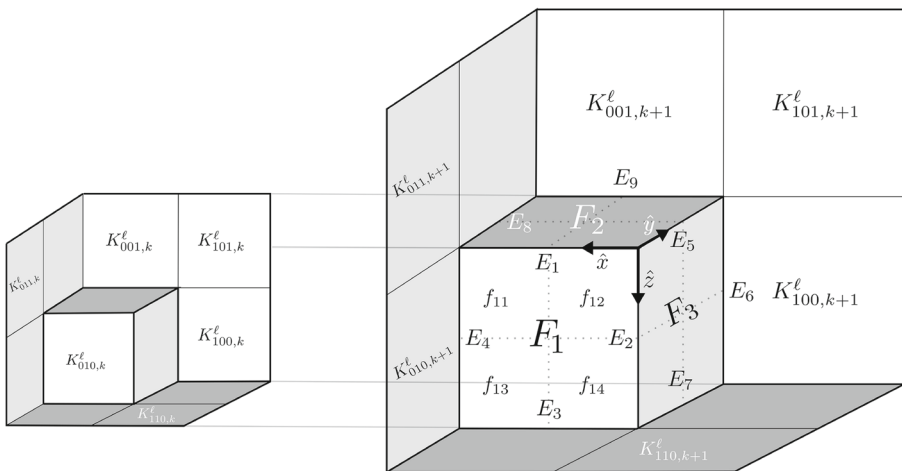


**Fig. 10** Separation of mesh levels  $\mathcal{L}_k^\ell$  (elements moved to the left) and  $\mathcal{L}_{k+1}^\ell$ , with the interfaces  $F_1, F_2, F_3$  and edges  $E_1, \dots, E_9$  marked. The local system of coordinates is given by  $\hat{x}, \hat{y}, \hat{z}$  is also represented (with  $\hat{y}$  pointing upwards from the page)

$[[\Pi_{\text{hp,disc}}^{\ell,p} u]]_{E_1} = ([[ \Pi_{\text{hp,disc}}^{\ell,p} u ]_{F_1}]_{E_1}$ . Let  $n$  denote the normal on face  $F_1$  pointing outwards from  $K_{010,k+1}^\ell$ ; the lifting of the jump on edge  $E_1$  is given by

$$\mathfrak{L}^{E_1}(\Pi_{\text{hp,disc}}^{\ell,p} u) = \begin{cases} \left( [[\Pi_{\text{hp,disc}}^{\ell,p} u]]_{E_1} \cdot n \right) (1 - 2\hat{y}/h_E)(1 - 2\hat{z}/h_E) & \text{in } K_{011,k}^\ell \cup K_{111,k}^\ell \\ 0 & \text{elsewhere.} \end{cases} \tag{49}$$

After having defined the other edge liftings  $\mathfrak{L}^{E_i}$ ,  $i = 2, \dots, 9$ , in the same way, we can introduce the full edge lifting operator

$$\mathfrak{L}^E = \sum_{i=1}^9 \mathfrak{L}^{E_i}.$$

We now introduce the face lifting operator for the face  $F_1$ , the other liftings being derived in the same way. We have

$$\mathfrak{L}^{F_1}(\Pi_{\text{hp,disc}}^{\ell,p} u) = \begin{cases} \mathfrak{L}^E(\Pi_{\text{hp,disc}}^{\ell,p} u) + \left( [[\Pi_{\text{hp,disc}}^{\ell,p} u + \mathfrak{L}^E(\Pi_{\text{hp,disc}}^{\ell,p} u)]_{F_1} \cdot n \right) (1 - 2\hat{y}/h_E) & \text{in } K_{n,k}^\ell, n \in \{010, 011, 110, 111\} \\ 0 & \text{otherwise,} \end{cases} \tag{50}$$

where  $n$  is again the normal on face  $F_1$  pointing outwards from  $K_{010,k+1}^\ell$ . Then, the global lifting  $\mathfrak{L}^k$  between mesh levels  $\mathcal{L}_k^\ell$  and  $\mathcal{L}_{k+1}^\ell$  is the sum of the local liftings on the three interfaces:

$$\mathfrak{L}^k = \mathfrak{L}^{F_1} + \mathfrak{L}^{F_2} + \mathfrak{L}^{F_3}. \tag{51}$$

Note that the lifting thus defined has support only in the elements belonging to mesh level  $\mathcal{L}_k^\ell$ .

We now turn to the terminal layer, i.e., to the jumps of  $\Pi_{\text{hp,disc}}^{\ell,p} u$  between the element  $K_{000,0}^\ell = (0, 2^{-\ell})^3$  and the elements of  $\mathcal{L}_1^\ell$ . The (three) faces belonging to the interface are all regular, but  $\Pi_{\text{hp,disc}}^{\ell,p} u$  is defined as a constant in  $K_{000,0}^\ell$ , see (47). One has to lift the nodal jumps at all the nodes of  $K_{000,0}^\ell$  except the origin. Then, the same procedure as for the other mesh layers (applied to the nodally lifted polynomial) gives a lifting operator  $\mathfrak{L}^0$ .

The full lifting operator is thus given by the sum of the local operators, as

$$\mathfrak{L} = \sum_{k=0}^{\ell-1} \mathfrak{L}^k, \tag{52}$$

with all  $\mathfrak{L}^k$  constructed as in (51). Such a lifting permits to obtain a conforming projector into  $X_{\text{hp}}^{\ell,p}$ , with approximation error bounded by a multiple of the approximation error of the discontinuous operator  $\Pi_{\text{hp,disc}}^{\ell,p}$ , as stated in the next proposition, that is proven in [73].

**Proposition 4** [73, Proposition 5.3] *The discontinuous projection operator  $\Pi_{hp}^{\ell,p}$  defined in (47) and the lifting operator  $\mathfrak{L}$  defined in (52) are such that*

$$\Pi_{hp}^{\ell,p} = \Pi_{hp, \text{disc}}^{\ell,p} + \mathfrak{L}\Pi_{hp, \text{disc}}^{\ell,p} : X \rightarrow X_{hp}^{\ell,p}$$

*is conforming in  $H^1(Q)$  and there exists  $C > 0$  independent of  $p$  such that*

$$\begin{aligned} \sum_{K \in \mathcal{G}^\ell} \frac{1}{h_K^2} \|u - \Pi_{hp}^{\ell,p} u\|_{L^2(K)}^2 + \|\nabla(u - \Pi_{hp}^{\ell,p} u)\|_{L^2(K)}^2 \\ \leq Cp^{18} \sum_{K \in \mathcal{G}^\ell} \frac{1}{h_K^2} \|\eta\|_{L^2(K)}^2 + \|\nabla\eta\|_{L^2(K)}^2 \end{aligned}$$

Here,  $\eta = u - \Pi_{hp, \text{disc}}^{\ell,p} u$ .

The exponential convergence of the conforming approximation, stated in Proposition 3, is a direct consequence of the last results.

*Proof of Proposition 3* Inequality (42) follows from Proposition 4 and Lemma 8, once the algebraic term in  $p$  of inequality (48) has been absorbed in the exponential by a change of constants. □

*Remark 8* Recall that  $\Gamma = \{(x_1, x_2, x_3) \in \partial Q : x_1 x_2 x_3 \neq 0\}$  contains the faces of the boundary of  $Q$  not abutting at the singularity. All liftings obtained by the operator (52) admit traces which vanish on  $\Gamma$ . I.e., for all  $v \in \mathcal{J}_\gamma^\infty(Q)$ ,

$$\left(\Pi_{hp}^{\ell,p} v\right)_{|\Gamma} = \left(\Pi_{hp, \text{disc}}^{\ell,p} v\right)_{|\Gamma}.$$

Therefore, by Remark 7, if  $v|_\Gamma = 0$ , then also  $\left(\Pi_{hp}^{\ell,p} v\right)_{|\Gamma} = 0$ .

### A.3 Combination of patches

We conclude this section by considering the approximation in a domain which contains the singular point in its interior. Let then  $R = (-1, 1)^3$ . The definition of the weighted space follows directly from the definition of the spaces in  $Q$ , by keeping the weight  $r = |x|$  to be the distance from the origin.

The construction of the graded mesh is done by decomposing  $R$  into eight sub-cubes of unitary edge and by collecting the elements of the sub-meshes (called here “patches”) obtained by symmetry from  $\mathcal{G}^\ell$ . The projector  $\Pi_{hp}^{\ell,p}$  in  $R$  can also be straightforwardly constructed by combining local projectors obtained by symmetry; we show that it is continuous on interpatch faces, hence conforming on the whole cube  $R$ .

We detail the construction for two patches; the rest follows by iterating this argument. Specifically, we consider the two cubes

$$Q^+ = (0, 1)^3 \quad Q^- = (-1, 0) \times (0, 1)^2,$$

and introduce the reflection operator

$$\psi^\pm : Q^+ \rightarrow Q^- \quad \psi^\pm : (x_1, x_2, x_3) \mapsto (-x_1, x_2, x_3).$$

Note that  $(\psi^\pm)^{-1} = \psi^\pm$ . Then, the mesh on the domain  $Q^\pm = \overline{Q^+ \cup Q^-}$  is given by

$$\mathcal{G}^{\ell,\pm} = \mathcal{G}^\ell \cup \mathcal{G}^{\ell,-}, \quad \mathcal{G}^{\ell,-} = \{\psi^\pm(K) : K \in \mathcal{G}^\ell\},$$

see Fig. 11.

The projection operator for functions  $v \in \mathcal{J}_\gamma^\infty(Q^\pm)$  can be easily constructed by reflection

$$(\Pi_{\text{hp}}^{\ell,p,\pm} v)|_K = \begin{cases} \Pi_{\text{hp}|_K}^{\ell,p} v & \text{if } K \in \mathcal{G}^\ell \\ \left( \Pi_{\text{hp}|_K}^{\ell,p} (v \circ \psi^\pm) \right) \circ \psi^\pm & \text{if } K \in \mathcal{G}^{\ell,-}. \end{cases}$$

The operator thus obtained is continuous hence conforming, as discussed in the next lemma.

**Lemma 9** *The operator  $\Pi_{\text{hp}}^{\ell,p,\pm}$  is conforming in  $H^1(Q^\pm)$ . Furthermore, if  $\gamma \geq \gamma_0 > 3/2$  and  $\mathfrak{d} \geq 1$ , then for all  $u \in \mathcal{J}_\gamma^\omega(Q^\pm; C, A, \mathfrak{d})$  there exist  $C_{\text{hp}}^\pm, b_{\text{hp}}$  such that, for all  $\ell \in \mathbb{N}$ , with  $p \geq c_0^\pm \ell^\mathfrak{d}$  for a sufficiently large  $c_0^\pm > 0$  independent of  $\ell$ , there holds*

$$\|u - \Pi_{\text{hp}}^{\ell,p,\pm} u\|_{H^1(Q^\pm)} \leq C_{\text{hp}}^\pm e^{-b_{\text{hp}}^\pm \ell}. \tag{53}$$

Furthermore, there holds  $\dim(X_{\text{hp}}^{\ell,p}) \simeq \ell^{3\mathfrak{d}+1}$ .

*Proof*  $\Pi_{\text{hp}}^{\ell,p,\pm}$  is continuous in the sub-patches  $Q^+$  and  $Q^-$ . It remains to check the continuity across the interpatch interface  $F^\pm = \{0\} \times (0, 1)^2$ . By construction, all elemental faces belonging to the interface are regular, hence, by Lemma 7, the discontinuous projector  $\Pi_{\text{hp},\text{disc}}^{\ell,p}$  is continuous across these faces.

We consider the error contribution from interior mesh layers, i.e., from all elements in  $\mathcal{L}_j^\ell, j > 0$ . For all faces  $F$  in interior mesh layers which are situated

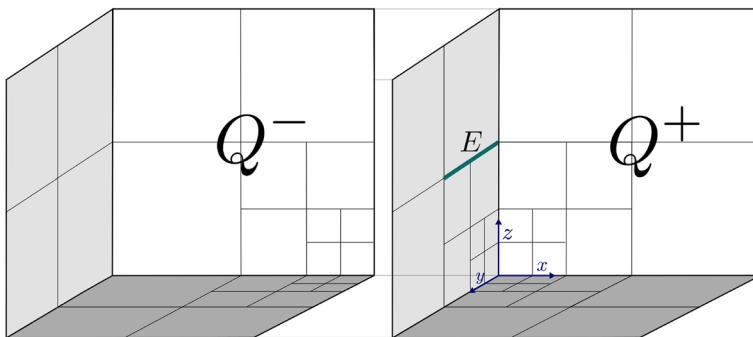


**Fig. 11** The mesh patches  $\mathcal{G}^{\ell,-}$  on  $Q^-$  and  $\mathcal{G}^\ell$  on  $Q^+$ . An edge  $E$  belonging to the interpatch interface is highlighted

perpendicular to  $F^\pm$ , we have

$$\llbracket \Pi_{\text{hp, disc}}^{\ell, p} u + \mathfrak{L}^E(\Pi_{\text{hp, disc}}^{\ell, p} u) \rrbracket_F \cdot n = 0.$$

We now consider any edge  $E$  belonging to  $F^\pm$  and separating the mesh levels  $\mathcal{L}_k^\ell$  and  $\mathcal{L}_{k+1}^\ell$ , see Fig. 11 for an example. By the continuity of the discontinuous projector across regular faces

$$\llbracket \Pi_{\text{hp, disc}}^{\ell, p} u \rrbracket_E = \llbracket \Pi_{\text{hp, disc}}^{\ell, p, -} u \rrbracket_E,$$

where  $\Pi_{\text{hp, disc}}^{\ell, p, -}$  is the discontinuous projector in patch  $\mathcal{G}^{\ell, -}$ . Therefore, from definitions (49), (50), and (51), we conclude that the projection operator is continuous across interior mesh layers  $\mathcal{L}_k^\ell$ ,  $k > 0$ .

When dealing with the terminal layer  $\mathcal{L}_0^\ell$ , we note that the discontinuous projector is constant hence continuous. The nodal liftings are continuous by the symmetry of their construction; the edge liftings are then continuous by the same argument as in interior mesh layers, and this gives the continuity between patches.

Finally, (53) follows from the application of the corresponding approximation results in each patch. □

We can directly extend the construction in the proof of the above lemma to the remaining patches  $R^m = (0, a_1) \times (0, a_2) \times (0, a_3)$  with  $(a_1, a_2, a_3) \in \{-1, 1\}^3$ ,  $m = 0, \dots, 7$ . Recall that  $\Pi_{\text{hp}}^{\ell, p, m}$  is the conforming  $hp$  projector in patch  $R^m$ , obtained by reflection from the one defined in  $(0, 1)^3$ , see (55). Recall also that the functions  $\psi^m$  are the reflections from  $(0, 1)^3$  to  $R^m$ . For  $\gamma > 3/2$ , given the finite element space on  $R = \bigcup_m R^m$ ,

$$X_{\text{hp}}^{\ell, p}(R) = \{v \in H^1(R) : v \circ \psi^m \in X_{\text{hp}}^{\ell, p}, m = 0, \dots, 7\},$$

we define the global projector

$$\Pi_{\text{hp}}^{\ell, p, R} : \mathcal{J}_\gamma^\infty(R) \rightarrow X_{\text{hp}}^{\ell, p}(R) \quad \text{such that} \quad \Pi_{\text{hp}}^{\ell, p, R} v|_{R^m} = \Pi_{\text{hp}}^{\ell, p, m} v|_{R^m}. \quad (54)$$

Then, by the same arguments as in Lemma 9 applied to all interpatch interface, there holds the following result.

**Corollary 1** *The operator  $\Pi_{\text{hp}}^{\ell, p, R}$  defined in (54) is conforming in  $H^1(R)$ . Furthermore, if  $\gamma \geq \gamma_0 > 3/2$  and  $\mathfrak{d} \geq 1$ , then for all  $u \in \mathcal{J}_\gamma^\infty(R; C, A, \mathfrak{d})$  exist constants  $C_{\text{hp}}^R, b_{\text{hp}}^R$  (that depend on  $C, A$ , and  $\mathfrak{d}$ ) such that, for every  $\ell \in \mathbb{N}$  there holds, with  $p \geq c_0^R \ell^\mathfrak{d}$  for some  $c_0^R > 0$  independent of  $\ell$ , the error bound*

$$\|u - \Pi_{\text{hp}}^{\ell, p, R} u\|_{H^1(Q^\pm)} \leq C_{\text{hp}}^R e^{-b_{\text{hp}}^R \ell}.$$

Furthermore,  $\dim(X_{\text{hp}}^{\ell, p}) \simeq \ell^{3\mathfrak{d}+1}$ .

### Appendix B. Extension of rank bounds to domains with internal singularity

As a corollary to Theorem 1, we show here how the result can be generalized to functions that have the singularity in an internal point of the domain. As an example, we will consider the case of the axiparallel cube  $R = (-1, 1)^3$  and of functions in the weighted analytic class  $\mathcal{J}_\gamma^\infty(R; C, A, \delta)$  with singularity at the origin. The cube  $R$  can be decomposed into eight congruent cubes, all with the singularity situated at one corner, that we will denote by  $R^m, m = 0, \dots, 7$ . For each  $m$ , there exist  $(a_1, a_2, a_3) \in \{-1, 1\}^3$  such that  $R^m = (0, a_1) \times (0, a_2) \times (0, a_3)$ . We do not need to specify any particular ordering, but choose, without loss of generality  $R^0 = Q$ . We will denote  $\psi^m : Q \rightarrow R^m$  the linear transformation from  $Q = R^0$  to  $R^m$  such that for all  $(x_1, x_2, x_3) \in Q$

$$\psi^m : \begin{pmatrix} x_1 \\ x_2 \\ x_3 \end{pmatrix} \mapsto \begin{pmatrix} a_1 & & \\ & a_2 & \\ & & a_3 \end{pmatrix} \begin{pmatrix} x_1 \\ x_2 \\ x_3 \end{pmatrix}, \quad \text{with } (a_1, a_2, a_3) \in \{-1, 1\}^3,$$

i.e.,  $\psi^m$  only operates reflections with respect to interpatch interfaces. Note that  $\psi^0$  is the identity.

Furthermore, we define by  $\mathcal{A}^{\ell,m}$  the analysis operator (see Section 3.1.4) of patch  $R^m$ , such that

$$\mathcal{A}^{\ell,m} v|_{R^m} \in \mathbb{R}^{2^\ell \times 2^\ell \times 2^\ell} \quad \text{and} \quad \mathcal{A}^{\ell,m} v = \mathcal{A}^\ell (v \circ \psi^m).$$

#### B.1 Quasi interpolation on $R$

We can then define the local  $hp$  projection and interpolation operators in the patches  $R^m, m = 0, \dots, 7$ , in the same way, i.e., as

$$\Pi_{hp}^{\ell,p,m} v = \left( \Pi_{hp}^{\ell,p} (v \circ \psi^m) \right) \circ (\psi^m)^{-1} \quad \text{and} \quad \mathcal{I}^{\ell,m} v = \left( \mathcal{I}^\ell (v \circ \psi^m) \right) \circ (\psi^m)^{-1} \tag{55}$$

in each  $R^m$ . The definition of the local quasi interpolation operators also follows directly, by setting  $\mathfrak{P}^{\ell,m} = \mathcal{I}^{\ell,m} \Pi_{hp}^{\ell,p,m}$ , for  $m = 0, \dots, 7$ . Then, the global (on  $R$ ) quasi interpolation operator is the operator  $\mathfrak{P}_{|R^m}^{\ell,R}$  such that  $\mathfrak{P}_{|R^m}^{\ell,R} = \mathfrak{P}^{\ell,m}$  for all  $m = 0, \dots, 7$ .

#### B.2 Patchwise QTT formats

It is now straightforward to consider the ‘‘patchwise QTT’’ formats which are constructed by adding a patch index to the formats considered so far. For a function  $u \in \mathcal{J}_\gamma^\infty(R)$ , we consider the tensor  $A \in \mathbb{R}^{8 \times 2^\ell \times 2^\ell \times 2^\ell}$  such that for  $m = 0, \dots, 7$

$$A_{m,\dots,\dots} = \mathcal{A}^{\ell,m} \mathfrak{P}^{\ell,m} u.$$

Then, writing with the usual notation  $i = \overline{i_1 \dots i_\ell}, j = \overline{j_1 \dots j_\ell}$  and  $k = \overline{k_1 \dots k_\ell}$ ,



- $A$  admits a *patchwise, classic QTT* decomposition if

$$A_{m,i,j,k} = U_{m,:}^1(i_1) \cdots U^\ell(i_\ell) V^1(j_1) \cdots V^\ell(j_\ell) W^1(k_1) \cdots W^\ell(k_\ell)$$

for all  $m = 0, \dots, 7$ ,  $(i, j, k) \in \{0, \dots, 2^\ell - 1\}^3$  and where  $U_{m,:}^1(i_1)$  indicates the  $m$ th row of  $U^1(i_1)$  with cores defined as in (14) and the following convention on ranks

$$r_0 := 8, \quad r_{3\ell} := 1.$$

Note that the only modification with respect to Definition 3 is the convention  $r_0 = 8$ .

- $A$  admits a *patchwise, transposed order QTT* decomposition if

$$A_{m,i,j,k} = U_{m,:}^1(\overline{i_1 j_1 k_1}) \cdots U^\ell(\overline{i_\ell j_\ell k_\ell}) \tag{56}$$

with cores as in Definition 4 and with the restriction on the ranks  $r_0 = 8, r_\ell = 1$ .

- $A$  admits a *patchwise, Tucker QTT* decomposition if

$$A_{m,i,j,k} = \sum_{\beta_1, \beta_2, \beta_3=1}^{R_1, R_2, R_3} G_{\beta_1, \beta_2, \beta_3}^m U_{\beta_1}^1(i_1) U^2(i_2) \cdots U^\ell(i_\ell) V_{\beta_2}^1(j_1) V^2(j_2) \cdots V^\ell(j_\ell) W_{\beta_3}^1(k_1) W^2(k_2) \cdots W^\ell(k_\ell). \tag{57}$$

where, clearly, the Tucker core is now a four-dimensional array of size  $8 \times R_1 \times R_2 \times R_3$ .

Let  $\mathcal{T}^{\ell,R}$  be the tensor product mesh on  $R$  given by

$$\mathcal{T}^{\ell,R} = \{(2^{-\ell}i, 2^{-\ell}(i + 1)) \times (2^{-\ell}j, 2^{-\ell}(j + 1)) \times (2^{-\ell}k, 2^{-\ell}(k + 1)), (i, j, k) \in \{-2^\ell + 1, \dots, 2^\ell - 1\}^3\}.$$

We define the finite element space in  $R$  as

$$X^{\ell,R} = \left\{ v \in H_0^1(R) : v|_K \in \mathbb{Q}_1(K), \text{ for all } K \in \mathcal{T}^{\ell,R} \right\}.$$

The following proposition is then a direct consequence of Theorem 1 and of Corollary 1.

**Proposition 5** *Assume  $\gamma > 3/2$ ,  $C_u > 0$ ,  $A_u > 0$ ,  $\mathfrak{d} \geq 1$ , and  $0 < \varepsilon_0 \ll 1$ . Furthermore, assume the function  $u$  belongs to the weighted Gevrey class  $u \in \mathcal{J}_\gamma^\omega(R; C_u, A_u, \gamma, \mathfrak{d}) \cap H_0^1(R)$ . Then, for all  $0 < \varepsilon \leq \varepsilon_0$ , there exists  $\ell \in \mathbb{N}$  and  $v_{\text{qtd}}^\ell \in X^{\ell,R}$  such that*

$$\|u - v_{\text{qtd}}^\ell\|_{H^1(Q)} \leq \varepsilon$$

and the multi-dimensional array  $V_{\text{qtd}}^\ell \in \mathbb{R}^{8 \times 2^\ell \times 2^\ell \times 2^\ell}$  such that  $(V_{\text{qtd}}^\ell)_{m, :, :, :} = \mathcal{A}^{\ell,m} v_{\text{qtd}}^\ell$ ,  $m = 0, \dots, 7$  admits a patchwise representation with

$$N_{\text{dof}} \leq C |\log \varepsilon|^K$$

degrees of freedom, with a positive constant  $C$  independent of  $\varepsilon$  and

$$\kappa = \begin{cases} 4\mathfrak{d} + 3 & \text{for patchwise classic QTT,} \\ 6\mathfrak{d} + 1 & \text{for patchwise transposed order QTT,} \\ 3\mathfrak{d} + 3 & \text{for patchwise Tucker QTT.} \end{cases}$$

*Proof* Here, we retrace the steps of the proofs of Lemmas 2, 3, and 5, generalizing them to the multipatch case.

**Patchwise classic QTT** The tensor  $V_{\text{qtt}}^\ell$  can be written as the product

$$(V_{\text{qtd}}^\ell)_{m,i,j,k} = U^0(m)U^1(i_1) \cdots U^\ell(i_\ell)V^1(j_1) \cdots V^\ell(j_\ell)W^1(k_1) \cdots W^\ell(k_\ell),$$

where the bounds on the ranks of the cores  $U^1, \dots, U^\ell$  and the first rank of the core  $V^1$  are multiplied by 8, while the other bounds are left unchanged with respect to the single patch case. The multiplication of the cores  $U^0$  and  $U^1$  gives the multipatch formulation.

**Patchwise transposed order QTT** The row space of the unfolding matrices

$$V_{\overline{m\xi_1\eta_1\zeta_1}, \overline{\xi_2\eta_2\zeta_2}}^{(q)} = (V_{\text{qtd}}^\ell)_{m, \overline{\xi_1\xi_2}, \overline{\eta_1\eta_2}, \overline{\zeta_1\zeta_2}}$$

defined for  $m \in 0, \dots, 7$ ,  $\xi_1, \eta_1, \zeta_1 \in \{0, \dots, 2^q - 1\}$ , and  $\xi_2, \eta_2, \zeta_2 \in \{0, \dots, 2^{\ell-q} - 1\}$  is bounded asymptotically by the same quantity as the one of the unfolding matrix in (30), by symmetry. Thus,  $V_{\text{qtd}}^\ell$  admits a decomposition such that

$$(V_{\text{qtd}}^\ell)_{m,i,j,k} = U^0(m)U^1(\overline{i_1j_1k_1}) \cdots U^\ell(\overline{i_\ell j_\ell k_\ell}).$$

By multiplying  $U_0(m)$  and  $U_1(\overline{i_1j_1k_1})$  for all  $m = 0, \dots, 7$  and  $i_1, j_1, k_1 \in \{0, 1\}$ , we obtain a representation of the form (56).

**Patchwise Tucker QTT** We Tucker-decompose the tensor  $V_{\text{qtd}}^\ell$ , thus obtaining, by the same arguments that we used for (32),

$$V_{\text{qtd}}^\ell = \sum_{\beta_1, \beta_2, \beta_3=1}^{R_T} \sum_{\beta_0=1}^{R_P} G_{\beta_0, \beta_1, \beta_2, \beta_3} Z_{\beta_0} \otimes U_{\beta_1} \otimes V_{\beta_2} \otimes W_{\beta_3},$$

where  $R_T \leq C\ell^{\mathfrak{d}+1}$ . Then, by contracting the core  $G$  and the factor  $Z$  over the index  $\beta_0$  and by deriving the existence of the block QTT decomposition of the Tucker factors  $U, V, W$  as in (33), we obtain the existence of a representation of  $V_{\text{qtd}}^\ell$  of the form (57). □

*Remark 9* In Proposition 5, we consider the approximation of functions in the cube  $R = (-1, 1)$  for ease of notation. Nonetheless, the argument and the result extend, without major modification, to  $\tilde{R} = (-a_1, b_1) \times (-a_2, b_2) \times (-a_3, b_3)$ , with  $a_i, b_i > 0, i = 1, 2, 3$ , and with a point singularity at the origin. This implies, by translation, that given a cube of fixed size, we can obtain bounds on patchwise quantized tensor representations that are *uniform in the location of the singularity*.

### Appendix C. QTT representation of prolongation matrices

In order to evaluate the error  $\varepsilon_\ell$ , we need a tensor of  $\nabla u_{\text{qtd}}^{\ell,\delta}$  evaluated on the background mesh with  $L$  levels of refinement and have it represented using the respective tensor decomposition without accessing all its elements. This can be implemented as a multiplication by the prolongation matrices in the respective tensor format. To introduce the prolongation matrices, we start by considering the one-dimensional piecewise linear space on the background mesh with  $\ell$  levels (recall that  $I_j^\ell = (2^{-\ell}j, 2^{-\ell}(j + 1))$ )

$$X_{1d,0}^\ell = \{v \in H^1((0, 1)) : v(1) = 0 \text{ and } v|_{I_j^\ell} \in \mathbb{P}_1(I_j^\ell), j = 0, \dots, 2^\ell - 1\}.$$

Furthermore, we introduce the one-dimensional analysis operator  $\mathcal{A}_{1d}^\ell : H^1((0, 1)) \rightarrow \mathbb{R}^{2^\ell}$  as

$$\left(\mathcal{A}_{1d}^\ell v\right)_i = v(2^{-\ell}i), \quad i = 0, \dots, 2^\ell - 1.$$

Then, for every  $L > \ell$ , the one-dimensional prolongation operator  $P_{\text{p.l.}}^{(\ell \rightarrow L)} \in \mathbb{R}^{2^L \times 2^\ell}$  is realized by the matrix such that

$$P_{\text{p.l.}}^{(\ell \rightarrow L)} \left(\mathcal{A}_{1d}^\ell v_{\text{qtd}}^\ell\right) = \mathcal{A}_{1d}^L v_{\text{qtd}}^\ell \quad \text{for all } v_{\text{qtd}}^\ell \in X_{1d,0}^\ell. \tag{58}$$

In the same vein, the one-dimensional prolongation operator for piecewise constant function is such that

$$P_{\text{p.c.}}^{(\ell \rightarrow L)} \left(\mathcal{A}_{1d}^\ell v_{\text{qtd}}^\ell\right) = \mathcal{A}_{1d}^L v_{\text{qtd}}^\ell$$

for all

$$v_{\text{qtd}}^\ell \in X_{\text{p.c.,1d}}^\ell = \{v \in L^\infty((0, 1)) : v|_{[x_j, x_{j+1}]} \in \mathbb{P}_0([x_j, x_{j+1}]), j = 0, \dots, 2^\ell - 1\}.$$

Recall that we consider functions  $u$  such that  $u|_\Gamma = 0$ , where  $\Gamma = \partial Q \setminus \{x = (x_1, x_2, x_3) \in \partial Q : x_1 x_2 x_3 = 0\}$ . In this case, the three-dimensional prolongation matrices from mesh level  $\ell$  to  $L > \ell$ , can be written as a tensor product of the one-dimensional piecewise linear and piecewise constant prolongation matrices, which read:

$$P_{\text{p.l.}}^{(\ell \rightarrow L)} = 2^{\ell-L} \left( I^{(\ell)} \otimes \begin{bmatrix} 2^{L-\ell} \\ \vdots \\ 2 \\ 1 \end{bmatrix} + J^{(\ell)} \otimes \begin{bmatrix} 0 \\ 1 \\ \vdots \\ 2^{L-\ell} - 1 \end{bmatrix} \right) \in \mathbb{R}^{2^L \times 2^\ell} \tag{59}$$

and

$$P_{\text{p.c.}}^{(\ell \rightarrow L)} = I^{(\ell)} \otimes \begin{bmatrix} 1 \\ \vdots \\ 1 \end{bmatrix}_{2^{L-\ell}} \in \mathbb{R}^{2^L \times 2^\ell},$$

respectively, where we used the notation

$$I^{(\ell)} = \begin{bmatrix} 1 & & & \\ & \ddots & & \\ & & \ddots & \\ & & & 1 \end{bmatrix}_{2^\ell \times 2^\ell}, \quad S^{(\ell)} = \begin{bmatrix} 0 & 1 & & \\ & \ddots & \ddots & \\ & & \ddots & 1 \\ & & & 0 \end{bmatrix}_{2^\ell \times 2^\ell}.$$

The matrix  $P_{\text{p.c.}}^{(\ell \rightarrow L)}$  can be represented with QTT ranks  $1, 1, \dots, 1$ , as it has Kronecker product structure, since  $I^{(\ell)} = (I^{(1)})^{\otimes \ell}$  and

$$P_{\text{p.c.}}^{(\ell \rightarrow L)} = I^{(\ell)} \otimes e^{\otimes (L-\ell)}, \quad e = \begin{bmatrix} 1 \\ 1 \end{bmatrix}.$$

We now show, in Proposition 6 below, that  $P_{\text{p.l.}}^{(\ell \rightarrow L)}$  also has low-rank QTT structure. For convenience, we introduce the matricization operator  $\mathcal{M} : \mathbb{R}^{r_1 \times m \times n \times r_2} \rightarrow \mathbb{R}^{mr_1 \times nr_2}$  such that:

$$(\mathcal{M}(X))_{\overline{\alpha_1 i}, \overline{\alpha_2 j}} = (X(i, j))_{\alpha_1, \alpha_2},$$

$$i = 1, \dots, m, \quad j = 1, \dots, n, \quad \alpha_i = 1, \dots, r_i, \quad i = 1, 2,$$

that allows to recast tensor cores as matrices. The following proposition holds.

**Proposition 6** *The matrix  $P_{\text{p.l.}}^{(\ell \rightarrow L)}$ ,  $L > \ell$ , defined in (59) has explicit QTT representation with ranks  $2, 2, \dots, 2$ . In particular, for each  $i_1, \dots, i_L \in \{0, 1\}$ ,  $j_1, \dots, j_\ell \in \{0, 1\}$  and  $j_{\ell+1}, \dots, j_L \in \{0\}$ :*

$$\left( P_{\text{p.l.}}^{(\ell \rightarrow L)} \right)_{\overline{i_1 \dots i_L, j_1 \dots j_L}} = Q_1(i_1, j_1) \dots Q_L(i_L, j_L)$$

where the matricizations read

$$\begin{aligned} \mathcal{M}(Q_1) &= \begin{bmatrix} I & J \end{bmatrix}, \\ \mathcal{M}(Q_i) &= \begin{bmatrix} I & J \\ & J^\top \end{bmatrix}, \quad i = 2, \dots, \ell, \\ \mathcal{M}(Q_i) &= \frac{1}{2} \begin{bmatrix} p & \delta_1 \\ \delta_2 & q \end{bmatrix}, \quad i = \ell + 1, \dots, L - 1, \\ \mathcal{M}(Q_L) &= \frac{1}{2} \begin{bmatrix} p \\ \delta_2 \end{bmatrix}, \end{aligned}$$

with blocks given by

$$I = \begin{bmatrix} 1 & 0 \\ 0 & 1 \end{bmatrix}, \quad J = \begin{bmatrix} 0 & 1 \\ 0 & 0 \end{bmatrix}, \quad p = \begin{bmatrix} 2 \\ 1 \end{bmatrix}, \quad q = \begin{bmatrix} 1 \\ 2 \end{bmatrix}, \quad \delta_1 = \begin{bmatrix} 1 \\ 0 \end{bmatrix}, \quad \delta_2 = \begin{bmatrix} 0 \\ 1 \end{bmatrix}.$$

*Proof* First, we introduce the notation

$$p^{(i)} = 2^{-i} \begin{bmatrix} 2^i \\ \vdots \\ 2 \\ 1 \end{bmatrix}, \quad q^{(i)} = 2^{-i} \begin{bmatrix} 0 \\ 1 \\ \vdots \\ 2^i - 1 \end{bmatrix},$$

so that

$$P_{p.l.}^{(\ell \rightarrow L)} = I^{(\ell)} \otimes p^{(L-\ell)} + J^{(\ell)} \otimes q^{(L-\ell)}.$$

Since  $I^{(\ell)} = I \otimes I^{(\ell-1)}$  and  $J^{(\ell)} = I \otimes J^{(\ell-1)} + J \otimes (J^\top)^{\otimes(\ell-1)}$  and using the operation  $\otimes$  that denotes the strong Kronecker product between block matrices, in which matrix-matrix multiplication of blocks is replaced by a Kronecker product<sup>6</sup>, we obtain

$$\begin{aligned} P_{p.l.}^{(\ell \rightarrow L)} &= [I \ J] \otimes \begin{bmatrix} I^{(\ell-1)} & J^{(\ell-1)} \\ & (J^\top)^{\otimes(\ell-1)} \end{bmatrix} \otimes \begin{bmatrix} p^{(L-\ell)} \\ q^{(L-\ell)} \end{bmatrix} \\ &= [I \ J] \otimes [I \ J]^{*\otimes(\ell-1)} \otimes \begin{bmatrix} p^{(L-\ell)} \\ q^{(L-\ell)} \end{bmatrix}. \end{aligned}$$

We complete the proof by the observations that

$$\begin{bmatrix} p^{(i)} \\ q^{(i)} \end{bmatrix} = \frac{1}{2} \begin{bmatrix} p & \delta_1 \\ \delta_2 & q \end{bmatrix} \otimes \begin{bmatrix} p^{(i-1)} \\ q^{(i-1)} \end{bmatrix}, \quad i > 1, \quad p^{(1)} = \frac{1}{2} \begin{bmatrix} 2 \\ 1 \end{bmatrix}, \quad q^{(1)} = \frac{1}{2} \begin{bmatrix} 0 \\ 1 \end{bmatrix}.$$

□

**Corollary 2** Let  $v_{\text{qtt}}^\ell \in X_{\text{id},0}^\ell$  and let  $\mathcal{A}_{\text{id}}^\ell v_{\text{qtt}}^\ell$  have QTT ranks  $r_1, r_2, \dots, r_{\ell-1}$ . Then, for any  $L > \ell$ , the vector  $\mathcal{A}_{\text{id}}^L v_{\text{qtt}}^\ell = \{v_{\text{qtt}}^\ell(x_i)\}_{i=0}^{2^L-1}$ ,  $x_i = 2^{-L} i$  can be represented with QTT ranks equal to  $2r_1, 2r_2, \dots, 2r_{\ell-1}$ .

*Proof* According to Proposition 6, the matrix  $P_{p.l.}^{(\ell \rightarrow L)}$  has ranks  $2, 2, \dots, 2$ . The statement then follows from the fact that the multiplication in (58) of a TT-matrix with ranks  $R_1, \dots, R_{\ell-1}$  by a TT-vector with the ranks  $r_1, \dots, r_{\ell-1}$ , leads to the TT representation with ranks  $R_1 r_1, \dots, R_{\ell-1} r_{\ell-1}$ , see [65]. □

The multidimensional prolongation matrices are assembled as Kronecker products of the one-dimensional matrices  $P_{p.l.}^{(\ell \rightarrow L)}$  and/or  $P_{p.c.}^{(\ell \rightarrow L)}$ . For example, to find the values of  $v_{\text{qtt}}^\ell \in X^\ell$  on a mesh with  $L$  levels, the matrix

$$P_{p.l.}^{(\ell \rightarrow L)} \otimes P_{p.l.}^{(\ell \rightarrow L)} \otimes P_{p.l.}^{(\ell \rightarrow L)}$$

represented in the respective format is applied to the coefficient vector  $\mathcal{A}^\ell v_{\text{qtt}}^\ell$ .

<sup>6</sup>Formally, the strong Kronecker product of two  $2 \times 2$  block matrices is defined as the following  $2 \times 2$  block matrix:

$$\begin{bmatrix} A_{11} & A_{12} \\ A_{21} & A_{22} \end{bmatrix} \otimes \begin{bmatrix} B_{11} & B_{12} \\ B_{21} & B_{22} \end{bmatrix} = \begin{bmatrix} A_{11} \otimes B_{11} + A_{12} \otimes B_{21} & A_{11} \otimes B_{12} + A_{12} \otimes B_{22} \\ A_{21} \otimes B_{11} + A_{22} \otimes B_{21} & A_{21} \otimes B_{12} + A_{22} \otimes B_{22} \end{bmatrix}.$$

**Acknowledgements** The authors are grateful to the reviewers for their comments which contributed to the improvement of the paper. Ch. Schwab acknowledges stimulating discussions at WS1936 at the Mathematical Research Institute Oberwolfach 02-06Sep2019.

**Funding** Open access funding provided by Swiss Federal Institute of Technology Zurich. M. Rakhuba was supported by ETH Grant ETH-44 17-1.

## Declarations

**Conflict of interest** The authors declare no competing interests.

**Open Access** This article is licensed under a Creative Commons Attribution 4.0 International License, which permits use, sharing, adaptation, distribution and reproduction in any medium or format, as long as you give appropriate credit to the original author(s) and the source, provide a link to the Creative Commons licence, and indicate if changes were made. The images or other third party material in this article are included in the article's Creative Commons licence, unless indicated otherwise in a credit line to the material. If material is not included in the article's Creative Commons licence and your intended use is not permitted by statutory regulation or exceeds the permitted use, you will need to obtain permission directly from the copyright holder. To view a copy of this licence, visit <http://creativecommons.org/licenses/by/4.0/>.

## References

1. Ali, M., Nouy, A.: Approximation with tensor networks. Part I: Approximation Spaces. arXiv e-prints arXiv:2007.00118 (2020)
2. Ali, M., Nouy, A.: Approximation with tensor networks. Part II: Approximation Rates for Smoothness Classes. arXiv e-prints arXiv:2007.00128 (2020)
3. Ali, M., Nouy, A.: Approximation with tensor networks. Part III: Multivariate Approximation. arXiv e-prints arXiv:2101.11932 (2021)
4. Babuška, I., Guo, B.Q.: The h-p version of the finite element method for problems with nonhomogeneous essential boundary condition. *Comput. Methods Appl. Mech. Eng.* **74**(1), 1–28 (1989). [https://doi.org/10.1016/0045-7825\(89\)90083-2](https://doi.org/10.1016/0045-7825(89)90083-2)
5. Bachmayr, M., Kazeev, V.: Stability of low-rank tensor representations and structured multilevel preconditioning for elliptic PDEs. *Found. Comput. Math.* **20**(5), 1175–1236 (2020). <https://doi.org/10.1007/s10208-020-09446-z>
6. Bachmayr, M., Schneider, R., Uschmajew, A.: Tensor networks and hierarchical tensors for the solution of high-dimensional partial differential equations. *Found. Comput. Math.* **16**(6), 1423–1472 (2016). <https://doi.org/10.1007/s10208-016-9317-9>
7. Ballani, J., Grasedyck, L.: Tree adaptive approximation in the hierarchical tensor format. *SIAM J. Sci. Comput.* **36**(4), A1415–A1431 (2014). <https://doi.org/10.1137/130926328>
8. Ballani, J., Grasedyck, L., Kluge, M.: Black box approximation of tensors in hierarchical Tucker format. *Linear Algebra Appl.* **438**(2), 639–657 (2013). <https://doi.org/10.1016/j.laa.2011.08.010>
9. Beylkin, G., Monzón, L.: Approximation by exponential sums revisited. *Appl. Comput. Harmon. A.* **28**(2), 131–149 (2010)
10. Boyer, R.H., Lindquist, R.W.: Maximal analytic extension of the Kerr metric. *J. Mathematical Phys.* **8**, 265–281 (1967). <https://doi.org/10.1063/1.1705193>
11. Cancès, E., Chakir, R., Maday, Y.: Numerical analysis of nonlinear eigenvalue problems. *J. Sci. Comput.* **45**(1-3), 90–117 (2010). <https://doi.org/10.1007/s10915-010-9358-1>, <http://www.scopus.com/inward/record.url?eid=2-s2.0-77956139484&partnerID=ZOTx3y1>
12. Cancès, E., Defranceschi, M., Kutzelnigg, W., Le Bris, C., Maday, Y.: Computational quantum chemistry: A primer. In: *Handbook of Numerical Analysis, Vol. X, Handb. Numer. Anal., X*, pp. 3–270, North-Holland, Amsterdam (2003)
13. Cancès, E., Le Bris, C., Maday, Y.: *Méthodes mathématiques en chimie quantique : une introduction*. Springer (2006)

14. Costabel, M., Dauge, M., Nicaise, S.: Mellin analysis of weighted Sobolev spaces with non-homogeneous norms on cones. Springer, New York. [https://doi.org/10.1007/978-1-4419-1341-8\\_4](https://doi.org/10.1007/978-1-4419-1341-8_4) (2010)
15. Costabel, M., Dauge, M., Nicaise, S.: Analytic regularity for linear elliptic systems in polygons and polyhedra. *Math. Model. Methods. Appl. Sci.* **22**(08), <https://doi.org/10.1142/S0218202512500157> (2012)
16. Costabel, M., Dauge, M., Nicaise, S.: Weighted analytic regularity in polyhedra. *Comput. Math. Appl* **67**(4), 807–817 (2014). <https://doi.org/10.1016/j.camwa.2013.03.006>
17. Costabel, M., Dauge, M., Schwab, C.: Exponential convergence of hp-FEM for Maxwell equations with weighted regularization in polygonal domains. *Math. Model. Methods. Appl. Sci.* **15**(4), 575–622 (2005). <http://www.worldscientific.com/doi/abs/10.1142/S0218202505000480>
18. Dolgov, S., Khoromskij, B.: Two-level QTT-tucker format for optimized tensor calculus. *SIAM J. Matrix An. Appl.* **34**(2), 593–623 (2013). <https://doi.org/10.1137/120882597>
19. Dolgov, S.V., Khoromskij, B.N., Oseledets, I.V.: Fast solution of parabolic problems in the tensor train/quantized tensor train format with initial application to the Fokker–Planck equation. *SIAM J. Sci. Comput.* **34**(6), A3016–A3038 (2012)
20. Feischl, M., Schwab, C.: Exponential convergence in  $H^1$  of hp-FEM for Gevrey regularity with isotropic singularities. *Numer. Math.* **144**(2), 323–346 (2020). <https://doi.org/10.1007/s00211-019-01085-z>
21. Flad, H., Schneider, R., Schulze, B.W.: Asymptotic regularity of solutions to Hartree–Fock equations with Coulomb potential. *Mathematical Methods in the Applied Sciences* (June) 2172–2201. <https://doi.org/10.1002/mma.1021/abstract> (2008)
22. Fournais, S., Hoffmann-Ostenhof, M., Hoffmann-Ostenhof, T., Østergaard Sørensen, T.: Analytic structure of many-body Coulombic wave functions. *Comm. Math. Phys.* **289**(1), 291–310 (2009). <https://doi.org/10.1007/s00220-008-0664-5>
23. Fournais, S., Hoffmann-Ostenhof, M., Hoffmann-Ostenhof, T., Østergaard Sørensen, T.: Analytic structure of solutions to multiconfiguration equations. *J. Phys. A* **42**(31), 315208, 11 (2009). <https://doi.org/10.1088/1751-8113/42/31/315208>
24. Georgoulis, E.H.: Inverse-type estimates on hp-finite element spaces and applications. *Math. Comput.* **77**(261), 201–219 (2008). <https://doi.org/10.1090/S0025-5718-07-02068-6>
25. Girault, V., Raviart, P.A.: *Finite Element Methods for Navier-Stokes Equations* Springer Series in Computational Mathematics, vol. 5. Springer, Berlin (1986). <https://doi.org/10.1007/978-3-642-61623-5>
26. Grasedyck, L.: Polynomial approximation in Hierarchical Tucker format by vector-tensorization. Preprint 308, Institut für Geometrie und Praktische Mathematik, RWTH Aachen. [http://www.igpm.rwth-aachen.de/Download/reports/pdf/IGPM308\\_k.pdf](http://www.igpm.rwth-aachen.de/Download/reports/pdf/IGPM308_k.pdf) (2010)
27. Grasedyck, L., Kressner, D., Tobler, C.: A literature survey of low-rank tensor approximation techniques. *GAMM-Mitt.* **36**(1), 53–78 (2013)
28. Grisvard, P.: *Elliptic problems in nonsmooth domains*. Monographs and Studies in Mathematics, vol. 24, p. xiv+410. Pitman (Advanced Publishing Program), Boston, MA (1985)
29. Guo, B., Babuška, I.: The h-p version of the finite element method - Part 1: The basic approximation results. *Comput. Mech.* **1**(1), 21–41 (1986). <https://doi.org/10.1007/BF00298636>
30. Guo, B., Babuška, I.: The h-p version of the finite element method - Part 2: General results and applications. *Comput. Mech.* **1**(3), 203–220 (1986). <https://doi.org/10.1007/BF00272624>
31. Guo, B., Schwab, C.: Analytic regularity of Stokes flow on polygonal domains in countably weighted Sobolev spaces. *J. Comput. Appl. Math.* **190**(1–2), 487–519 (2006). <https://doi.org/10.1016/J.CAM.2005.02.018>
32. Hackbusch, W.: *Tensor spaces and numerical tensor calculus*. Springer Series in Computational Mathematics, vol. 42, p. xxiv+500. Springer, Heidelberg (2012). <https://doi.org/10.1007/978-3-642-28027-6>
33. Hackbusch, W.: *Hierarchical Matrices: Algorithms and Analysis* Springer Series in Computational Mathematics, vol. 49. Springer, Heidelberg (2015). <https://doi.org/10.1007/978-3-662-47324-5>
34. Hackbusch, W., Khoromskij, B.N.: Low-rank Kronecker-product approximation to multi-dimensional nonlocal operators. Part I. separable approximation of multi-variate functions. *Computing* **76**(3–4), 177–202 (2006)
35. Hackbusch, W., Khoromskij, B.N., Tyrtshnikov, E.E.: Approximate iterations for structured matrices. *Numer. Math.* **109**(3), 365–383 (2008). <https://doi.org/10.1007/s00211-008-0143-0>

36. Kazeev, V.: Quantized Tensor-Structured Finite Elements for Second-Order Elliptic PDEs in Two Dimensions, Ph.D. thesis, ETH Zürich. <https://doi.org/10.3929/ethz-a-010554062> (2015)
37. Kazeev, V., Khoromskij, B.: Low-rank explicit QTT representation of the Laplace operator and its inverse. *SIAM J. Matrix Anal. Appl.* **33**(3), 742–758 (2012). <https://doi.org/10.1137/100820479>
38. Kazeev, V., Oseledets, I., Rakhuba, M., Schwab, C.: QTT-Finite-element approximation for multi-scale problems i: model problems in one dimension. *Adv. Comput. Math.* **43**(2), 411–442 (2017). <https://doi.org/10.1007/s10444-016-9491-y>
39. Kazeev, V., Oseledets, I., Rakhuba, M., Schwab, C.: Quantized tensor FEM for multiscale problems: diffusion problems in two and three dimensions, accepted for publication in *SIAM J. Multiscale Methods* (2022). arXiv e-prints arXiv:2006.01455 (2020)
40. Kazeev, V., Schwab, C.: Quantized tensor-structured finite elements for second-order elliptic PDEs in two dimensions. *Numer. Math.* **138**(1), 133–190 (2018). <https://doi.org/10.1007/s00211-017-0899-1>
41. Khoromskaia, V., Khoromskij, B., Schneider, R.: QTT representation of the Hartree and exchange operators in electronic structure calculations. *Comput. Methods Appl. Math.* **11**(3), 327–341 (2011). <https://doi.org/10.2478/cmam-2011-0018>
42. Khoromskij, B.N.:  $\mathcal{O}(d \log n)$ -quantics approximation of  $n$ - $d$  tensors in high-dimensional numerical modeling. *Constr. Approx.* **34**(2), 257–280 (2011). <https://doi.org/10.1007/s00365-011-9131-1>
43. Khoromskij, B.N.: Tensor Numerical Methods in Scientific Computing Radon Series on Computational and Applied Mathematics, vol. 19. De Gruyter, Berlin (2018)
44. Khoromskij, B.N., Oseledets, I.O.: Quantics-TT collocation approximation of parameter-dependent and stochastic elliptic PDEs. *Comput. Methods Appl. Math.* **10**(4), 376–394 (2010). <https://doi.org/10.2478/cmam-2010-0023>
45. Khrulkov, V., Hrinchuk, O., Oseledets, I.V.: Generalized tensor models for recurrent neural networks. *CoRR arXiv:1901.10801* (2019)
46. Kolda, T.G., Bader, B.W.: Tensor decompositions and applications. *SIAM Rev.* **51**(3), 455–500 (2009). <https://doi.org/10.1137/07070111X>
47. Kondrat'ev, V.A.: Boundary value problems for elliptic equations in domains with conical or angular points. *Trudy Moskovskogo Matematičeskogo Obščestva* **16**, 209–292 (1967)
48. Kozlov, V., Maz'ya, V., Rossmann, J.: Spectral Problems Associated with Corner Singularities of Solutions to Elliptic Equations *Mathematical Surveys and Monographs*, vol. 85. American Mathematical Society, Providence, Rhode Island (2001). <https://doi.org/10.1090/surv/085>
49. Kozlov, V., Maz'ya, V.G., Rossmann, J.: Elliptic boundary value problems in domains with point singularities. American Mathematical Society (1997)
50. Landau, L., Lifshitz, E.: Quantum mechanics: Non-Relativistic theory. Course of theoretical physics elsevier (1981)
51. Levine, Y., Sharir, O., Cohen, N., Shashua, A.: Quantum entanglement in deep learning architectures. *Phys. Rev. Lett.* **122**(6), 065301, 7 (2019). <https://doi.org/10.1103/PhysRevLett.122.065301>
52. Lieb, E.H., Simon, B.: The Hartree-Fock theory for Coulomb systems. *Comm. Math. Phys.* **53**(3), 185–194 (1977). <http://projecteuclid.org/euclid.cmp/1103900699>
53. Luskin, M., Ortner, C.: Atomistic-to-continuum coupling. *Acta. Numer.* **22**, 397–508 (2013). <https://doi.org/10.1017/S0962492913000068>
54. Maday, Y., Marcati, C.: Analyticity and hp discontinuous Galerkin approximation of nonlinear Schrödinger eigenproblems. arXiv:1912.07483 (2019)
55. Maday, Y., Marcati, C.: Regularity and hp discontinuous Galerkin finite element approximation of linear elliptic eigenvalue problems with singular potentials. *Math. Models Methods Appl. Sci.* **29**(8), 1585–1617 (2019). <https://doi.org/10.1142/S0218202519500295>
56. Marcati, C.: Discontinuous hp finite element methods for elliptic eigenvalue problems with singular potentials. Phd thesis, Sorbonne Université. <https://tel.archives-ouvertes.fr/tel-02072774> (2018)
57. Marcati, C., Rakhuba, M., Schwab, C.: Tensor rank bounds for singularities in polyhedra. In preparation
58. Marcati, C., Rakhuba, M., Ulander, J.E.M.: Low-rank tensor approximation of singularly perturbed boundary value problems in one dimension. *Calcolo. A Quarterly on Numerical Analysis and Theory of Computation* **59**(1), Paper No. 2, 32 (2022). <https://doi.org/10.1007/s10092-021-00439-0>
59. Marcati, C., Schwab, C.: Analytic regularity for the incompressible Navier-Stokes equations in polygons. *SIAM J. Math. Anal.* **52**(3), 2945–2968 (2020). <https://doi.org/10.1137/19M1247334>



60. Maz'ya, V., Rossmann, J.: Elliptic Equations in Polyhedral Domains Mathematical Surveys and Monographs, vol. 162. American Mathematical Society, Providence, Rhode Island (2010). <https://doi.org/10.1090/surv/162>
61. Nouy, A.: Higher-order principal component analysis for the approximation of tensors in tree-based low-rank formats. *Numer. Math.* **141**(3), 743–789 (2019). <https://doi.org/10.1007/s00211-018-1017-8>
62. Oseledets, I.: DMRG approach to fast linear algebra in the TT-format. *Comput. Methods Appl. Math.* **11**(3), 382–393 (2011). <https://doi.org/10.2478/cmam-2011-0021>
63. Oseledets, I., Tyrtshnikov, E.: TT-cross approximation for multidimensional arrays. *Linear Algebra Appl.* **432**(1), 70–88 (2010). <https://doi.org/10.1016/j.laa.2009.07.024>
64. Oseledets, I.V.: Approximation of  $2^d \times 2^d$  matrices using tensor decomposition. *SIAM J Matrix Anal. Appl.* **31**(4), 2130–2145 (2010). <https://doi.org/10.1137/090757861>
65. Oseledets, I.V.: Tensor-train decomposition. *SIAM J. Sci. Comput.* **33**(5), 2295–2317 (2011). <https://doi.org/10.1137/090752286>
66. Oseledets, I.V.: Constructive representation of functions in low-rank tensor formats. *Constr. Approx.* **37**(1), 1–18 (2013). <https://doi.org/10.1007/s00365-012-9175-x>
67. Oseledets, I.V., Savostyanov, D.V., Tyrtshnikov, E.: Linear algebra for tensor problems. *Computing* **85**(3), 169–188 (2009). <https://doi.org/10.1007/s00607-009-0047-6>
68. Rakhuba, M.: Robust alternating direction implicit solver in quantized tensor formats for a three-dimensional elliptic PDE. *SIAM J. Sci. Comput.* **43**(2), A800–A827 (2021). <https://doi.org/10.1137/19M1280156>
69. Rakhuba, M., Oseledets, I.: Grid-based electronic structure calculations: The tensor decomposition approach. *J. Comput. Phys.* **312**, 19–30 (2016)
70. Samarskii, A.A., Galaktionov, V.A., Kurdyumov, S.P., Mikhailov, A.P.: Blow-up in quasilinear parabolic equations, De Gruyter Expositions in Mathematics, vol. 19. Walter de Gruyter & Co., Berlin (1995). <https://doi.org/10.1515/9783110889864.535>. Translated from the 1987 Russian original by Michael Grinfeld and revised by the authors
71. Scherer, K.: On optimal global error bounds obtained by scaled local error estimates. *Numer. Math.* **36**(2), 151–176 (1980/81). <https://doi.org/10.1007/BF01396756>
72. Schollwöck, U.: The density-matrix renormalization group in the age of matrix product states. *Ann. Phys.* **326**(1), 96–192 (2011). <https://doi.org/10.1016/j.aop.2010.09.012>
73. Schötzau, D., Schwab, C.: Exponential convergence for  $hp$ -version and spectral finite element methods for elliptic problems in polyhedra. *Math. Models Methods Appl. Sci.* **25**(9), 1617–1661 (2015). <https://doi.org/10.1142/S0218202515500438>
74. Schötzau, D., Schwab, C.: Exponential convergence of  $hp$ -FEM for elliptic problems in polyhedra: mixed boundary conditions and anisotropic polynomial degrees. *Found. Comput. Math.* **18**(3), 595–660 (2018). <https://doi.org/10.1007/s10208-017-9349-9>
75. Schötzau, D., Schwab, C., Wihler, T.P.:  $hp$ -dGFEM for second order elliptic problems in polyhedra. II: Exponential convergence. *SIAM J. Numer. Anal.* **51**(4), 2005–2035 (2013). <https://doi.org/10.1137/090774276>
76. Schötzau, D., Schwab, C., Wihler, T.P.:  $hp$ -dGFEM for second-order mixed elliptic problems in polyhedra. *Math. Comput.* **85**(299), 1051–1083 (2016). <https://doi.org/10.1090/mcom/3062>, <http://www.ams.org/mcom/2016-85-299/S0025-5718-2015-03062-2/>
77. Schwab, C.:  $P$ - and  $H_p$ -Finite Element Methods. Numerical Mathematics and Scientific Computation. The Clarendon Press, Oxford University Press, New York (1998). Theory and applications in solid and fluid mechanics
78. Tyrtshnikov, E.E.: Tensor approximations of matrices generated by asymptotically smooth functions. *Mat. Sb.* **194**(6), 147–160 (2003). <https://doi.org/10.1070/SM2003v194n06ABEH000747>
79. Visser, M.: The Kerr spacetime—a brief introduction. In: The Kerr Spacetime, pp. 3–37. Cambridge Univ. Press, Cambridge (2009)